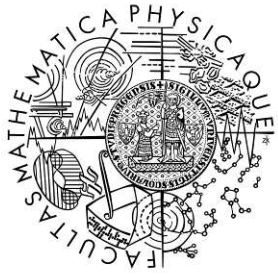

FACULTY
OF MATHEMATICS
AND PHYSICS
Charles University

DOCTORAL THESIS

Hana Chaloupecká

Sudden release of toxic gas in built-up environment

Department of Atmospheric Physics

Supervisor of the doctoral thesis: prof. Zbyněk Jaňour, DrSc.

Study programme: Physics
Specialization: Meteorology and Climatology

Prague 2019

I declare that I carried out this doctoral thesis independently, and only with the cited sources, literature and other professional sources.

I understand that my work relates to the rights and obligations under the Act No. 121/2000 Coll., the Copyright Act, as amended, in particular the fact that the Charles University has the right to conclude a license agreement on the use of this work as a school work pursuant to Section 60 paragraph 1 of the Copyright Act.

In Prague 1.1.2019 Hana Chaloupecká

I would like to thank my supervisor and all the members of the Laboratory of Environmental Aerodynamics for pieces of advice during writing of my dissertation thesis. I would also like to thank my family for supporting me spiritually throughout writing this thesis and in my life in general.

Title: Sudden release of toxic gas in built-up environment

Author: Hana Chaloupecká

Department: Department of Atmospheric Physics, Faculty of Mathematics and Physics, Charles University

Supervisor of the doctoral thesis: prof. Zbyněk Jaňour, DrSc., Department of Atmospheric Physics, Faculty of Mathematics and Physics, Charles University

Abstract:

The dissertation thesis deals with short-term gas releases (puffs) in an urban canopy studied utilizing wind-tunnel modelling. The urban canopy was composed of buildings with pitched roofs organised into closed courtyards. Into it, a ground-level point gas source was placed. The first part of the thesis is focused on specific definitions of puff characteristics. New definitions of puff arrival and departure times are presented. Various definitions of puff arrival time were applied on the same datasets and the results were compared. Moreover, it was studied how slight changes in determination of puff departure time can affect its values and other derived puff characteristics. The second part of the thesis is focused on modelling of probability density functions of puff characteristics with knowledge of sampling positions towards the gas source and mean values of concentrations valid for long-term gas sources. The found equations will be utilized in an operational model. The outputs in the form of the probability density functions of puff characteristics distinguishes my model from the usually utilized operational models, in which only the ensemble-averaged puff outline and concentration field can be predicted.

Keywords: wind tunnel, short-term gas leakage, puff, continuous release, operational model.

CONTENTS

1. Introduction

This dissertation thesis deals with leakages of gases investigated utilizing wind-tunnel modelling. It specialises in short-term gas leakages. The thesis consists of four papers: Evaluation of a new method for puff arrival time as assessed through wind tunnel modelling (journal Process Safety and Environmental Protection 111, 194-210, 2017), Sensitivity of puff characteristics to maximum-concentration-based definition of departure time (journal Journal of Loss Prevention in the Process Industries 56, 242-253, 2018), Model of arrival time for gas clouds in urban canopy (book Air Pollution Modeling and its Application vol. XXVI., 2019), Equations of a new puff model for idealized urban canopy (journal Process Safety and Environmental Protection, submitted). The papers in the dissertation thesis are the originals from the journals but with a changed format to follow the standards for dissertation theses as written at https://www.mff.cuni.cz/cs/studenti/doktorske-studium.

The short-term gas leakages are in contrast with long-term gas leakages discussed only in a small number of studies. The short-term gas releases are predominant in emergency situations. They can be caused accidentally or deliberately. An example of deliberately caused leakages of gases is chemical attacks (e.g. Syria 2014-15, 2016 chlorine leakage, 2013, 2017 sarine leakage or Iraq 2006-7 chlorine leakage - Wikipedia, 2018). Accidental releases can happen for instance in chemical plants (e.g. ammonia leak in Maharashtra - PTI, 2018). The Magazine Time listed top ten environmental disasters in history as follows (Time, 2018):

- Chernobyl
- Bhopal
- Kuwaiti Oil Fires
- Love Canal
- The Exxon Valdez
- Tokaimura Nuclear Plant
- Minamata Disease
- Three Mile Island
- The Aral Sea

- Seveso Dioxin Cloud

Four of the listed disasters are associated with leakages (gas leakages - Bhopal, Seveso Dioxin Cloud, nuclear accidents - Chernobyl, Toakimura Nuclear Plant). This underlines the importance of the investigation of such processes. As these huge disasters have changed industry and its legislation, the introduction of the dissertation takes closer look at the biggest one – Bhopal accident. Then the way how to investigate such leakages is introduced and the content of the rest of the dissertation is introduced.

1.1. Bhopal accident

1.1.1. Situation

After becoming independent in 1947, India had problems with food shortage. This problem was solved by the Green Revolution in the early 1960s. The Green Revolution changed agriculture from the traditional farming to an industrial system that utilizes tractors, pesticides etc. (e.g., Varma and Varma, 2005).

Bhopal is the capital city of the state Mashya Pradesh in central India (Figure 1). It is situated in an agricultural region. In 1984, the city had population of about 1,000,000 (Havens et al., 2012).

Figure 1. Location of Bhopal in India (the map created utilizing www.google.com/maps).

1.1.2. Union Carbide Corporation (UCC)

UCC is an American company, which was established at the beginning of the 20th century. The company originally produced only industrial gases (oxygene, propane, ammonia,…), metallurgical specialties and plastic goods. But parasites started destroying crops in America in the 1950s. Hence, the chemical industry invented new pesticides to eradicate them. One of the pesticides was Experimental Insecticide Seven Seven (abbreviation Sevin). During its production, phosgene and monomethylamine were reacted by creation of methyl isocyanate (MIC; Dutta, 2002).

MIC is highly reactive and very toxic. Its toxicity is greater following inhalation than oral ingestion. MIC causes death after much longer time (hours to days) than cyanides (usually minutes). Moreover, MIC poisoning leads to long term effects and the death is caused by less ppm than cyanides (less than 10 ppm). The exposure limits to MIC were set as 0.02 ppm during 8 hours in the USA. At room temperature, MIC is a flammable, colorless liquid. Its boiling point is 39.1 degrees Celsius. To prevent explosion, it has to be kept at a temperature near zero. It is odorless; one can notice its presence only by starting of eyes watering and throat irritation (Varma 1986; Varma 1989; Dutta, 2002). MIC was tested by UCC‘s toxicologists on rats. But as the results were too terrifying, UCC banned to publish them (Dutta, 2002).

By 1983, UCC had 14 plants in India. It held 50.9% stake in the Indian subsidiary. The rest was owned by Indian investors. This ratio was unusual since normally foreign investors could own only 40% stake. But UCC got an exception because of its sophistication technology and potential for export (Dutta, 2002).

1.1.3. Bhopal factory

The Bhopal factory Union Carbide India Limited (UCIL) was built in Bhopal in 1969. It should have helped in the development of the region (Varma and Varma, 2005). UCIL was a packaged transfer almost without any Indian organization helping with technology etc. (Varma, 1986). It was granted a license to manufacture 5 000 tons of Sevin a year. The Argentinean agronomic engineer, who worked for UCC, advised an alternative batch production of MIC to meet the production. The reason was dangerousness of storing such a huge quantity of MIC in the factory. But UCC turned down his suggestion saying that the factory will be as inoffensive as a chocolate factory. UCIL was located one km from the railway station and three km from two major hospitals (Figure 2). This location was against authorities, who advised to

locate the factory to an industrial zone 25 km away (Reinhold, 1985; Varma and Varma, 2005). The reason why the factory could have been built such close to density populated site was that UCC officials did not mention that the factory will be utilizing the most toxic gases available in the chemical industry (Dutta, 2002).

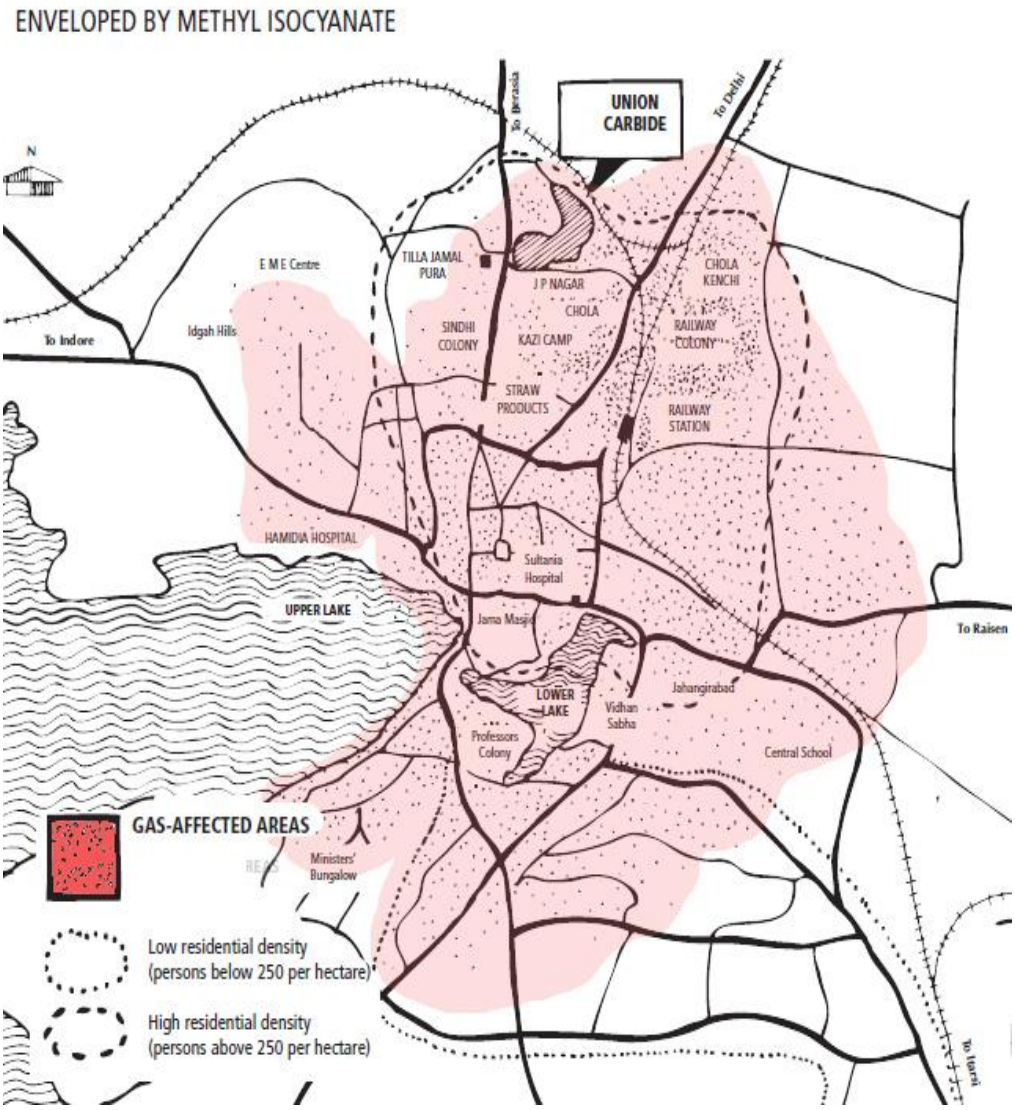

Figure 2. Placement of the factory in the town (adopted from http://www.indiaenvironmentportal.org.in).

1.1.4. Years before the accident

Crop failures and famine in the 1980s caused that farmers did not invest in pesticides as much as in the past (Broughton, 2005). Hence, UCIL profits dropped and the production of pesticides was also dropped (Abbasi, 2018). In the early 1980s a few accidents occurred in the factory (Abbasi, 2018):

- December 1981

  A worker died and two other were injured after an exposure of phosgene.

- January 1982

  25 workers hospitalized after an exposure of phosgene.
- February 1982

  25 workers hospitalized because of leaks of chlorine, MIC, hydrochlorid acid.

Hence, three American engineers from UCC came to Bhopal to confirm that everything was functioning according to the UCC standards. Their report described many problems with the factory (Dutta, 2002). It is doubtful whether the recommendations suggested in the report were implemented (Varma and Varma, 2005).

- October 1982

  4 workers injured and many people nearby affected (eye irritation, breathlessness) by MIC exposure (Dutta, 2002).
- December 1982

  16 workers and neighboring shanties affected by a chlorine leak.

UCIL was also criticized by local journalists. In 1983, UCC commanded cost cutting. Hence, 200 skilled workers were asked to resign. Moreover, number of workers at shifts were reduced by half, a supervisor position was eliminated, the period of safety training was decreased from six months to fifteen days (Dutta, 2002). In autumn 1983, the managing director of UCIL ordered shutting down of the principal safety systems as the factory was no longer active. But sixty tons of MIC were still stored in tanks. Therefore, many engineers and operators left UCIL to find more secure and satisfactory employment (Dutta, 2002). Ram (1984) and Vaidyanathan (1985) suggested that such manner of UCIL functioning was able only because of the relations between the Indian government and UCIL. Many relatives of the ministers were on the UCIL payroll and the UCIL guest house was at the disposal for the government (Varma and Varma, 2005).

In October 1984, refrigeration system of a MIC tank was shut down and vent gas scrubber to neutralize MIC vapors were put in a passive mode to save costs. In November 1984, operators tried to transfer MIC from the tank 610 but they failed. The same happened on 2nd December 1984. The plan was to wash the lines to clean the blockage but no slip blind required for isolation was inserted (Abbassi, 2018).

1.1.5. Accident

Water got into the tank 610 containing over 40 tons of MIC during the cleaning operation at night on 2nd December 1984. It reacted with MIC and generated heat above its boiling point. Hence, the liquid was transformed into gas (Diamond, 1985). The reason why the water for cleaning internal pipes mixed with MIC was a faulty valve (Fortun, 2001). The pressure and temperature in the tank increased and MIC and other reaction products burst past the ruptured disc into the atmosphere (Varma and Varma, 2005).

There are many reasons why the accident was so enormous. The tank was 87% full but the recommended capacity was only 50% at the West Virginia plant and 60% at the Bhopal plant owned by UCC (Reinhold, 1985; Varadarajan, 1985). The safety systems were under-designed and inoperative. Tanks containing MIC were not kept under refrigeration as requested. Moreover, the alarm was set at 20 degrees Celsius, which is by 9 degrees higher temperature than the one requested by the UCC manual. The reason was that the temperature of MIC was probably normally at or above 15 degrees Celsius in Bhopal (Dutta, 2002). The factory workers warmed neighborhood communities at least one hour later since the leak started (Dutta, 2002). The police did not know what had leaked. Hence, they blared with loud speakers: ”Run, run! Poison gas is spreading”. But by running, people inhaled more gas. The correct instructions were to lie down on the ground and cover the face with wet cloths. This is probably the reason why houseflies, as the only animals in Bhopal, were not affected by the leakage. They lay still on the ground (Varma and Varma, 2005). The other problem in Bhopal was misrepresentation of facts. Shortly before the accident, an Indian Minister said that the phosgene in UCIL is not a poisonous gas and therefore the factory is totally safe. After the leakage, top UCIL managers informed that the gas cannot be from UCIL, as it was shut down. After the confirmation of the leakage, a UCIL medical officer announced that the gas was not fatal and could cause just a minor irritant (Abbasi, 2018).

1.1.6. Consequences

The leaked gas caused irritation in eyes and difficulty in breathing. The gas caused chemically induced SARS. Many people died in the first four days due to pulmonary edema. No specific treatment of SARS exists. Only supporting therapy can be provided (Varma and Varma, 2005). MIC has also long-term toxicity as Ranjan et al. (2003) reported. For instance, parents exposed by MIC had much shorter boys than

parents who were not exposed to MIC. In the next two decades 15 000 to 20 000 people died because of the accident (Sharma, 2005). Another more than half a million people were exposed to the gas (Cassels, 1993).

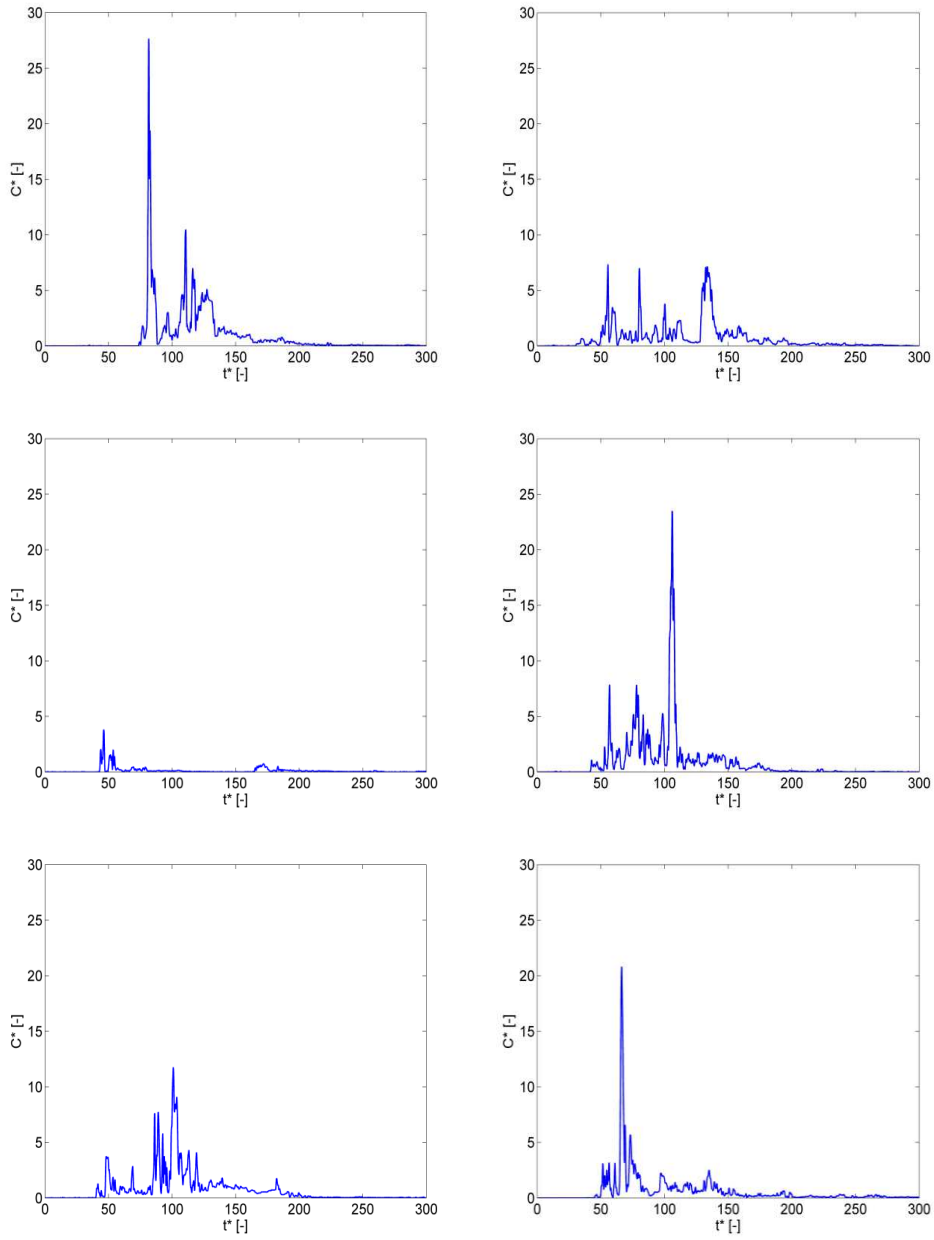

Figure 3. A few short-term gas leakage realisations under the same mean ambient and leakage conditions.

1.2. Investigation of short-term gas releases

The duration of leakages during accidents is very often less than one hour (Chaloupecká et al., 2017). Therefore, they do not belong to the mean field but the turbulent part of the atmospheric spectrum, instead (Van der Hoven, 1957). Under the same mean ambient and leakage conditions many different accident scenarios

can occur (e.g., Zimmerman and Chatwin, 1995). An example of this behaviour is shown in Figure 3. Figure 3 displays a few concentration time series measured at the same place for different leakage realisations under the same mean ambient and leakage conditions. This huge number of different accident courses is the main reason why research of short-term gas leakages is so difficult and only a small number of studies examining these processes in the literature exists. The solution how to explore this variability in the results is a repetition of leakage realisations under the same mean conditions many times to obtain statistically representative datasets.

The study of short-term gas leakages can be performed using mathematical models, field campaigns or wind-tunnel experiments:

1.2.1. Mathematical models

The Direct Numerical Simulation (DNS, e.g. Moser et al., 1999; Schlatter and Örlü, 2010), which solves the Navier-Stokes equations without any turbulence model, provides accurate results. But its demands on calculations (number of the grid points proportional to the 9/4 power of the Reynolds number and the cost of the computation scales like the third power of the Reynolds number) are for high Reynolds numbers out of range even for available supercomputers, as stated by VKI (2016). Because of the time demands, the DNS is not a suitable tool for investigation of short-term gas leakages nowadays.

The DNS computes all the scales of motion (Figure 4b). Nevertheless, one can compute not all, but only the large scales, which are more affected by boundary conditions than the small ones, and utilize a subgrid model for the small scales. This approach is used in the Large Eddy Simulation (LES, Figure 4c, e.g. Piomelli, 1999; Kobayashi, 2006). Though the LES in comparison with the DNS decreases demands on computers, they stay still very high (e.g., Zhiyin, 2015). For instance, using the LES for a full aircraft at flight Reynolds numbers is not expected to be earlier than 2070 as stated by Spalart (2000). Even in the project COST ES1006, which was specialized in short-term gas leakages and lasted for three years, modellers were able to simulate only a very limited number of puff realisations (20-25) utilizing the LES (e.g., Baumann-Stanzer et al., 2015). Such a number is up to an order of magnitude less than by utilizing wind-tunnel modelling that is therefore able to provide representative datasets (e.g., Baumann-Stanzer et al., 2015).

Further decrease of the time demands on the time calculations can be achieved by Reynolds' averaging (e.g., Stull, 2012). It utilizes averaging over a time interval much longer than all the time scales of the turbulent flow (e.g., Pal Arya, 1999). Applying this averaging on the Navier Stokes equations, one obtains the Reynolds Averaged Navier Stokes equations (RANS, e.g. Kajishima and Taira, 2017; Lien and Yee, 2004). These equations can be utilized in the combination with the LES, which is performed in the Detached Eddy Simulation (DES, e.g. Spalart, 2009; Yalçın et al., 2018). Nevertheless, the RANS are usually used in the engineering practice on their own (e.g., Zhiyin, 2015).

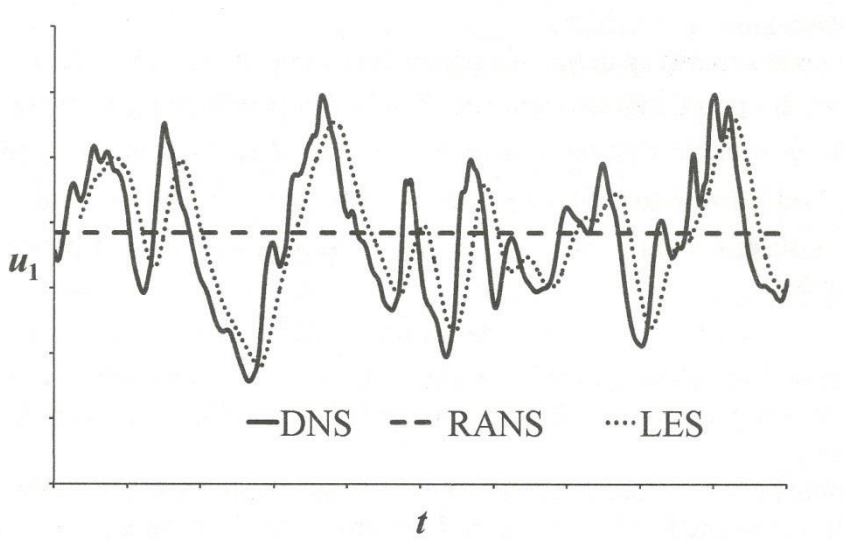

a.

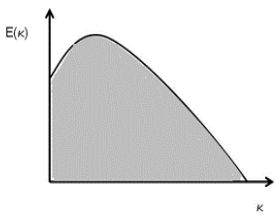

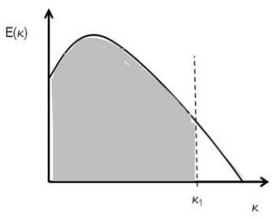

b. c.

Figure 4. Mathematical modelling: Mathematical models (adopted from Uruba, 2009; a), Energy spectrum of turbulent flow with highlighted computed scales for DNS (b) and LES (c).

In an operational practice usage of even much simpler approach, which provides results in almost no time, is usual to estimate of a situation after an accident (e.g., Pal Arya, 1999; Sahin and Ali, 2016). Besides the time issue, one of the reasons for their usage is their recommendation in regulatory guidelines (Hanna et al., 1982; Bluett et al., 2004). This approach is called the Gaussian dispersion modelling. The Gaussian models can be divided into two main types, the plume and the puff. The basic of the plume type (e.g., Pal Arya, 1999) is a constant mean transport wind in the horizontal plane and the Gaussian concentration distributions in the directions perpendicular to the wind direction. It is applicable for accidents in which the gas leaks for a relatively long time (e.g. hours to days). The puff type (e.g., Pal Arya, 1999) has the Gaussian concentration distribution in all three directions and it is useful for those cases in which the duration of the leakage is on the time scale for which the turbulent motions in flow are crucial.

1.2.2. Field campaigns

In field campaigns, variable atmospheric conditions make the achievement of the same mean ambient conditions for long periods nearly impossible and puff ensemble size is very limited (e.g., Baumann-Stanzer et al., 2015). For continuous releases, the commonly used averaging times (10 min or 30 min) are not enough to produce meaningful time mean values. But longer averaging times are usually not possible because of changes in the atmospheric boundary conditions (Schatzmann et al., 1997).

1.2.3. Wind-tunnel experiments

In wind-tunnel experiments, the real world is diminished into a scale model. The experiments are based on the similarity of actions that occur at the model placed into the wind-tunnel (Figure 5) and in the reality. To achieve this similarity, geometric and dynamic similarity of the model and the reality is required (e.g. Jaňour 2001; Bezpalcová, 2007 or Chaloupecká, 2012).

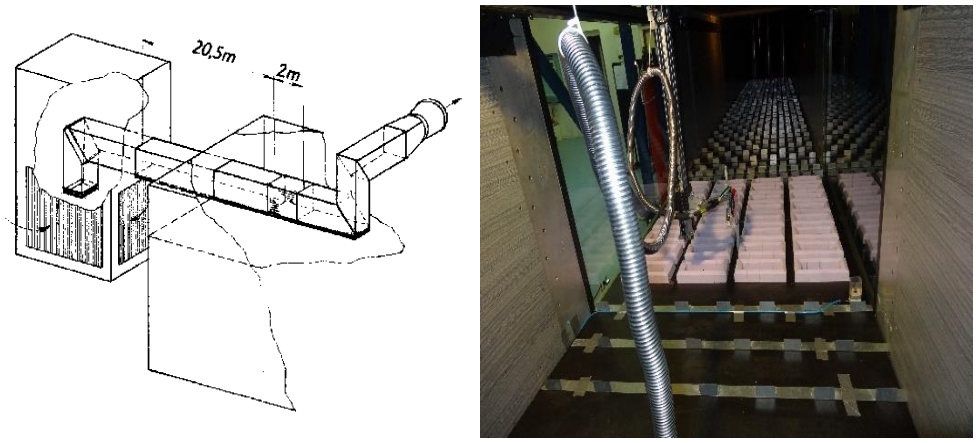

a. b.

Figure 5. Scheme of the open low speed wind tunnel in Nový Knín (a) and a model in scale 1:400 placed in the tunnel (b).

The geometric similarity requires development of a model in a defined scale to the reality and modelling of the boundary layer in the same scale. In the experiments presented in the thesis, boundary layer in 1:400 scale with a neutral stratification and a model in the same scale (Figure 5b) were used. The modelled boundary layer characteristics (roughness length 1.87 m, zero plane displacement 2.96 m, power law exponent α=0.27) agree with the recommendations of VDI (2000) for flows found in cities (Grimmond and Oke, 1999; Britter and Hanna, 2003). The vertical profiles of the mean velocity and the intensity of turbulence of velocity component along the main wind direction at the inlet section are displayed in Figure 6.

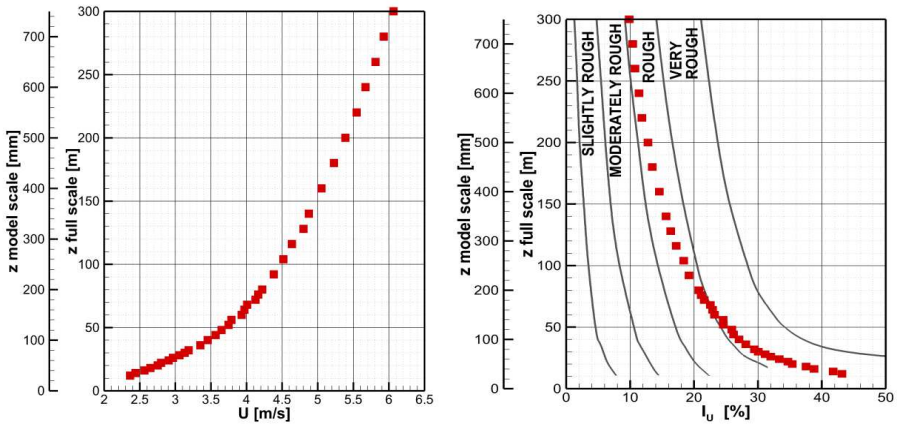

a. Vertical profile of the mean velocity U. b. Vertical profile of the turbulence intensity I_U with intervals for various roughness classes according to VDI (2000).

Figure 6. Vertical profiles of the mean velocity and the intensity of turbulence of velocity component along the main wind direction U at the inlet section.

To achieve the dynamic similarity, having the same ratio between individual forces that affect air particles at the model and in the reality is required. These ratios of forces are called similarity numbers. The approach how to achieve the same similarity numbers in the reality and in the wind tunnel experiments at the model in Figure 5b is described below (more information can be found in Jaňour, 2001; Bezpalcová, 2007; Chaloupecká, 2012).

- Strouhal number – Its value is 1 for each steady flow that is used during the wind tunnel modelling. The same type of flow is assumed in the reality.
- Richardson number – In both, the reality and the wind tunnel, the case of neutral stratification is studied.
- Rossby number – The influence of this number can be neglected if processes in the surface layer and small areas (approximately smaller than 5 km) are being studied.
- Reynolds number – Townsend hypothesis (Jaňour, 2001) can be utilized. An example of its application is displayed in Figure 7. The colour crosses show the results of measurements at four different sampling positions at the model (displayed in Figure 5b) at the height of human breathing zone. The horizontal axis displays Reynolds number $Re = \frac{U_{ref}H}{\nu}$. In this relation, U_{ref} is reference speed (measured at the middle height of the tunnel), H characteristic length (the height of modelled buildings in Figure 5b), ν kinematic viscosity of air. The vertical axis shows dimensionless value of mean concentrations. Concentrations are defined for a point source by the relation $C^* = \frac{CU_{ref}H^2}{Q}$ (VDI, 2000). In this relation, C is concentration, Q source intensity. The Figure reveals that independence of the mean dimensionless concentrations on Reynolds number is achieved for approximately Re≥20,000. Hence, the experiments have to be conducted only for Re≥20,000.

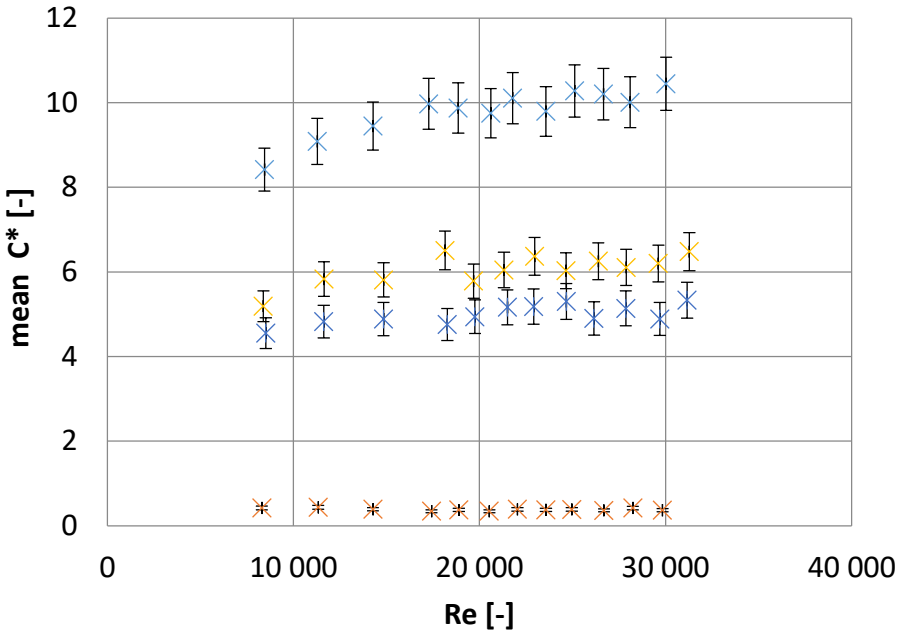

Figure 7. Townsend hypothesis: finding the critical Re from which value of the mean C* is independent of the Re value.

- Prandtl number – Its value is automatically preserved if air is utilized in the wind tunnel.
- Eckert number – This number can be neglected because the velocity of flow in the reality and in the model scale is much less than the velocity of sound.
- Schmidt number – This number has the same value in the tunnel and the reality if air is utilized in the tunnel.

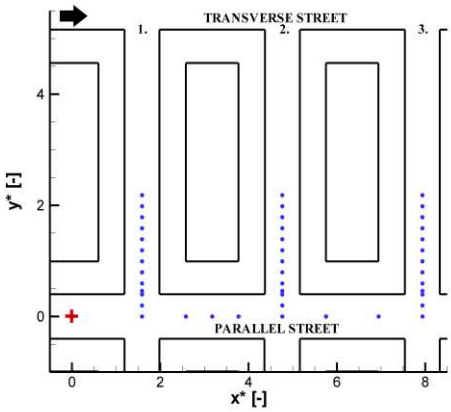

Figure 8. Zoomed investigated section of the model: red cross - position of source, blue circles - sampling positions, arrow - flow direction; $x^* = \frac{x}{H}, y^* = \frac{y}{H}$, where x, y are horizontal positions, H is characteristic length.

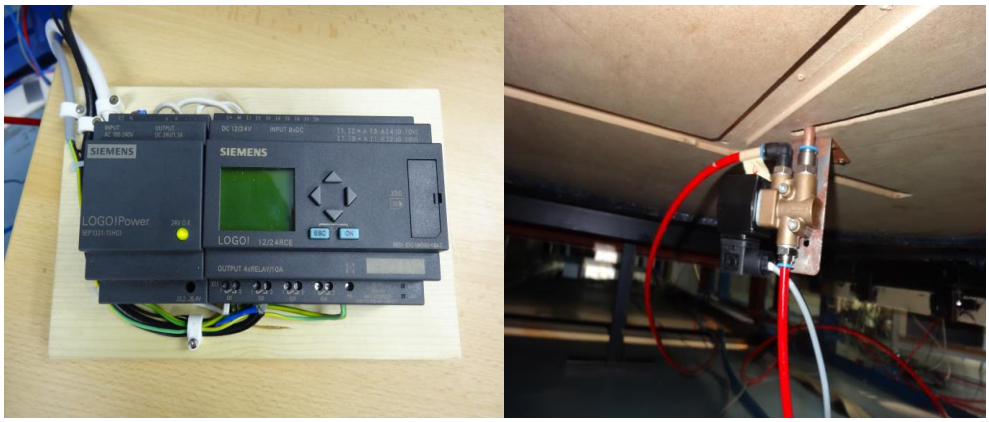

a. b.

Figure 9. SIEMENS Programme Logic Controler LOGO! (a) and Norgren electromagnetic valve ND5 (b).

Source		
source type	short-term, ground-level, point, gas	
number of sources	1	
source placement at the model (Figure 8)	x*=0, y*=0, z*=0	
type of released medium	passive gas – ethane	
	physical characteristics:	
	molecular weight	30.069 kg/mol
	gas density at 0°C and 1.013 bar	1.3551 kg/m^3
	density ratio to air	1.0481
	vapour pressure at 20°C	37.64 bar
release characteristics	mean release duration	1s (+- 2%)
	mean released gas volume	5.6 ml (+- 4%)
experimental details	pipe with 8 mm inner orifice	

Table 1. Basic description of the release characteristics (ethane characteristics - Engineering ToolBox, 2018) following recommendations of the project COST ES1006 (Andronopoulos et al., 2015).

The leakage is simulated by tracer gas. Pure ethane was utilized during conducting of my experiments (Table 1). Short-time gas discharges were created by a source composed of Programmable Logic Controller (PLC) Siemens LOGO! 12/24 RCE 0BA 7

and electromagnetic 3/2 valve ND5 (Figure 9) in the experiments. The source is capable of a discharge creation of defined time durations. The basic principle of the creation of the releases is as follows:

The gas is transported in a hose to an input valve orifice.

a) It flows continually through the output orifice that empties outside the tunnel – in Figure 10 the right upper orifice - until the voltage is set to the valve by PLC.

b) While the valve is under voltage, gas is transported to the second output orifice – in Figure 10 the left upper orifice - that empties into the bottom of the tunnel and a "cloud" of gas is created in the wind tunnel.

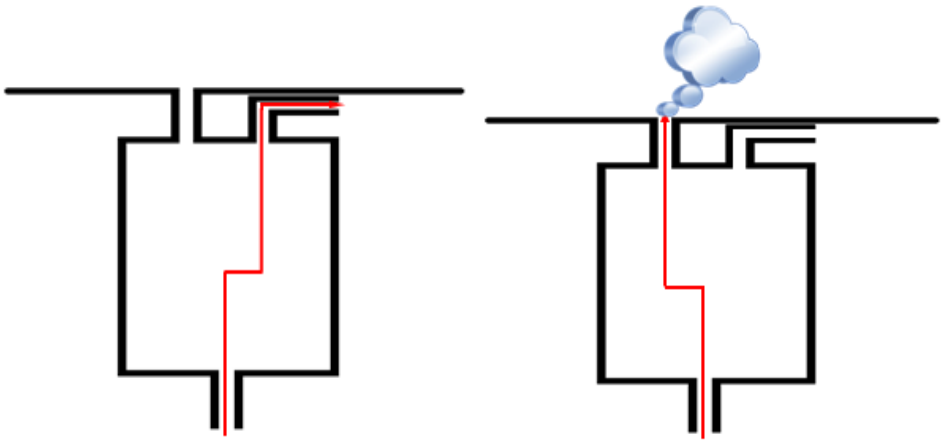

a. b.

Figure 10. Puff creation: valve without voltage (a), valve under voltage (b).

The time course of a simulated leakage in the tunnel is recorded at exposed places of the model (Figure 8) by a concentration measurement device - e.g. Laser photoacoustic spectrometry (Civiš et al., 2001) or Flame ionisation detector (HFR400, 2017), the device utilized in the measurements described in this thesis.

The measurement with Fast Flame Ionisation Detector (FFID) is based on the knowledge that during combustion of hydrocarbons ions are created. In the FFID sample head (Figure 11), the tracer gas (air with hydrocarbons) is mixed with the fuel gas (hydrogen) at the nozzle exit. Then air is added. The hydrocarbons are burnt in flames and the number of ions, which is proportional to the total mass of hydrocarbons, is created. Ions are collected at a collector electrode and the output signal is obtained by FFID. The frequency response of FFID must be evaluated (flick

test, Figure 11). The response is a function of sampling system tube dimensions and pressures. The FFID signal must be calibrated, which is done utilizing a gas with the known value of ppm (typically mixture of air and hydrocarbon utilized as the tracer gas; HFR400, 2017).

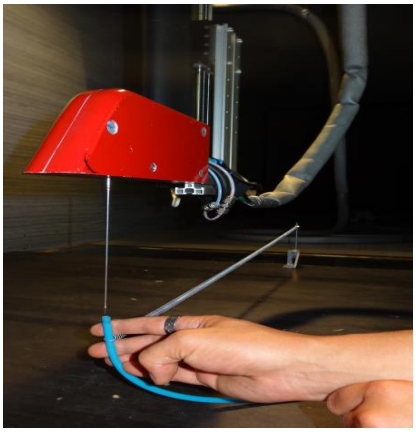

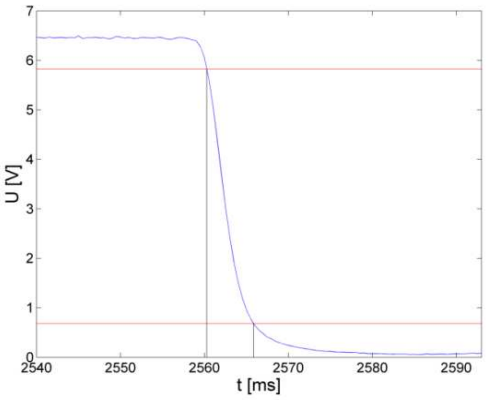

a. b.

Figure 11. Flick test: realisation of the test (a); test results (b) (adopted from Chaloupecká et al., 2017).

As a result of the measurements, concentration time series are obtained. These concentration time series must be then analysed. By this analysis, puff characteristics are obtained to evaluate short-term gas releases at individual exposed locations. The commonly examined puff characteristics (e.g., Zhou and Hanna, 2007; Chaloupecká et al., 2018; Figure 12) are:

- arrival time (at)

  Arrival time is the time when the gas cloud gets to the exposed place.
- maximum concentration (maximum C)

  Maximum concentration is the highest value of concentration registered during the presence of the gas cloud at the exposed place.
- high percentiles of concentrations (e.g., 99th percentile of C)

  High percentiles of concentrations are the percentiles counted from the time interval when the gas cloud was present at the exposed place.
- dosage

  Dosage is the total sum of concentrations registered during the presence of the gas cloud at the exposed place.
- departure time (dt)

  Departure time is the time when the gas cloud left the exposed place.

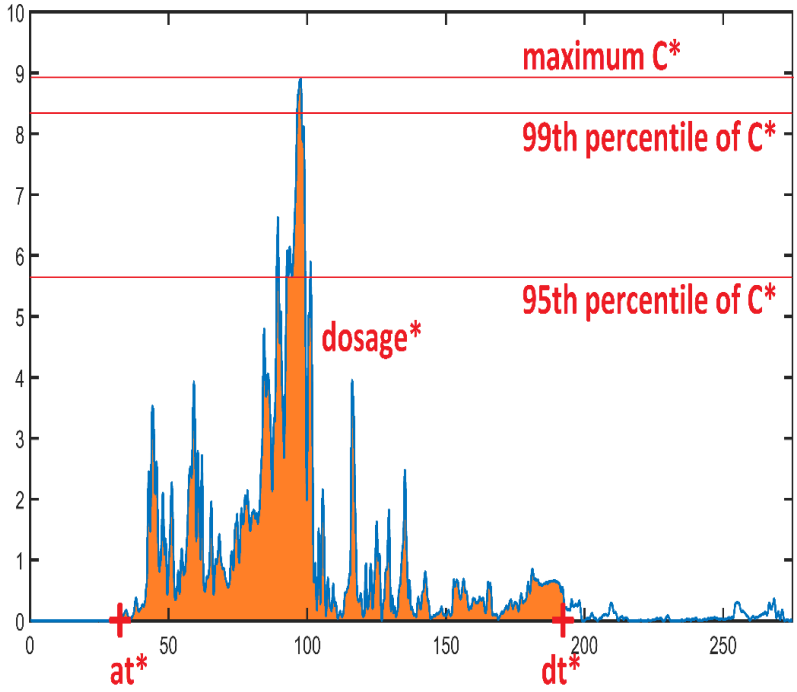

Figure 12. Puff characteristics.

The definitions of puff characteristics above are only general and concrete specifications must be chosen to use them in practise. The main problem is that a non-zero signal is obtained by the device even when the gas cloud is not present at the sampling position. The main reason is the noise of the equipment utilized for concentration measurements, the residue of tracer gas as well as dust particles sucked into the detector (Chaloupecká et al., 2017). Therefore, the first part of my dissertation deals with the problem of specific definitions of puff characteristics.

The issue of puff arrival determination is described in the first chapter after the introduction. Different researchers overcome the difficulties in puff arrival determination by utilizing various arrival time definitions. Two main approaches exist in the literature.

The first approach does not find the first time at which the maximum concentration is detected, but the time when a maximum concentration is registered, referred as travel time (e.g., Zhou and Hanna, 2007).

The second approach tries to find the first moment when the gas cloud gets to the sampling place. A few sub-approaches of this approach can be found. These are a visual method, a method utilizing a dosage and a method based on a threshold criterion.

The visual method (e.g., Yee et al., 1998) uses eyesight. It has both, advantages as well as disadvantages. The biggest advantage of this approach is that a human is more capable, compared with an inflexible algorithm, in coming to a decision whether an increase in concentration is caused by a gas cloud or not. The disadvantage is a degree of subjectivity arises via this approach to the analysis and high time demands.

The dosage method (e.g., Harms et al., 2011) uses 5% of the total dosage reached at the sampling place for the definition of arrival time. Harms et al. (2013) report that this definition enables puffs with different concentrations to have a uniform arrival time.

The last method utilizes the threshold criterion. Many approaches how to determine the threshold in the literature exist. One can find three main approaches. The first approach uses a value that is dependent on a specific released substance and the threshold is chosen according to the hazardousness of the gas, such as a lower flammability limit (e.g., Pontiggia et al., 2011). One can also choose the threshold based on the course of a recorded signal. This value can be related to the recorded maximum concentration (e.g., Zhou and Hanna, 2007). Another option is to look at the statistical characteristics of background noise. The chosen threshold can be the same for all the sampling positions. Doran et al. (2006) utilized a quantity which was higher than the detectable minimum, as well as the residual values from a previous realisation for all sampling places. But the problem with only one threshold for all the sampling positions is that these residual values are different for the places close to and distant from the gas source. A higher threshold chosen according to the residual values found close to the source may cause delayed puff arrival detection at places distant from the source. Hence, this method could have problems for places very differently distanced from the source. The other option is to choose different thresholds at different places (e.g., Chaloupecká et al., 2016).

One can look at only one value to make a decision whether the gas cloud reached the sampling position or not. But concentration time series can contain false very high values caused by sucking in a dust particle during measurements. The solution to this problem is to require the detection of a value of at least the threshold quantity in a specific time interval (Doran et al., 2007). But this requirement is problematic because of the concentration time series intermittency. Chaloupecká et al. (2016) therefore require the detection of values of at least the threshold quantity, not in the entire time interval, but in a specific percentage of cases instead.

In the chapter dealing with the puff arrival, a new threshold method of determining the puff arrival time as well as comparison of the results utilizing various methods is presented. Zhou and Hanna (2007) find the threshold of the realisation by looking at the whole concentration time series. But the cloud arrival could probably be better recognised if we look only at the behaviour of the beginning of the concentration time series before the cloud arrival. But this time is unknown. However, we can utilize concentration time series registered before the cloud release. This is the central idea of the new method as presented in the chapter. Moreover, we compare the results with other methods applied to the same dataset. This comparison is important, since widely different arrival time definitions lead to different results but no comparative study exists.

The third chapter of the thesis deals with puff departure time. In comparison with the puff arrival time, the determination of puff departure time is much more challenging. The reason is that the gas cloud is torn at its back side. The gas can be detected only from time to time at the sampling place. In comparison with the departure time, the concentration arise after the puff arrival is more steep and therefore the puff arrival can be more easily found.

While the determination of the arrival time is definitely crucial for emergency services, the precise determination of departure time seems not to be as important at first glance. Departure time is useful to determine the end of the evacuation. But this decision can be made with information derived by the direct measurements utilizing detectors at the exposed locations (e.g., Mitchell et al., 2005). The predicted departure time is therefore only a helpful tool, which should estimate the time when firefighters and the army can perform direct measurements at the exposed location. However, the value of the departure time enters into the definitions of other variables, which help to evaluate the hazardous effects of the emergency incident – e.g. dosage, high percentiles of concentrations (e.g, Efthimiou et al., 2016; Yee and Chan, 1997).

In the chapter, it is shown how slight changes in the definition of departure time affect its values and other derived puff characteristics (dosage, high percentiles of concentrations). Moreover, a modified definition of departure time is introduced. The basic idea of the definition is creation of an envelope curve based on concentration local maxima around the concentration time series. The method trades on the fact that after the puff departure time the concentration levels change in time only very slowly in contrast with the time when the gas cloud is present at the sampling place. Hence, the departure time is set when the time changes in the concentration level almost stop.

The last two chapters of the thesis before the conclusion deal with modelling of probability density functions of puff characteristics at exposed places as a part of a new semi-empirical puff model. The reason for developing of the new semi-empirical puff model are the results found in the project COST ES1006. The project COST ES1006 revealed that fast puff models, which are the only option for estimating the situation after an accident during an emergency phase, give incorrect results (e.g., underestimation of mean dosage by one order of magnitude). However, the results of these models for long-term gas releases are not bad (Baumann-Stanzer et al., 2015). Hence, the solution might be to find relations that would recalculate the results valid for the long-term gas releases into the ones valid for the short-term gas releases.

We present these relations for the semi-empirical puff model valid for a built-up environment consisting of closed courtyards with pitched roofs (Figure 13). This urban area is typical for European city inner parts (Heathcote, 2014). To find the relations, wind tunnel experiments for both, short-term gas releases as well as long-term gas releases, were utilized. The developed model will consist of a model utilized for the continuous source and the equations introduced in the thesis. The outputs of the model are probability density functions of puff characteristics. The reason why not only one value as an output for each puff characteristic is good enough is that for short-term gas leakages, many possible dispersion scenarios for an exposed position and the same mean conditions exist (Zimmerman and Chatwin, 1995). The probability density function enables one to count the most probable value as well as the extreme cases which can occur. This stands our semi-empirical model apart from the models usually utilized during accidents in which only the ensemble-averaged puff outline and concentration field can be predicted (Pal Arya, 1999).

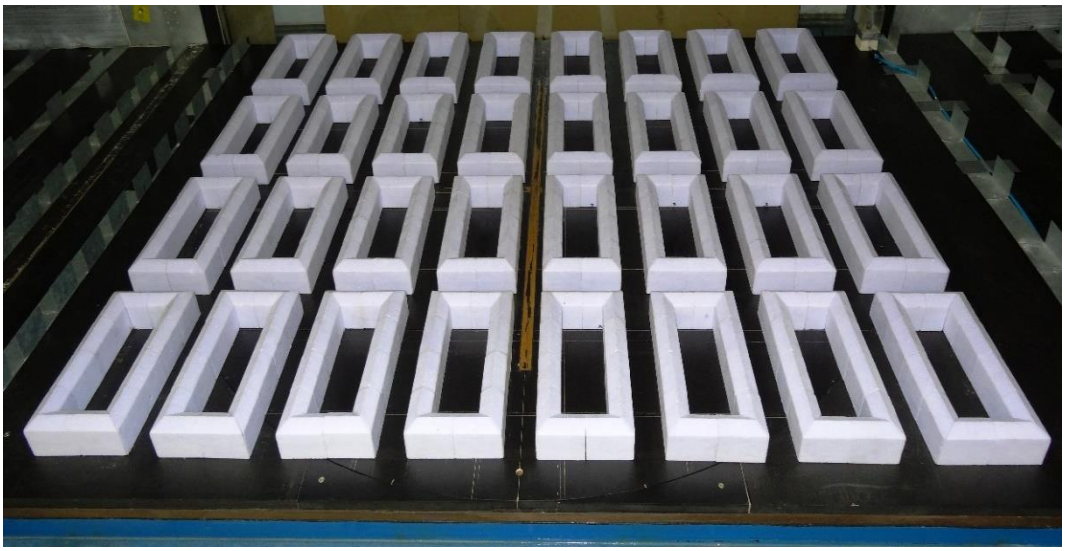

Figure 13. Idealized urban area placed in the wind tunnel.

References

Abbasi, S.A., 2018. Bhopal disaster: Lessons learnt and ignored. Pondicherry University.

Andronopoulos, S., Barmplas, F., Bartzis, J.G., Baumann-Stanzer, K., Berbekar, E., Efthimiou, G., Gariazzo, C., Harms, F., Hellsten, A., Herring, S., Jurcakova, K., Leitl, B., Trini.Castelli, S., 2015. COST ES1006 – Model Evaluation Protocol, COST Action ES1006.

Baumann-Stanzer, K., Andronopoulos, S., Armand, P., Berbekar, E., Efthimiou, G., Fuka, V., Gariazzo, C., Gasparac, G., Harms, F., Hellsten, A., Jurcakova, K., Petrov, A., Rakai, A., Stenzel, S., Tavares ,R., Tinarelli, G., Trini Castelli, S., 2015. COST ES1006 – Model Evaluation Case Studies, COST Action ES1006.

Bezpalcová, K., 2007. Physical Modelling of Flow and Dispersion in Urban Canopy, Dissertation Thesis. Charles University.

Bluett, J., Gimson, N., Fisher, G., Heydenrych, C., Freeman, T., Goldfrey, J., 2004. Good Practice Guide for Atmospheric Dispersion Modelling. Ministry for the Environment, New Zealand.

Britter, R.E., Hanna, S.R.,2003. FLOW AND DISPERSION IN URBAN AREAS. Annual Review of Fluid Mechanics 35, 469-496.

Broughton, E., 2005. The Bhopal disaster and its aftermath: a review. Environmental Health, 4-6.

Cassels, J., 1993. Uncertain promise of law: Lessons from Bhopal. Toronto, Canada: University of Toronto Press.

Civiš, S., Zelinger, Z., Střižik, M., Jaňour, Z., 2001. Simulation of Air Pollution in a Wind Tunnel. Spectroscopy from Space, NATO Science Series (Series II: Mathematics, Physics, and Chemistry), vol 20. Springer, Dordrecht.

Chaloupecká, H., 2012. Flow and dispersion in urban areas. Diploma thesis. Charles University.

Chaloupecká, H., Jaňour, Z., Nosek, Š., 2016. Short-term gas dispersion in idealised urban canopy in street parallel with flow direction. EPJ Web of Conferences 114.

Chaloupecká, H., Jaňour, Z., Jurčáková, K., kellnerová, R., 2017. Evaluation of a new method of puff arrival time as assessed through wind tunnel modelling, Process Safety and Environmental protection 111, 194-210.

Chaloupecká, H., Jaňour, Z., Jurčáková, K., Kellnerová, R., 2018. Sensitivity of puff characteristics to maximum-concentration-based definition of departure time, Journal of Loss prevention in the Process Industries 56, 242-253.

Diamond, S., 1985.The Bhopal disaster: How it happened. The New York Times, p. A1.

Doran, J.C., Allwine, K.J., Clawson, K.L., Carter, R.G., 2006. 6.2 RETENTION OF TRACER GAS FROM INSTANTANEOUS RELEASES OF SF6 IN AN URBAN ENVIRONMENT. 14th Joint Conference on the Applications of Air Pollution Meteorology with the Air and Waste Management Association.

Doran, J.C., Alwine, K.J., Flaherty, J.E., Clawson, K.L., Carter, R.G., 2007. Characteristics of puff dispersion in an urban environment. Atmospheric Environment 41, 3440-3452.

Dutta, S., 2002. The Bhopal Gas Tragedy. ICFAI Center for Management Research, p. 9.

Efthimiou, G.C., Andronopoulos, S., Tolias, I., Venetsanos, A., 2016. Prediction of the upper tail of concentration probability distributions of a continuous point source release in urban environments. Environmental Fluid Mechanic 16 (5), 899–921.

Engineering ToolBox, https://www.engineeringtoolbox.com/ethane-d_1417.html, accessed 30.12.2018

Fortun, K., 2001. Advocacy after Bhopal: Environmentalism, disaster, new global orders. University of Chicago Press.

Grimmond, C.S.B., Oke, T.R., 1999. Aerodynamic Properties of Urban Areas Derived from Analysis of Surface Form. Journal of Applied Meteorology 38, 1262-1292.

Hanna, S.R., Briggs, G.A., Hosker, Jr., R.P., 1982. Handbook on ATMOSPHERIC DIFFUSION. Technical Information CENTER, U. S. DEPARTMENT OF ENERGY, p. 102.

Harms, F., Leitl, B., Schatzmann, M., Patnaik, G., 2011. Validating LES-based flow and dispersion models. Journal of Wind Engineering and Industrial Aerodynamics 99, 289-295.

Harms, F., Hertwig, D., Leitl, B., Schatzman, M., Patnaik, G., 2013. CHARACTERIZATION OF TRANSIENT DISPERSION PROCESSES IN AN URBAN ENVIRONMENT. 14th Conference on Harmonisation within Atmospheric Dispersion Modelling for Regulatory Purposes.

Havens, J., Walker, H., Spicer, T., 2012. Bhopal atmospheric dispersion revisited. Journal of Hazardous Materials 233–234, 33-40.

Heathcote, E., 2014. The historic mixed-use courtyard buildings of central Europe. Global Property Insight, Financial Times.

HFR400, 2017. Atmospheric Fast FID, User Guide. Cambustion Ltd., Cambridge.

Jaňour, Z., 2001. Modelování mezní vrstvy atmosféry. p. 148, Karolinum.

Kajishima T., Taira K., 2017. Reynolds-Averaged Navier–Stokes Equations. Computational Fluid Dynamics, Springer.

Kobayashi, T., 2006. large Eddy simulation for engineering applications. Fluid Dynamics Research 38, 84-107.

Lien, F-S, Yee, E., 2004. NUMERICAL MODELLING OF THE TURBULENT FLOW DEVELOPING WITHIN AND OVER A 3-D BUILDING ARRAY, PART I: A HIGH-RESOLUTION REYNOLDS-AVERAGED NAVIER–STOKES APPROACH Boundary-Layer Meteorology 112, 427–466.

Mitchell, J.T., Edmonds, A.S., Cutter, S.L., Schmidtlein, M., McCarn, R., Hodgson, M.E., Duhé, S., 2005. Evacuation Behaviour in Response to the Graniteville, South Carolina, Chlorine Spill.. QUICK RESPONSE RESEARCH REPORT 178, University of South Carolina.

Moser,R.D., Kim, J. , Mansour, N.N., 1999. Direct numerical simulation of turbulent channel flow up to Reτ=590.Physics of Fluids 11, 943-945.

Pal Arya, S., 1999. Air Pollution Meteorology and Dispersion, Oxford University Press, p. 310.

Piomelli, U., 1999. Large-eddy simulation: achievements and challenges. Progress in Aerospace Sciences, 35, 335-362.

Pontiggia, M., Landucci, G., Busini, V., Derudi, M., Alba, M., Scaioni, M., Bonvicini, S., Cozzani, V., Rota, R., 2011. CFD model simulation of LPG dispersion in urban areas. Atmospheric Environment 45, 3913-3923.

PTI. Ammonia gas leaks from chemical plant in Maharashtra, 2018. http://timesofindia.indiatimes.com/articleshow/66921671.cms?utm_source=contentofinterest&utm_medium=text&utm_campaign=cppst

Ram, M., 1984. Counting the cost. Far Eastern Economic Review, 10–11.

Ranjan, N., Sarangi, S., Padmanabhan, V. T., Holleran, S., Ramakrishnan, R., & Varma, D. R., 2003. Methyl isocyanate exposure and growth patterns of adolescents in Bhopal. Journal of American Medical Association, 290, 1856-1857.

Reinhold, R., 1985. Disaster in Bhopal: Where does blame lie? The New York Times, p. A8.

Sahin, S., Ali, M., 2016. Emergency Planning Zones Estimation for Karachi-2 and Karachi-3 Nuclear Power Plants using Gaussian Puff Model, Science and Technology of Nuclear Installations, 6 pages.

Schatzmann, M., Rafailidis, S., Pavageau, M., 1997. Some remarks on the validation of small-scale dispersion models with field and laboratory data. Journal of Wind Engineering and Industrial Aerodynamics 67, 885-893.

SCHLATTER, P., ÖRLÜ, R., 2010. Assessment of direct numerical simulation data of turbulent boundary layers. Journal of Fluid Mechanics, 659, 116-126.

Sharma, D.C., 1954. Bhopal: 20 years on. Lancet. 365 (9454), 111-2.

Spalart, P.R., 2000. Strategies for turbulence modelling and simulations. international journal of heat fluid flow 21, 252-263.

Spalart, P.R., 2009. Detached Eddy Simulation, Annual Review of Fluid Mechanics 41, 181–202.

Stull, B.R., 2012. An Introduction to Boundary Layer Meteorology, Kluwer academic Publishers, p. 670.

Time,http://content.time.com/time/specials/packages/completelist/0,29569,1986457,00.html.

Uruba, V., 2009. Turbulence. Nakladatelství ČVUT, p. 141, Praha.

Vaidyanathan, A., 1985. A sorry technological tale from India. New Scientist, p. 21.

Van der Hoven, I., 1957. Power spectrum of horizontal wind speed in the frequency range from 0.0007 to 900 cycles per hour. Journal of Meteorology 14, 160-164.

Varadarajan, S.,1985. A scientific enquiry into the methylisocyanate leak in Bhopal. New Delhi, India: Council of Scientific and Industrial Research.

Varma, V. S., 1986. I. Bhopal: The Unfolding of a Tragedy. Alternatives, 11(1), 133–145.

Varma, D. R., 1989. Hydrogen cyanide and Bhopal. Lancet 2, 557-558.

Varma, R., Varma, D.R., 2005. The Bhopal Disaster of 1984. Bulletin of Science, Technology and Society 25(1), 37-45.

VDI - Verein Deutcher Ingenier, 2000. Environmental meteorology Physical modelling of flow and dispersion processes in the atmospheric boundary layer, Application of wind tunnels, VDI-Standard: VDI 3783 Blatt 12, Dusserdorf.

VKI, 2016. LES and related techniques: Theory and applications, von Karman Institute for Fluid dynamics.

Wikipedia, https://en.wikipedia.org/wiki/Chemical_warfare , accessed 25.12.2018.

Yalçın, Ö., Cengiz, K., Özyörük, Y., 2018. High-order detached eddy simulation of unsteady flow around NREL S826 airfoil, Journal of Wind Engineering and Industrial Aerodynamics 179, 125-134.

Yee, E., Chan, R.A., 1997. Simple model for the probability density function of concentration fluctuations in atmospheric plumes. Atmospheric Environment 31, 991–1002.

Yee, E., Kosteniuk, P.R., Bowers, J.F., 1998. A STUDY OF CONCENTRATION FLUCTUATIONS IN INSTANTANEOUS CLOUDS DISPERSING IN THE ATMOSPHERIC SURFACE LAYER FOR RELATIVE TURBULENT DIFFUSION: BASIC DESCRIPTIVE STATISTICS. Boundary-Layer Meteorology 87, 409-457.

Zhiyin, Y., 2015. Large-eddy simulation: Past, present and the future. Chinese Journal of Aeronautics 28(1), 11-24.

Zhou, Y., Hanna, S.R., 2007. Along-wind dispersion of puffs released in a built-up urban area. Boundary-Layer Meteorology 125, 469-486.

Zimmerman, W.B., Chatwin, P.C., 1995. Fluctuations in dense gas concentrations measured in a wind tunnel. Boundary Layer Meteorology 75, 321-352.

2. Evaluation of a new method for puff arrival time as assessed through wind tunnel modelling

Hana Chaloupecká[a,b*], Zbyněk Jaňour[a], Jiří Mikšovský[b], Klára Jurčáková[a], Radka Kellnerová[a]

[a] Institute of Thermomechanics, Czech Academy of Sciences, Czech Republic

[b] Faculty of Mathematics and Physics, Charles University in Prague, Czech Republic

Abstract

Deliberate or accidental gas leakages threaten people's lives. Short-duration releases of gas are influenced by actual phase of turbulent atmospheric flow and therefore the study of these situations requires multiple repetitions of the leakage under the same mean conditions. Such a set of experiments was conducted in a wind tunnel on a scaled model of an idealized urban canopy created by rectangular buildings with pitched roofs organized into closed courtyards. Concentration time series of high time resolution were measured by a fast flame ionisation detector. The arrival time of gas from short-duration discharges was investigated at a few places of detection. This paper introduces a new method of defining gas arrival time, one not only applicable in the post-processing analysis but also in the operative stage. Moreover, it shows the results of other commonly used gas arrival time definitions (visual and dosage methods and a method utilizing the maximum detected concentration). It was explored both, the change in the arrival time value in individual realisations and places as well as the change in statistical values calculated from ensembles (mean, median, quartiles). Furthermore, the dependence of the definitions of arrival time on their parameters is discussed.

Keywords: wind tunnel, short-term gas leakage, puff, arrival time, threshold, dosage.

2.1. Introduction

Air pollution studies are mainly concerned with long-term gas releases. Such releases are mostly releases from permanent sources of contaminants (e.g., smoke from factory stacks). But only a small number of studies examine short-term gas leaks. This scenario is predominant in emergency situations (e.g., chemical plant accidents), as suggested by Balczo et al. (2012). These gas leakages very often last less than one hour (e.g., the accident of the

industrial facility working under the EU Seveso II Directive described in Baumann-Stanzer et al. (2015), the Bhopal disaster - Varma and Varma, 2005 - or Orica's Kooragang Island chemical plant accidents in August and November 2011 - e.g. Wikipedia). Their dispersion differs from long-term releases since their leakage duration falls into the turbulent part of the atmospheric spectrum (e.g., Van der Hoven, 1957). Under the same mean ambient and leakage conditions many different accident scenarios can occur (e.g., Zimmerman and Chatwin, 1995). This fact contributes to the difficulty of conducting research into short-term gas releases. Many leakage realisations under the same mean conditions are needed for risk assessment (e.g., Zimmerman and Chatwin, 1995; Chaloupecká et al., 2016). In contrast to the dispersion from long-term gas sources, dispersion from short-term gas sources (puffs) computed by common emergency mathematical models (e.g., ALOHA - Jones et al., 2013; HotSpot - Homann et al., 2014) is inaccurate (e.g., mean dosage is underestimated by about one order of magnitude), since these models are typically based on time-averaged or parametric equations, as discussed in Baumann-Stanzer et al. (2015). Moreover, according to Baumann-Stanzer et al. (2015), these simple models provide only few output variables for puffs. Baumann-Stanzer et al. (2015) also report that advanced computational fluid dynamics (CFD) models (e.g., large eddy simulations, LES) are capable of simulating the variability of individual puffs. On the other hand, these LES models need rigorous validation and they are very expensive computationally, as stated e.g. by Zhiyin (2015) as well as Baumann-Stanzer et al. (2015). In field campaigns, variable atmospheric conditions make the achievement of the same mean ambient conditions for long periods nearly impossible and puff ensemble size is very limited (e.g., Baumann-Stanzer et al., 2015). In laboratory experiments, the ambient as well as leakage conditions can be controlled and therefore the wind tunnel represents the suitable research tool for short-term gas releases.

In wind tunnel experiments, the time course of leakage is recorded by a concentration measurement device at different exposed places. As a result of these near-point measurements, concentration time series are obtained. Concentration time series are then analysed to obtain the puff characteristics. One such characteristic to describe the gas cloud is its arrival time to the place of detection. The puff arrival time represents an important factor in determining safe courses of action for inhabitants in exposed areas.

In a concentration time series, the recognition of puff arrival is aggravated mainly by the noise of the equipment utilized for concentration measurements, the residue of tracer gas as well as dust particles sucked into the detector. Therefore, cloud arrival time cannot be

defined by the first detection of a non-zero concentration in the time series. Different researchers overcome these difficulties by utilizing various arrival time definitions. Some researchers do not find the first moment of gas arrival at the sampling place, but the time at which the maximum concentration is detected, referred to as travel time, instead (e.g., Zhou and Hanna, 2007). To find the first moment of gas presence at the sampling place, three main methods can be found in the literature. These methods are a visual method, a method utilizing a dosage and a method based on a threshold criterion. The visual method (e.g., Yee et al., 1998), which uses eyesight, has the advantage that a human is more capable, compared with an inflexible algorithm, in coming to a decision whether an increase in concentration is caused by a gas cloud or not. On the other hand, a degree of subjectivity arises via this approach to the analysis. In addition, the time demands of this approach make it impossible to analyse huge databases, but the visual method can serve as a comparison with results reached using the various automatic methods. The dosage method (e.g., Harms et al., 2011) uses 5% of the total dosage reached at the sampling place for the definition of arrival time. Harms et al. (2013) report that this definition enables puffs with different concentrations to have a uniform arrival time. The gas cloud arrival at the sampling place can also be defined by a threshold criterion. The choice of the threshold value changes widely from author to author. It can be classified into three main branches of approach. The first approach uses a value that is dependent on a specific released substance. The threshold is chosen according to the hazardousness of the gas, such as a lower flammability limit (e.g., Pontiggia et al., 2011). This method allows one to generate maps for emergency services with the affected zones highlighted according to their level of danger. The second approach is one in which the threshold value is dependent on the course of a recorded puff signal concentration. Zhou and Hanna (2007) chose the threshold value relative to the recorded maximum (peak) concentration. They determined the beginning of the puff as the time when the concentration exceeded a 10% maximum concentration. The third option is to look at the statistical characteristics of background noise. Doran et al. (2006) utilized a fixed threshold value, a quantity which was higher than the detectable minimum, as well as the residual values from a previous realisation for all sampling places. But these residual values are different for the places close to and distant from the gas source. A higher threshold chosen according to the residual values found close to the source may cause delayed puff arrival detection at places distant from the source. Therefore, this definition does not seem to be suitable for places very differently distanced from the source. This problem can be resolved by utilizing different thresholds at different places (e.g., Chaloupecká et al., 2016). Laboratory

concentration time series are very often measured by a fast flame ionisation detector. The detector can suck in a dust particle, thereby causing a false registration of a few very high concentration values in the time series. Looking at only one value, while searching for arrival time within a time series, can lead to incorrect values. Doran et al. (2007) therefore require the detection of a value of at least the threshold quantity in a specific time interval instead of a single value. But this requirement is problematic because of the concentration time series intermittency. Chaloupecká et al. (2016) therefore require the detection of values of at least the threshold quantity, not in the entire time interval, but in a specific percentage of cases instead.

Zhou and Hanna (2007) find the threshold of the realisation by looking at the whole concentration time series. But the cloud arrival could probably be better recognised if we look only at the behaviour of the beginning of the concentration time series. However, the problem is that we do not know at which time, after the gas discharge, the cloud arrives at the detection position and therefore, we cannot use this approach. Instead, we can utilize concentration time series registered before the cloud release. This is the central idea of the new method as presented in this paper. Moreover, we compare the results with other methods applied to the same dataset. This comparison is important, since widely different arrival time definitions lead to different results but no comparative study (as far as the authors know) exists.

In the paper, the experimental set-up and the data analysis is described in the section Materials and Methods. In this section, all the methods used for determining puff arrival time (visual method, threshold method utilizing residual concentration, dosage method, and threshold method utilizing the value of detected maximum concentration) are described. The Result section, which follows Materials and Methods, is divided into five subsections. The visual method is dealt with in the first subsection. The results of this method are then used as a comparative tool for the other three methods and are described in the subsequent three subsections. An Overview of the results is presented in the final subsection. Finally, the major outcomes are covered in the Conclusion section.

2.2. Materials and Methods

2.2.1. Experimental set-up

The experiments were conducted in the Laboratory of Environmental Aerodynamics of the Institute of Thermomechanics. The laboratory possesses an open, low-speed wind tunnel specialised in boundary layer modelling, with cross-dimensions of 1.5 m × 1.5 m. The

boundary layer is developed in a 20.5 m long section with the use of spires and roughness elements. A boundary layer in 1:400 scale with a neutral stratification was used in the experiments. The modelled boundary layer characteristics agree with the recommendations of VDI (2000) for flows found in cities (Grimmond and Oke, 1999; Britter and Hanna, 2003). The vertical profiles of the mean velocity and the intensity of turbulence of velocity component along the main wind direction at the inlet section are displayed in Fig. 1. In the section, a Prandtl probe used for velocity measurements was positioned at the wind tunnel centreline. Behind this section, the incoming flow comes to a test section, where measurements are conducted.

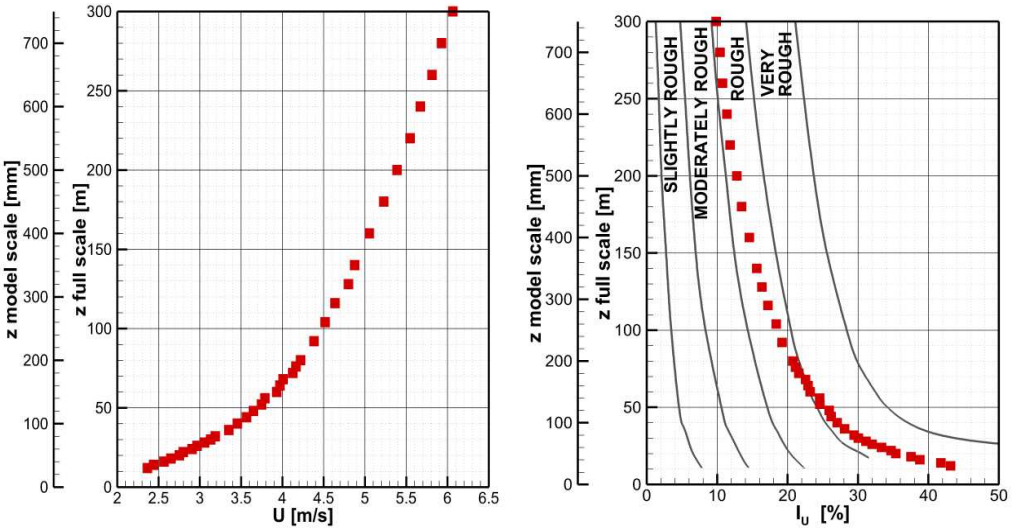

a. Vertical profile of the mean velocity U.

b. Vertical profile of the turbulence intensity I_U with intervals for various roughness classes according to VDI (2000).

Figure 1. Vertical profiles of the mean velocity and the intensity of turbulence of velocity component along the main wind direction U at the inlet section.

To the bottom of the test section, model is fixed. A model of an idealised urban canopy, as found in European city centres (e.g., Heathcote, 2014) and modelled to 1:400 scale (Fig. 2), was used. It consisted of houses which were 63 mm high and 38 mm wide. The houses had pitched roofs. The height of the roofs constituted 13 mm from the height of houses. The houses were organised into 150 mm x 300 mm courtyards (outer dimensions) placed 50 mm from each other. A short-duration, ground-level point gas source with a circular orifice of 4 mm in radius was used in the experiments. The tracer gas discharges were generated by an electromagnetic valve operated by a timer relay. The duration of discharges for majority of the experiments was 1 s. For the experiments with different discharge durations, the duration changed from 0.5 s to 10 s. The constant flow rate within each puff release with

value of 5.6 ml/s of tracer gas was set by a flowmeter. Pure ethane was used as the tracer gas. The placement of the source and measurement positions of concentrations within the model is displayed in Fig. 3. The measurement positions were chosen to cover the changes in puff behaviour with increasing distance from the source in both the parallel street and the transverse street. In the paper, identification codes P for positions along the parallel street and T for positions along the transverse street are used. The concentration time series were measured with a fast flame ionisation detector (FFID) at a human breathing zone (4 mm). The detector response time was measured by a flick test (HFR400 User Guide). The flick test showed that the response time is better than 6 ms (Fig. 4), which is in the estimated order of Kolmogorov and Batchelor time scales (e.g., Roberts and Webster, 2002). During the experiments, data were sampled at 1000 Hz rate and smoothed to 6 ms averages.

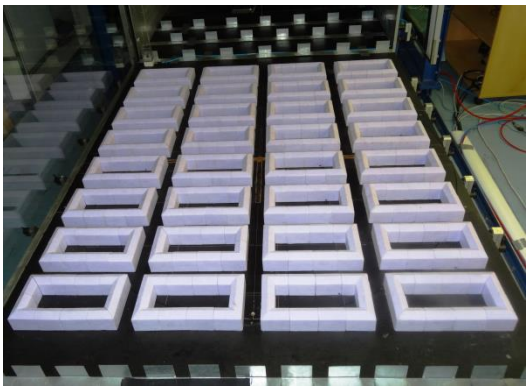

Figure 2. Model of an idealised urban canopy placed in the wind tunnel.

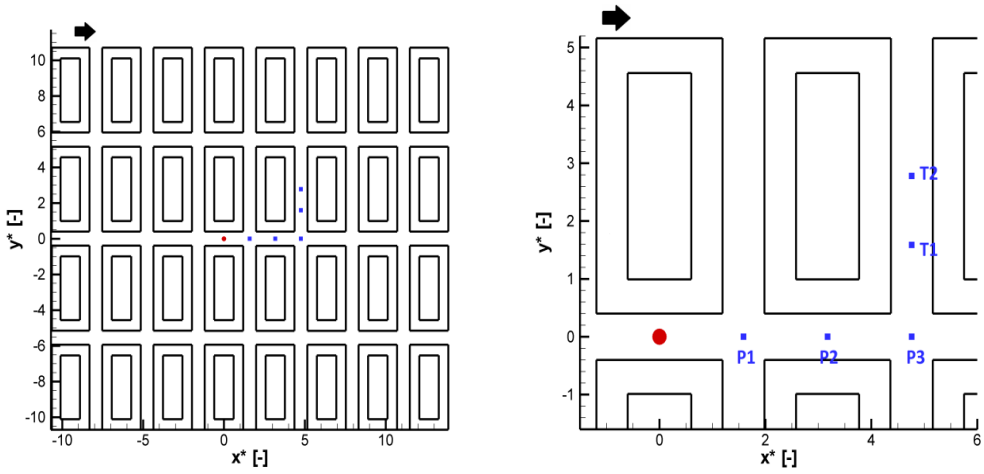

a. Non-zoomed scheme of model. b. Zoomed scheme of investigated area.

Figure 3. Scheme of model, source dimensions in scale (red filled circle – source location, arrow – direction of incoming flow, blue squares – sampling positions with identification codes - P parallel street, T - transverse street).

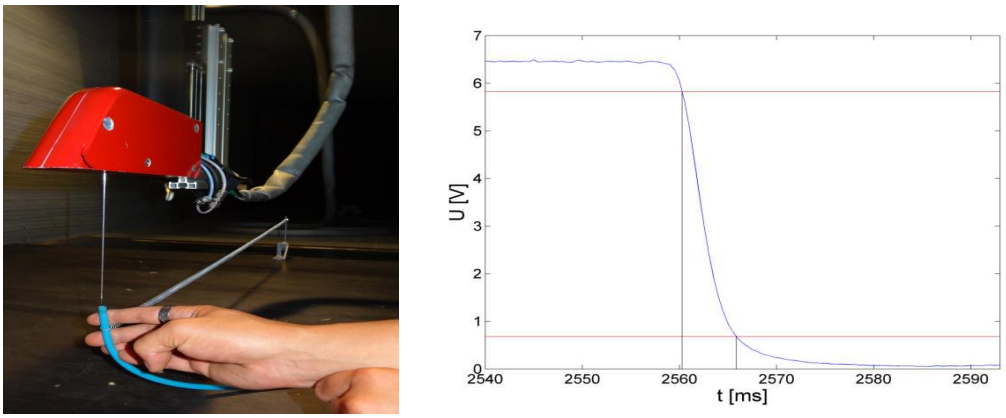

a. Flick test set-up.

b. Flick test results (zero time is set to beginning of constant signal of calibration gas measurement).

Figure 4. Flick test.

2.2.2. Data analysis

The results were converted into dimensionless forms according to relations in VDI (2000). To recalculate coordinates into a dimensionless form, the following relation was used:

$$x^* = \frac{x}{H}, y^* = \frac{y}{H} \quad (1)$$

In this relation, *H* stands for the characteristic height (the height of the modelled houses 63 mm), *x* and *y* are horizontal coordinates. To recalculate the recorded concentration time series into a dimensionless form, the following relation was used:

$$C^* = \frac{CU_{ref}H^2}{Q}. \quad (2)$$

In this relation, U_{ref} stands for the reference speed (measured at the middle height of the wind tunnel), *H* is the characteristic height and *Q* is the source intensity. This relation is valid for a point source (VDI, 2000). The tests of independence of dimensionless concentration values on Reynolds number and on source intensity were conducted to set appropriate experimental conditions. The correctness of the time scaling was checked as well. To recalculate time into a dimensionless form, the following relation was used:

$$t^* = \frac{tU_{ref}}{H}. \quad (3)$$

In this relation, U_{ref} stands for the reference speed, and *H* is the characteristic height.

The concentration time series of each realisation were analysed to obtain the arrival time value. The following methods were used:

1. Visual method

The visual method consists in depicting the time course of the concentration of one realisation into a graph (see Fig. 5 for one such example). From the graph, the time when the gas cloud arrives at the detection position is estimated by direct visual inspection.

2. Threshold method utilizing residual concentration

The new method presented in this paper uses a concentration time series registered before the cloud release. From this concentration time series, the 99th percentile (threshold) is counted. Time after the gas release at which this threshold is exceeded is found and then it is explored how many times this threshold is exceeded in the following time interval Δt = 100 ms ($\Delta t^* \sim 11$). The variable used during exploring is referred to as the intermittency factor (Yee et al., 1994). This variable constitutes the parameter utilized in the method. Yee et al. (1994) define the intermittency factor gamma as a fraction within the searched interval in which a significantly higher concentration above threshold is presented. If the intermittency factor of the explored time interval is higher than the permitted intermittency factor in the definition, the cloud arrival is registered by this method. In this paper, we will show the influence of the chosen value of the permitted intermittency factor on results at different places of measurement.

3. Dosage method

The dosage method utilizes the whole concentration time series of the realisation. The total dosage recorded during the realisation is counted. Then the algorithm searches for the moment when 5% of the total dosage is reached. The corresponding time is considered to be the arrival time in this method.

4. Threshold method utilizing the value of detected maximum concentration

The threshold value can be selected from the time series of a puff signal. Zhou and Hanna (2007) chose a threshold value relative to the recorded peak concentration. They determined

the beginning of the puff as the time when the concentration exceeds a 10% maximum concentration while calculating the puff duration.

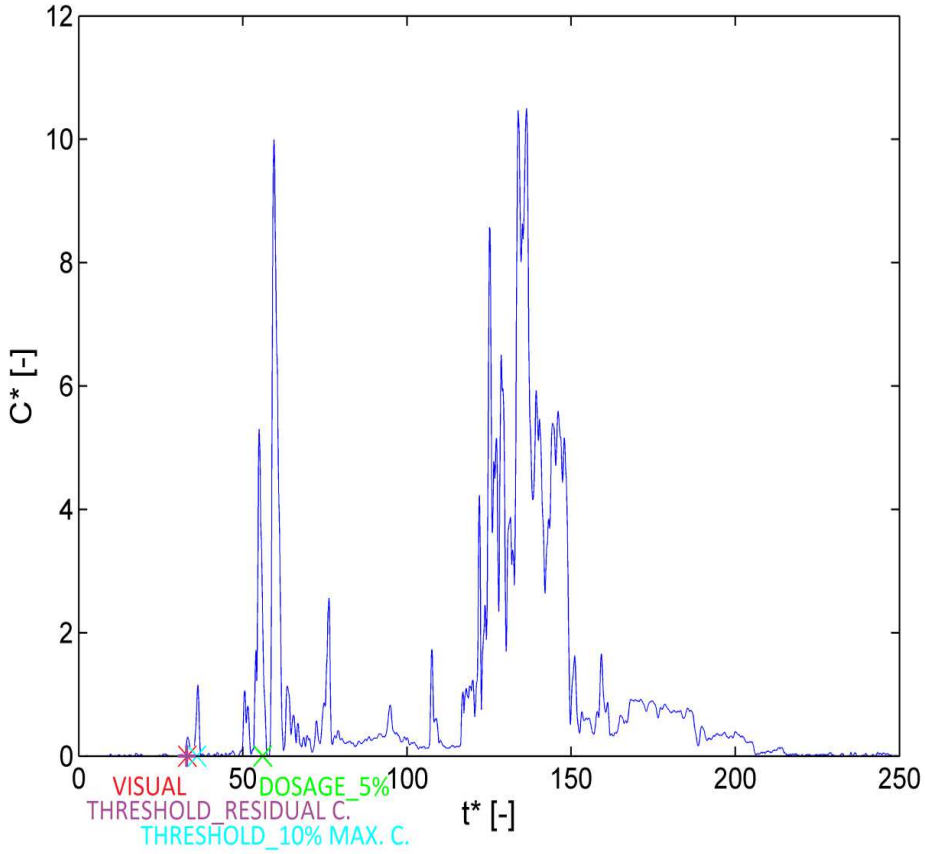

Figure 5. Example of one realisation with marked results for each separate method at the position T1.

The uncertainty of individual arrival times for all the methods is around $\Delta t^* = 0.7$. The automatic algorithm determines the arrival time of gas accurately for the given course of signal according to the given parameters in it. But using the visual method, some kind of subjectivity comes into the determination of puff arrival time. This subjectivity was evaluated as an added uncertainty for each individual arrival time as $\Delta t^* = 2$. At each measurement place, the experiment was repeated around 400 times to obtain a statistically representative dataset. The number of repetitions in the experiments of different release durations was 100. From the dataset, a sample of arrival time was computed. From this sample, the sample statistics were computed, which are visualized by means of box plots in the paper (see Fig. 6 for their structure). The box plots clearly depict the structure of the arrival time samples. In the box plots, 50% of the data are contained in the central boxes. The structure of the rest of the data is displayed by non-outliers, outliers and extreme values. To be able to compare

statistical values from the sample (e.g. a sample mean), its accuracy has to be estimated. The most common traditional approaches use an assumption of a sample statistical distribution (usually Gaussian). A typical example is the formula for the sample mean, $x = \bar{x} \pm t_p(\vartheta)\frac{\sigma}{\sqrt{n}}$, recommended as the norm by the "Guide to the Expression of Uncertainty in Measurements" (ISO, 1993). For our data, however, the assumptions of these methods are not generally met. Therefore, an alternative approach based on bootstrapping was used. Percentile Bootstrap Confidence Intervals based on 10000 bootstrap samples (e.g., Davison and Kinkley, 1999; Good, 2005 and 2006; Hesterberg et al., 2003) was utilized. In this way derived uncertainties for all utilized methods and selected parameters in the algorithms are written in Table 2.

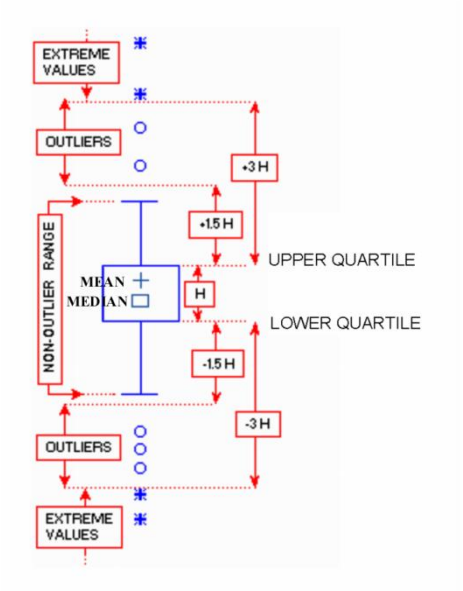

Figure 6. Scheme of boxplot (adopted with modifications from STATISTICA software documentation at http://documentation.statsoft.com).

Instrument	Accuracy	
Model manufactured to 1:400	1 mm	
Instruments placement to a sampling position	1 mm	
Approach flow direction	0.5°	
Cambustion HFR400 Atmosperic Fast FID	Noise	< 1%
	Peak-peak	< 1%
	Time response	< 6 ms
	Calibration	< 1%
Cole-Parmer Flowmeter	+-2% of full scale	
Prandtl tube with Baratron MKS, Type 226A/228A (MKS Instruments)	+-0.5% of full scale	

Table 1. Uncertainty of utilized instruments.

Method			1.	2.	3.			4.		
Value of used parameter			-	0.35	5%	0.09%	0.20%	10%	1%	2%
Position	P	Mean [%]	9	3	2	3	2	2	4	2
		Median [%]	10	4	2	4	3	3	4	3
		Lower quartile [%]	13	4	3	6	3	3	4	3
		Upper quartile [%]	9	5	3	6	4	4	5	4
	T	Mean [%]	6	5	4	5	5	5	5	5
		Median [%]	7	5	5	6, 18	7	5	5, 10	6
		Lower quartile [%]	8	4	4	11, 19	4, 19	5	8	4, 12
		Upper quartile [%]	7	6	5	8	6	5	6	7

Table 2. Uncertainties - 95th confidence intervals (in %) typical for the regions of measurement (P - parallel street, T - transverse street). In the boxes, in which two values are written (because of greater differences between the values), the first value belongs to the point of measurement closer to the source.

2.3. Results

2.3.1. Visual method

The results of the visual approach for five sampling positions are displayed in Fig. 7. The visual method, however subjective, has the advantage over an inflexible computer algorithm in that a human can better make a decision whether or not the observed non-zero concentration in a time series is caused by the presence of a gas cloud. Therefore, its results were used as reference for other automatic procedures. The results of the visual method show that the mean, median, lower and upper quartile of the arrival time, as derived from the datasets, increase as the distance from the gas source grows. The range of arrival time is much wider in the sampling places in the street situated perpendicular to the direction of flow (positions

T1 and T2) than in the street situated parallel (positions P1-P3) where the gas source is placed. Moreover, the data distributions are more asymmetric (skewed right) in the perpendicular than in the parallel street since the upper quartile is farther from the median than the lower quartile and the mean is greater than the median. Apart from the greater distance from the gas source, other reasons might be that the contaminant, in some realisations, gets into the street running transverse to the flow direction at a later time (e.g. because of its keeping in the corner vortex situated in the transverse street just beside the intersection).

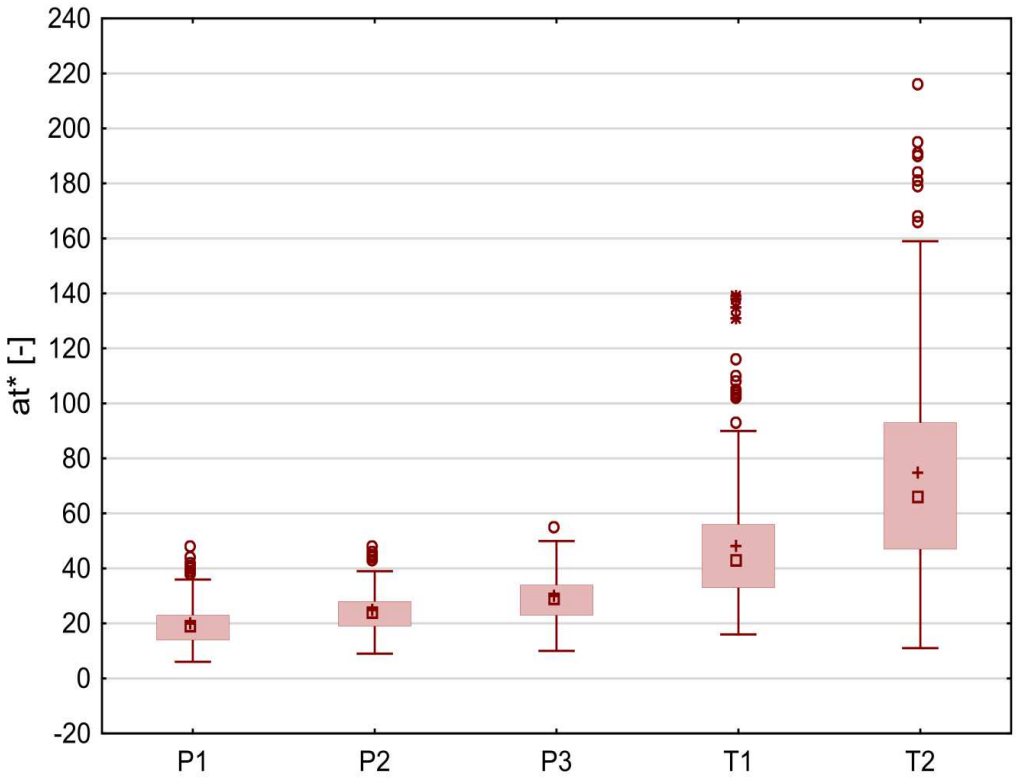

Figure 7. Times of arrival estimated by the visual method

2.3.2. Threshold method utilizing residual concentration

The second approach to the analysis is the threshold method utilizing a residual concentration. Using this approach, what intermittency level is appropriate in the definition must be first explored. For this reason, the results with different intermittency permitted in the definition, as displayed in Fig. 8, are compared with the visual method. The horizontal axis represents an intermittency factor gamma in the explored time interval Δt = 100 ms ($\Delta t^* \sim 11$) used in the threshold algorithm. The vertical axis indicates the percentage of cases in which the difference in the individual dimensionless arrival times, as found by both

approaches, is less than two, and which is regarded as an acceptable difference. In the graph, one can see that the curves first increase to a rather flat maximum and then drop off with the growing intermittency factor. For a higher intermittency factor (gamma approximately higher than 0.6), it holds that the further the sampling place is from the gas source, the higher the percentage of acceptable cases one finds. According to Fig. 8, the behaviour of the concentration time series for these five explored locations at the beginning after the gas cloud arrived can also be assessed. The closer the sampling place is located to the source, the more frequent take turns the moments in which almost no contaminant is detected with those with significant concentrations. At the position farthest from the source, the concentration values are within the explored short time interval after the gas arrival almost steadily above the threshold in many realisations. The curve maximum is reached for the intermittency between 0.3 to 0.4 depending on the sampling place. But the curve maximum is rather flat and not much difference can be detected in the observed percentages for these values of the intermittency factor. The results based on an intermittency factor of 0.35 are used in further analysis.

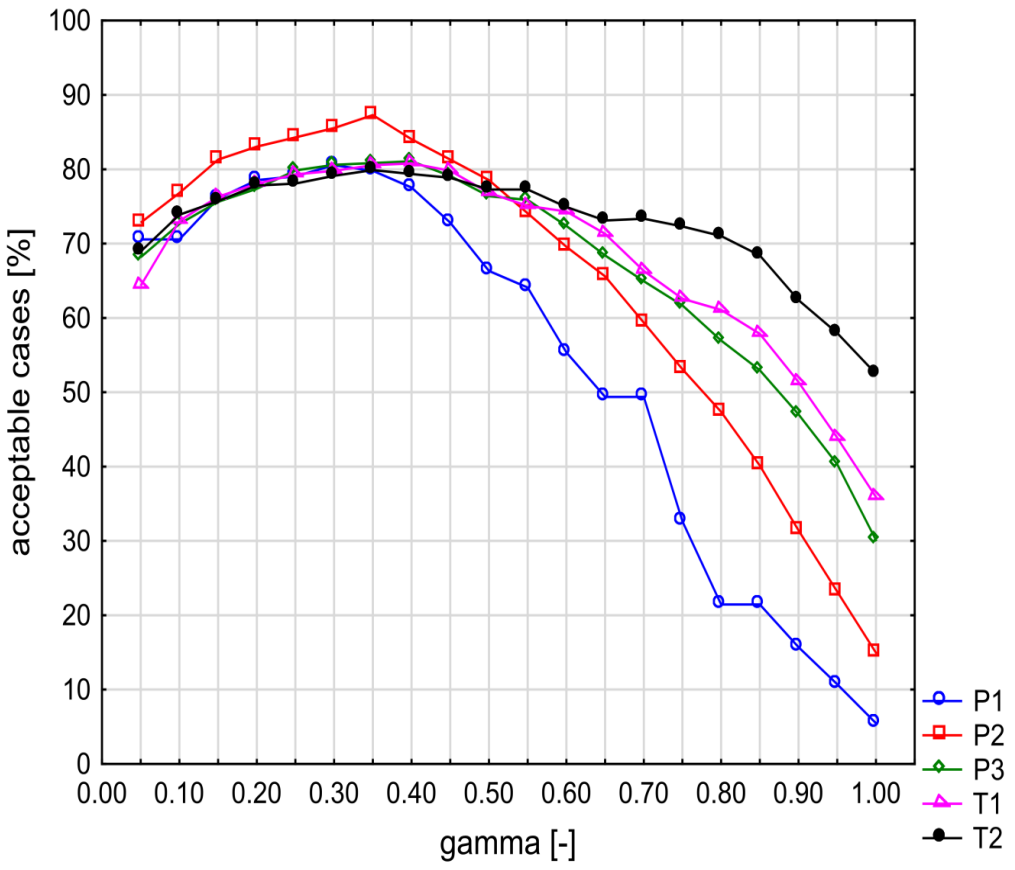

Figure 8. Comparing results of the threshold method with different intermittency gamma with a visual approach.

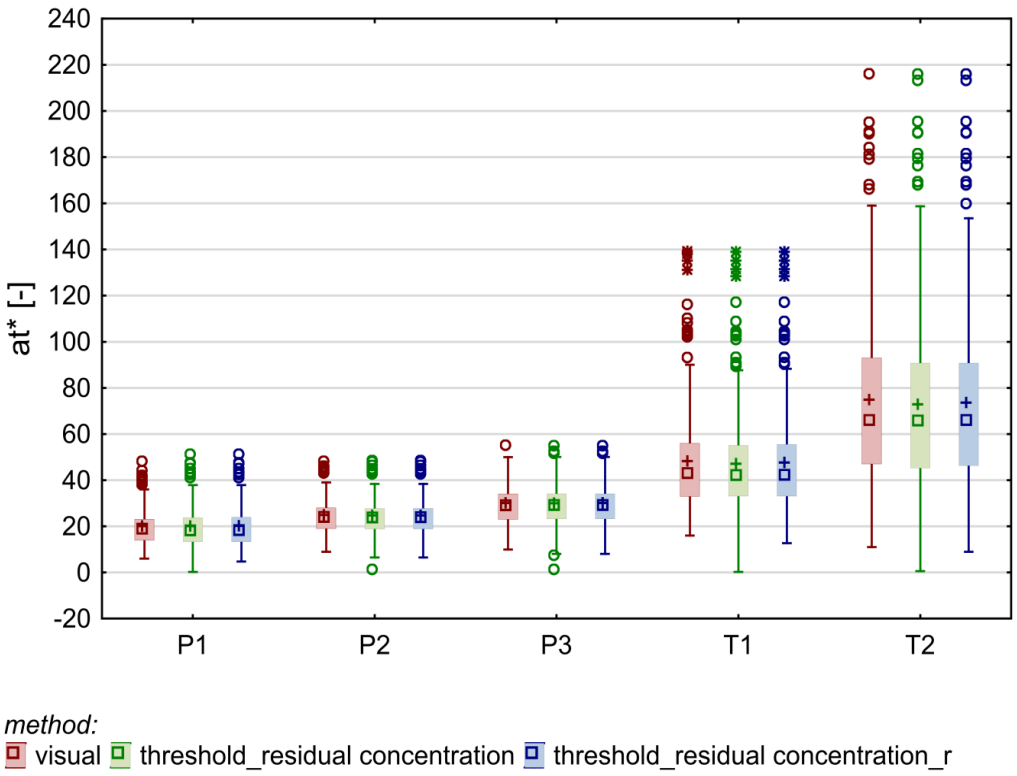

Figure 9. Visual and threshold method utilizing residual concentration.

In Fig. 9, the second box plot from the left for each sampling place displays the results for the threshold analysis utilizing the residual concentration. Compared to the visual approach, the mean, median, lower and upper quartile agree (they overlap in the 95% confidence interval). Apparently, the reason is the similarity in both methods of the approach utilized in the process of finding the arrival time. In the visual method, the graph displaying the time course of concentration at the sampling place beginning with the time of the gas cloud's release is explored. The knowledge of background concentrations level prior to the gas cloud's arrival in determining the puff arrival time is used, as in the threshold approach, using the 99th percentile of the time series prior to the gas discharge. A disadvantage of this method is that at each sampling position, in at least one realisation, the threshold procedure gives false — almost zero — gas arrival time to the sampling position. The reason is that concentrations a little higher than the threshold can be found just after the gas cloud release. But the number of such realisations is negligible in comparison with the entire size of the dataset (see scatter plot in Fig. 10 for instance). The values on the upper edge of the box plot (upper non-outlier values, upper outliers and extremes) seem to be more similar than those on the lower one. To improve the results on the lower edge of the box plot, the unreal results can be eliminated by adding a supplementary condition. This condition uses a minimum possible arrival time computed utilizing a uniform linear motion with constant velocity (from a knowledge of mean

wind speed at 3*H*) and the shortest distance of the sampling place from the gas source. Cases with an arrival time lower than the minimum possible are omitted in further analysis. These revised results are displayed in the third box plots from the left in Fig. 9. The revised results also agree with the visual approach in the observed statistics. But the lower edge of non-outliers is now similar with the visual approach.

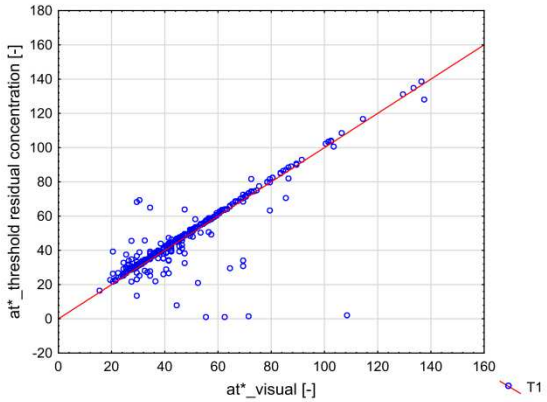

Figure 10. Scatter plot of arrival times according to visual and threshold method utilizing residual concentration.

To verify the independence of the threshold algorithm on a gas release duration, the experiments for durations from 0.5 s to 10 s were conducted. The results are presented in Fig. 11, which displays the same quantities on the axes as in Fig. 8. The appearance of the curves is very similar to those in Fig. 8 (the curves increase to a rather flat maximum and then decrease with the growing intermittency factor). The results reveal that the curves are organized neither increasingly nor decreasingly on the dependence of the gas duration. Therefore, the definition seems to be independent of the gas release duration.

2.3.3. Dosage method

The second to sixth box plot from the left in Figure 9, at each sampling place, shows the results for the dosage method. The second box plot displays the results for the definition of arrival time when 5% of the total dosage is counted. This percentage of dosage is, as far as the authors are aware, always utilized when using this method (e.g. Harms et al., 2009; Baumann-Stanzer et al., 2015). Compared to the visual approach, overestimations of the median, mean and lower and upper quartile of the arrival times are seen in all sampling positions. Only the upper outliers and extremes in the observed positions in the transverse street in Fig. 12 seem to be similar with those found by the visual approach compared to the same quantities for the positions in the street parallel to the flow. One reason may be the longer mean time interval, beginning with the cloud release and ending with the cloud arrival, to the sampling place. During this time interval, a concentration signal can be detected and

this increases the amount of the counted dosage before the cloud arrival. Another reason might be a decrease in the measured concentration due to the growing distance from the source. Therefore, the amount of the concentration counted before the cloud arrival represents a higher percentage of the total dosage, which is the detector exposed to in the individual realisations. The only quantity that seems to be similar (an overlap in the 95% confidence interval) in both approaches, and at all sampling locations, is the interquartile range. The scatter plots comparing the visual approach and the dosage method with a 5% total dosage utilized in the definition, as shown in Fig. 13, reveals how the results of individual realisations changes with the growing distance of the sampling place from the source. The red line indicates the positions with exactly the same results of the compared methods in the individual realisations. In the parallel street, the points in the scatter plots do not show a thin line shifted above the red line but instead the points generate relatively wide clouds in which just a weak relationship between both methods is seen. At the position within the transverse street closer to the source, a tendency to a linear relationship is seen, especially for the higher values of arrival time. This tendency is even more obvious at the position within the transverse street farthest from the source.

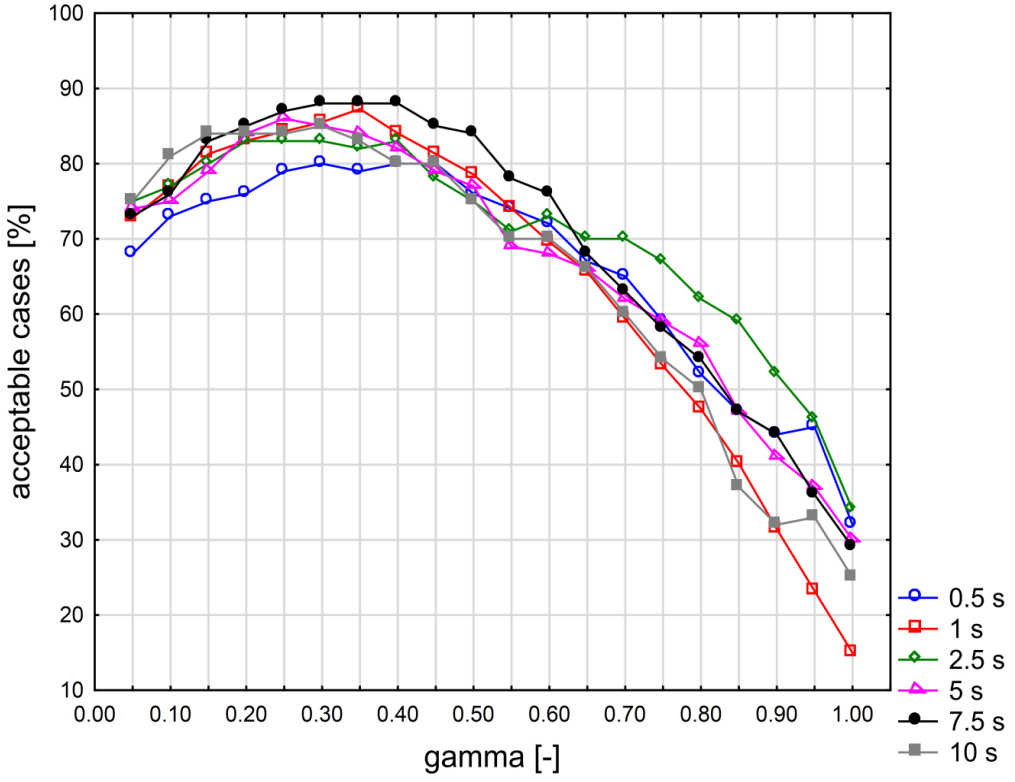

Figure 11. Comparing results of the threshold method with different intermittency factor gamma with a visual approach for experiments with different release durations at position P2.

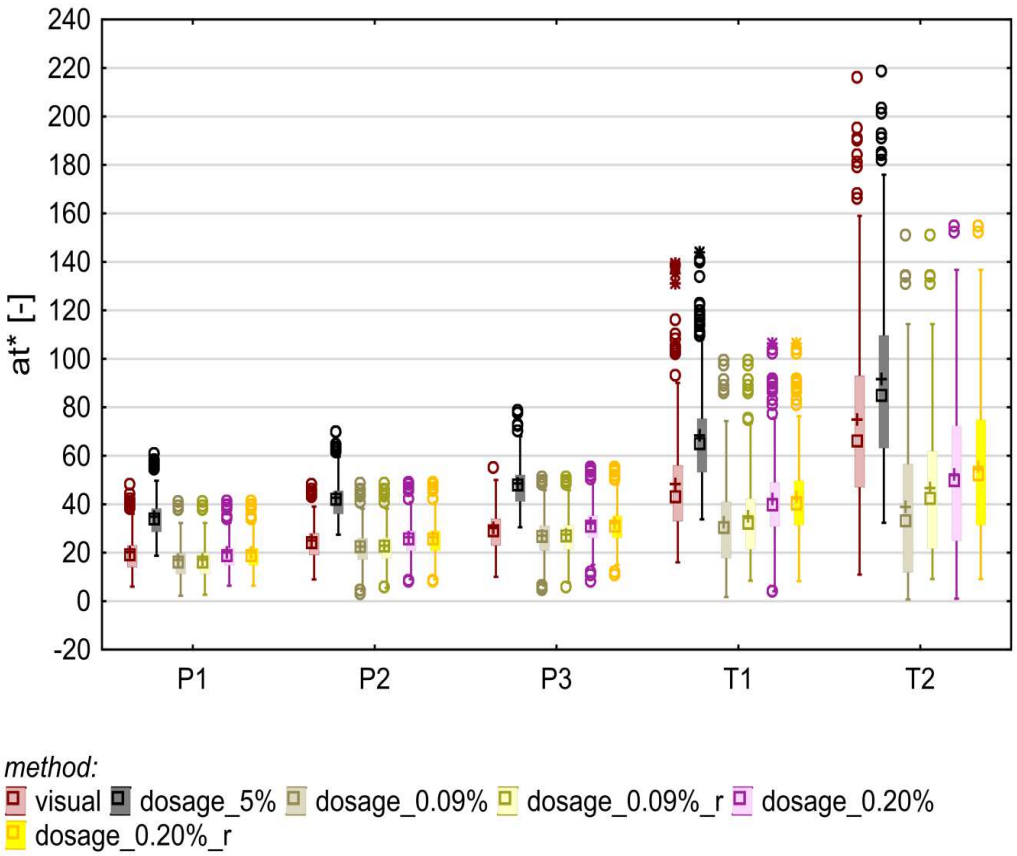

Figure 12. Visual and dosage method.

To find out whether a constant value of dosage is a good approximation for finding cloud arrival time, the percentage of dosage reached at the arrival times estimated by the visual method was calculated. The results (Fig. 14) revealed that the mean as well as median value of the counted dosages is much smaller than 5%. A greater percentage of dosage in the transverse street compared with the parallel street can be found. The largest percentages of dosage are reached in the sampling position farthest from the source. Because these values are extremes of the dataset, the difference between the mean and median value increases. In contrast, a decrease in the maximum percentage of dosage observed within the entire dataset at each sampling place with a growing distance from the source within the parallel street can be seen. At each sampling place, realisations in which almost no gas is detected before the gas cloud arrives can be found.

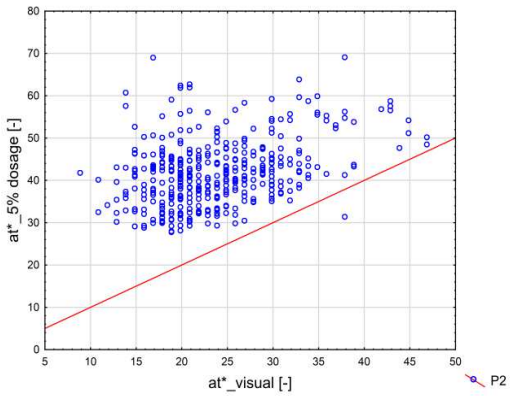

a. Scatter plot for the position P2.

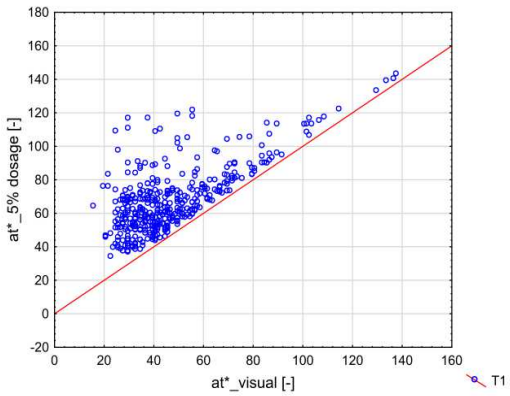

b. Scatter plot for the position T1.

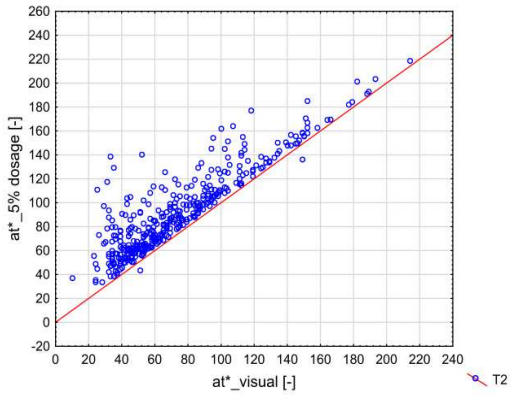

c. Scatter plot for the position T2.

Figure 13. Scatter plots of arrival times estimated by the visual and dosage method with 5% total dosage.

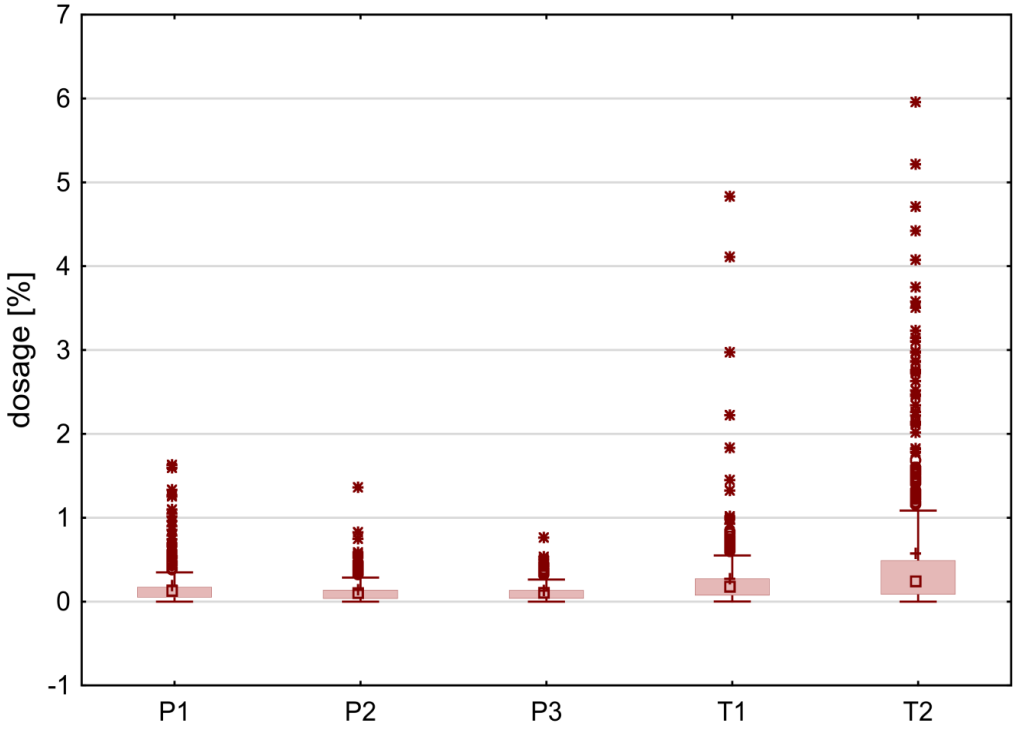

Figure 14. Percentage of dosage for visual method.

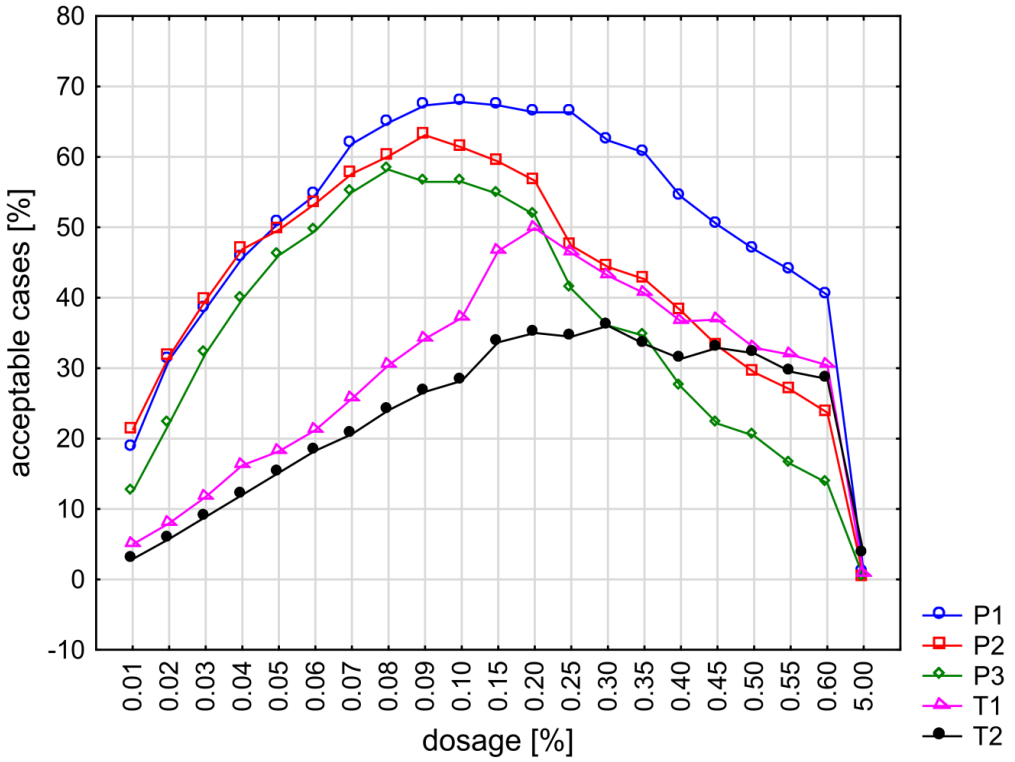

Figure 15. Comparing results of the dosage method with different percentages utilized in the definition with a visual approach.

To find an optimal dosage percentage, a systematic analysis was performed (Fig. 15). Dosage percentage was changed from 0.01 to 0.60 and obtained arrival times were compared with the results of the visual method. Similar to Fig. 8, the results are regarded as acceptable if their dimensionless time difference is less than two. The results for a 5% dosage used in the definition in Fig. 15, similar to Fig. 12, reveals that almost no results match. Only a few agreements are found at the sampling position farthest from the source. This fact can also be estimated using Fig. 14 in which a dosage of around 5% is observed in a few realisations for arrival times found by the visual approach. Various percentages of dosage in the algorithm were also used in order to discover the optimal one (Fig. 15). The optimum is evaluated similarly as in Fig. 8. Dissimilar behaviour of curves for places in the parallel and the transverse street can be seen. For the investigated locations in the parallel street, the results show curves reaching their maximum at approximately 0.1% of dosage in the definition and afterward have a decreasing character (at the P1 position the decrease after reaching maximum is very slow, the maximum is flat). In contrast, the curves displaying the results for places in the transverse street reach their maximum at a higher percentage of dosage utilized in the definition. At the T2 position, the curve seems to be nearly constant along a wide range of investigated percentages of dosage utilized in the algorithm. To sum up, Fig. 15 reveals that the optimum percentage of dosage utilized in the algorithm for the investigated

positions in the parallel street is 0.09. For the places in the transverse street, the optimal choice of dosage is 0.20. This is the percentage at which the curve for the T1 position has its maximum. This percentage is in the range at which the curves of T2 as well as P1 location are nearly at their maximum values. Moreover, Fig. 15 reveals that the further the sampling place is situated from the gas source, the smaller the maximum of the curve is observed. This statement is also true for the range of percentage of dosage from the lowest up to 0.20 utilized in the algorithm.

The third box plot from the left in Fig. 12 displays results for the dosage method with 0.09% of dosage in the definition. The means, medians, lower and upper quartiles within the transverse street are underestimated compared with the visual approach. At the positions within the parallel street, the situation is better. The values of these statistics overlap in the 95% confidence interval at the P2 and P3 positions. At the P1 location, this statement is true only for the lower and upper quartiles. Other observed statistics are underestimated. But according to Fig. 15, this location should agree best with the visual method from the explored locations as the percentage of agreements is the highest from the measured places. This circumstance can apparently cohere with the fact that a large majority of arrival times, from the cases that do not match with the visual approach (approximately 30% of the cases), are underestimated compared with the visual approach. The fourth box plot from the left in Fig. 12, at each sampling place, shows the results utilizing the same analysis as in the third box plot but with the physically impossible results removed. This elimination was created by using the same algorithm as in the previous cases. Comparing the revised results with the visual approach, the biggest differences can be seen at locations within the transverse street. At the T1 location, the number of removal cases is approximately 8%. At the T2 location, this number is much higher – almost 19%. But this improvement in the results is insufficient for the observed statistics of the results to overlap with the visual method in the 95th confidence interval.

The fifth box plot from the left in Fig. 12 shows results for the dosage method when utilizing 0.20% of dosage in the definition. Compared with the case with 0.09% of dosage in the definition, the results seem to be more similar with those found in the visual approach and therefore seems to be the best option of the percentage of dosage choice in the definition. The observed statistics from the datasets (means, medians, lower and upper quartile) overlap in the 95% confidence interval in all sampling positions within the parallel street. Moreover, the median, lower and upper quartile for the T1 position overlap in the 95% confidence

interval as well. The mean of the dataset is underestimated. The only position in which all the observed statistics are underestimated when compared to the visual approach is the position furthest from the source. In the scatter plots in Fig. 16, a tendency to a linear relation between the results of the investigated method can be seen. The number of cases which are significantly different is highest in the transverse street. This situation causes an underestimation of the observed statistics in comparison with the visual approach at the T2 location. In contrast with a 0.09% dosage in the definition, the number of cases eliminated in the revision process is much smaller (2% at T1 and 6% at T2). Just like in the method with a 0.09% dosage, the situation concerning the comparison of the observed statistics with the same statistics of the visual method is the same as in the non-revised case.

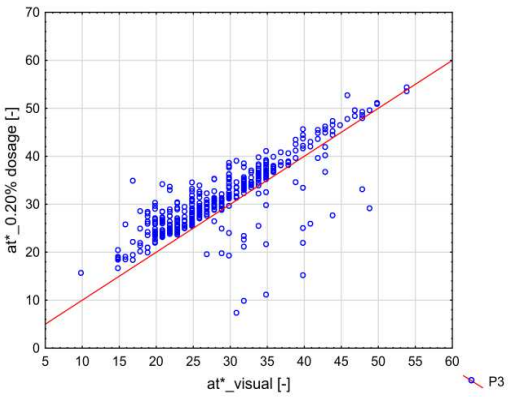

a. Scatter plot for the position P3.

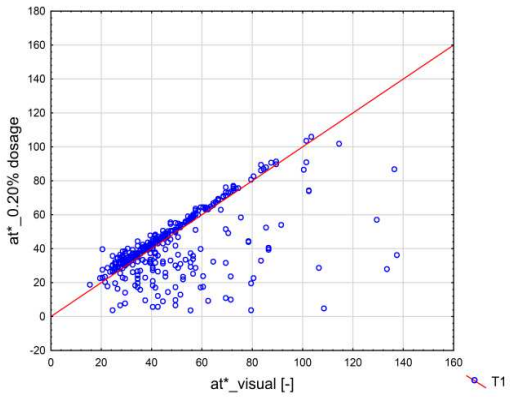

b. Scatter plot for the position T1.

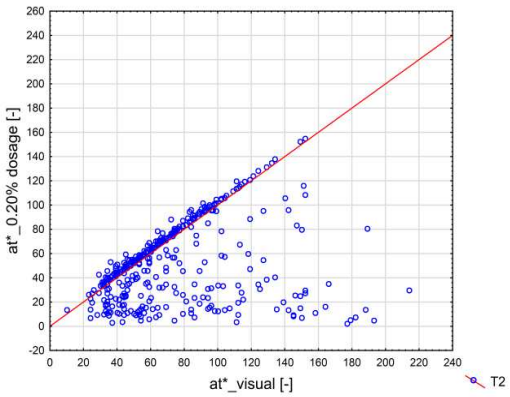

c. Scatter plot for the position T2.

Figure 16. Scatter plots of arrival times estimated by visual and dosage method with a 0.20% total dosage.

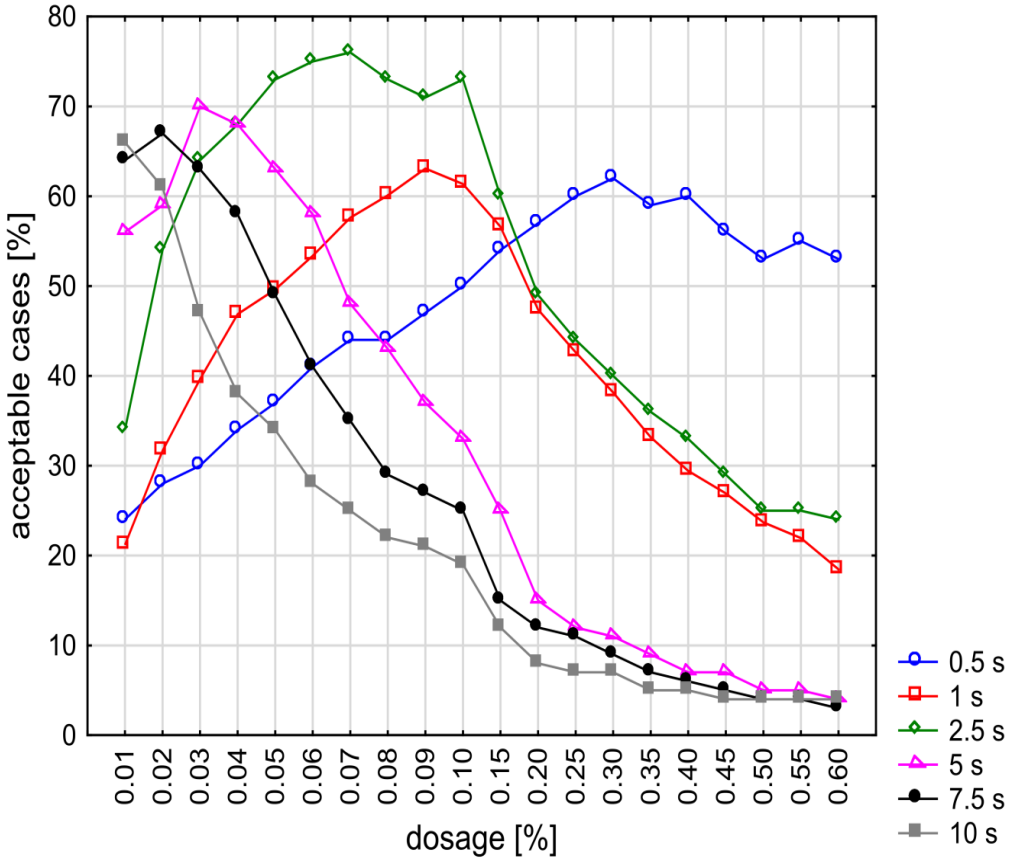

Figure 17. Comparing the results of the dosage method with different percentages of dosage with a visual approach for experiments with different release durations at position P2.

Fig. 17 shows the results for different puff durations. The horizontal axis shows the percentage of dosage used in the definition. The vertical axis displays the similarity of results with the visual approach. The cases are understood to be similar if their dimensionless time difference is less than two. Firstly, a logical conclusion of the utilized definition can be seen. The shorter the duration of the puff is, the higher the percentage of the dosage in the definition is needed in order to reach an optimal result. Secondly, the size of the observed maximum is organized neither increasingly nor decreasingly with respect to the leakage duration. Therefore, the size of the maximum seems not to depend on the duration of leakage. Moreover, for the puffs with longer duration (10 s, 7.5 s, 5 s), a faster decrease in the percentage of cases in which the results obtained by both procedures match after reaching a curve maximum can be seen than for the puffs with shorter duration (2.5 s, 1 s, 0.5 s).

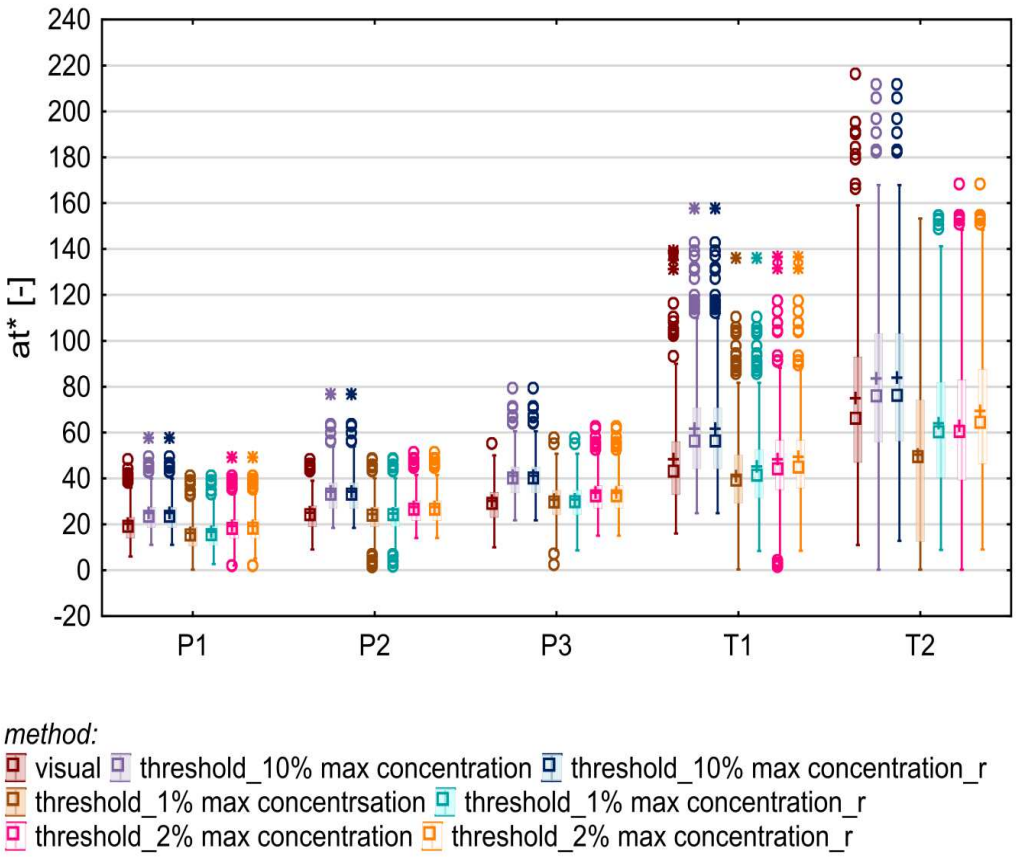

Figure 18. Arrival times estimated by visual method and threshold method utilizing maximum concentration.

2.3.4. Threshold method utilizing the value of detected maximum concentration

The second to seventh box plot at each sampling position in Fig. 18 shows results for the method utilizing the value of the detected maximum. Zhou and Hanna (2007) used 10% of the maximum as one possibility in determining the beginning of the puff. Comparing with the visual method, it should be noted that the observed statistics (mean, median, lower and upper quartile) in the majority of cases are overestimated. Fig. 19 depicts scatter plots for the explored method. At the P1 location, especially at the higher values, a tendency to a linear relationship between the results of both methods is slightly visible. But this tendency cannot be seen in the rest of the locations in the parallel street. In these locations, the points create a wide cloud. In the transverse street, a tendency to a linear relationship is more obvious than in the parallel street. In this method, the unreal results are observed only at the place furthest from the source (see Fig. 18). This slight change in the statistical values at position T2 in the revised method causes that the lower edge of the non-outliers is similar with the visual method.

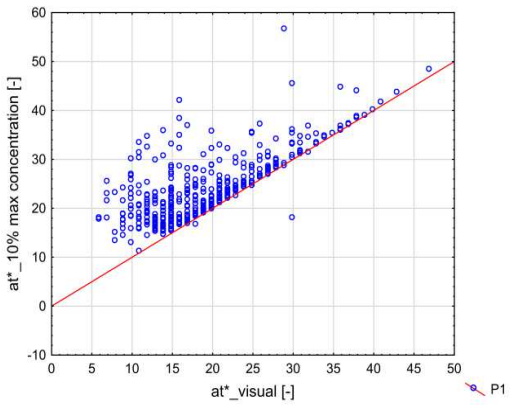

a. Scatter plot for the position P1.

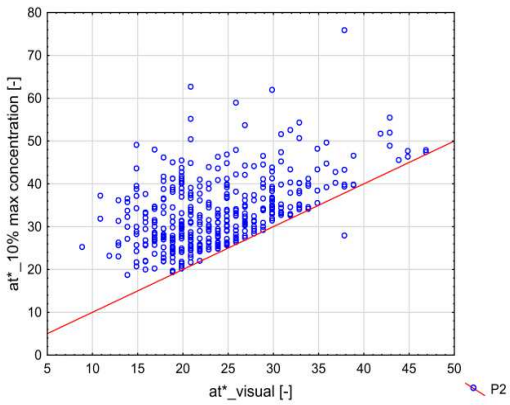

b. Scatter plot for the position P2.

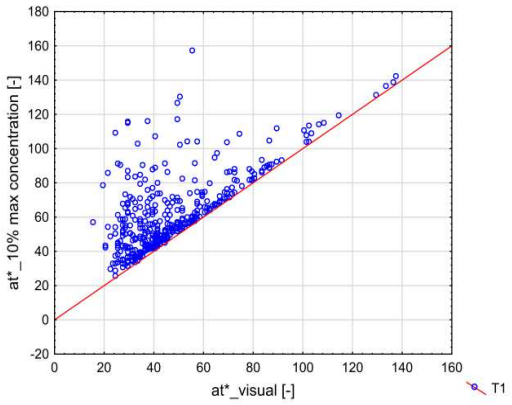

c. Scatter plot for the position T1.

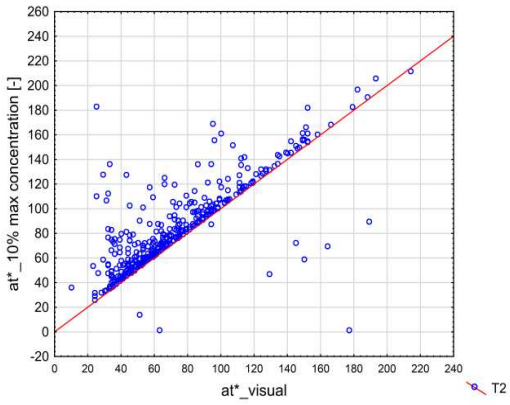

d. Scatter plot for the position T2.

Figure 19. Scatter plots of arrival times estimated by the visual method and a method utilizing a 10% maximum concentration.

Similar to both the dosage method (Fig. 15) and the threshold method, when utilizing the residual concentration (Fig. 8), an optimal percentage of maximum concentration is sought in the definition comparing the results for a different percentage choice with the visual method (Fig. 20). The results of both methods are evaluated as similar if their dimensionless time difference is less than two. In three of the cases, the maximum is reached immediately with the first tested percentage of maximum in the definition. At the last two positions, the maximum is found at the second smallest tested value. These results show that the measured concentrations are in order of few percentages of detected maximum during most realisations at the time when the cloud gets to the explored position.

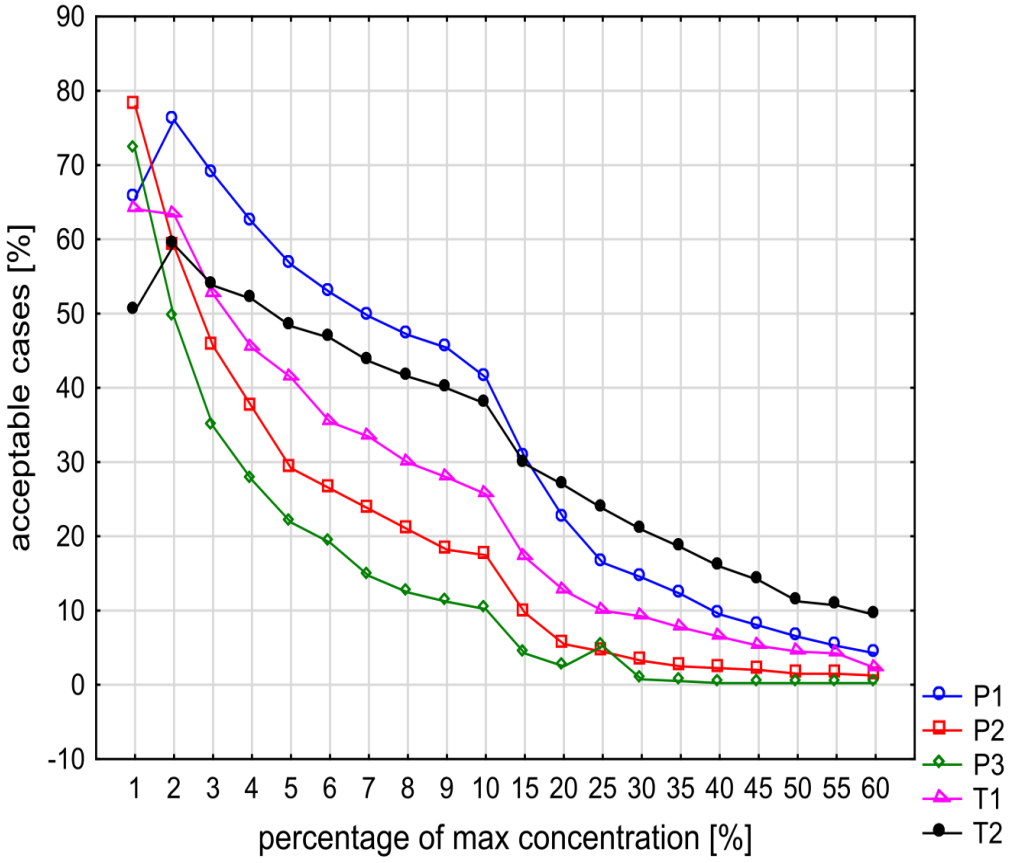

Figure 20. Comparing results of the threshold method utilizing different percentages of detected maximum concentration with the visual method.

The fourth box plot from the left at each sampling place in Fig. 18 shows the results for the method utilizing a 1% maximum concentration in the algorithm for arrival time. The means, medians and lower and upper quartile overlap in the 95% confidence interval at the P2 and P3 locations in the parallel street. But these statistics are, at the location P1, underestimated compared to the visual approach. It is the position in which Fig. 20 reveals the smallest percentage of agreement with the visual approach from the tested locations within the parallel street. But the percentage is still high – approximately 65% of all realisations. The reason is that the majority of the rest of the cases (almost 34%) are underestimated and the number of cases in which the values are smaller than those found by the visual approach but their dimensionless time difference is smaller than two is also very high (approximately 43%). In the transverse street, the only agreements are found at the T1 position for the median and upper quartile. Moreover, the cases in which the cloud gets to the detection position very late when compared with the median value, seem to be similarly evaluated. It is because the 90th percentile, as well as the 95th percentile, of the dataset at the T1 position match with the same statistics of the visual approach. In the rest of the cases, the observed statistics are underestimated when compared to the visual approach. After eliminating the physically

impossible results (approximately 10% of the cases at T1, and 22% at T2), the agreement of the observed statistics in the transverse street is much better (at T1 all these statistics match, and at T2 the only disagreement is the mean).

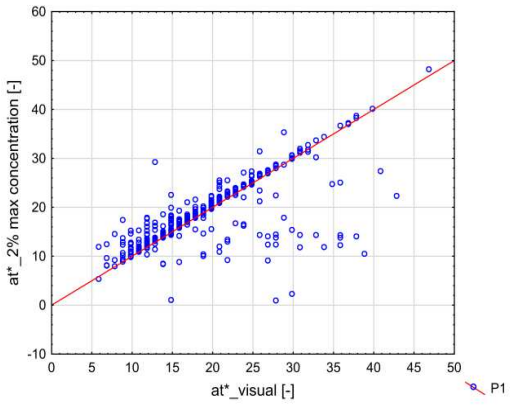

a. Scatter plot for the position P1.

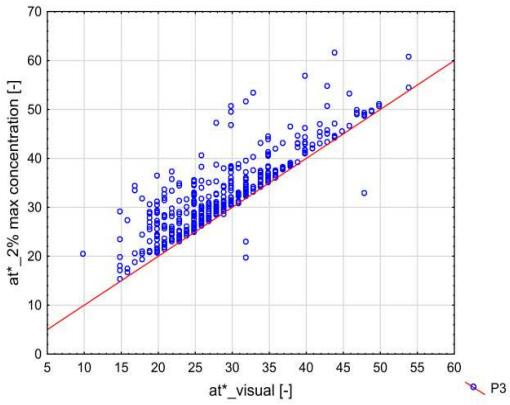

b. Scatter plot for the position P3.

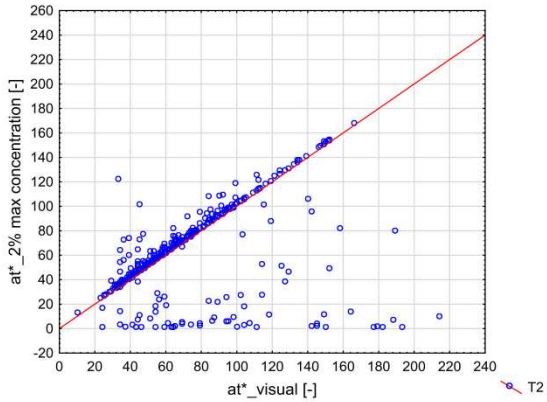

c. Scatter plot for the position T2.

Figure 21. Scatter plots of arrival times estimated by the visual method and a method utilizing a 2% maximum concentration.

The sixth box plot from the left at each sampling place in Fig. 18 shows the results when the definition of arrival time, using a 2% peak concentration, is employed. Utilizing a 2% peak concentration in the definition seems to be the best option since the observed statistical values match with the visual method in most cases out of the examined three possibilities in this type of definition. Within the parallel street, the observed statistics match in the 95% confidence interval with the visual method at the P1 and P2 positions. At the P3 location, this agreement is found only at the upper quartile. The rest of the observed statistics are examined by higher values. Moreover, this algorithm also evaluates the 90th and 95th percentile similar with the visual approach. Though it can be seen that the extreme cases in which the cloud gets to the place of detection very late are examined by an even higher value.

Within the transverse street, all observed statistics are similar to the visual approach at the T1 location. At the T2 position, the agreements are found only at the median and the upper quartile value. The mean and the lower quartile are underestimated. This finding probably coheres with a few false evaluations of near-zero arrival times and at the mean value also with on the contrary underestimation many of more extreme cases in which the cloud gets to the position of detection quite late compared to the median value. This latter fact negatively influences the 90th and 95th percentiles which are also underestimated (but only slightly). The scatter plots (in Fig. 21) show a tendency towards a linear relationship between the visual and the 2% maximum concentration methods. The scatter plot of the P3 location compared with the P1 location reveals slightly higher arrival times when compared with the visual approach. This fact coheres with the findings of the observed statistics discussed above. A revision of the analysis at the T2 location – eliminating approximately 9% of all cases – helps in reaching agreement between all observed statistics, compared to no agreement - except in the upper quartile for the unrevised case (the seventh box plot at each sampling place in Fig. 18).

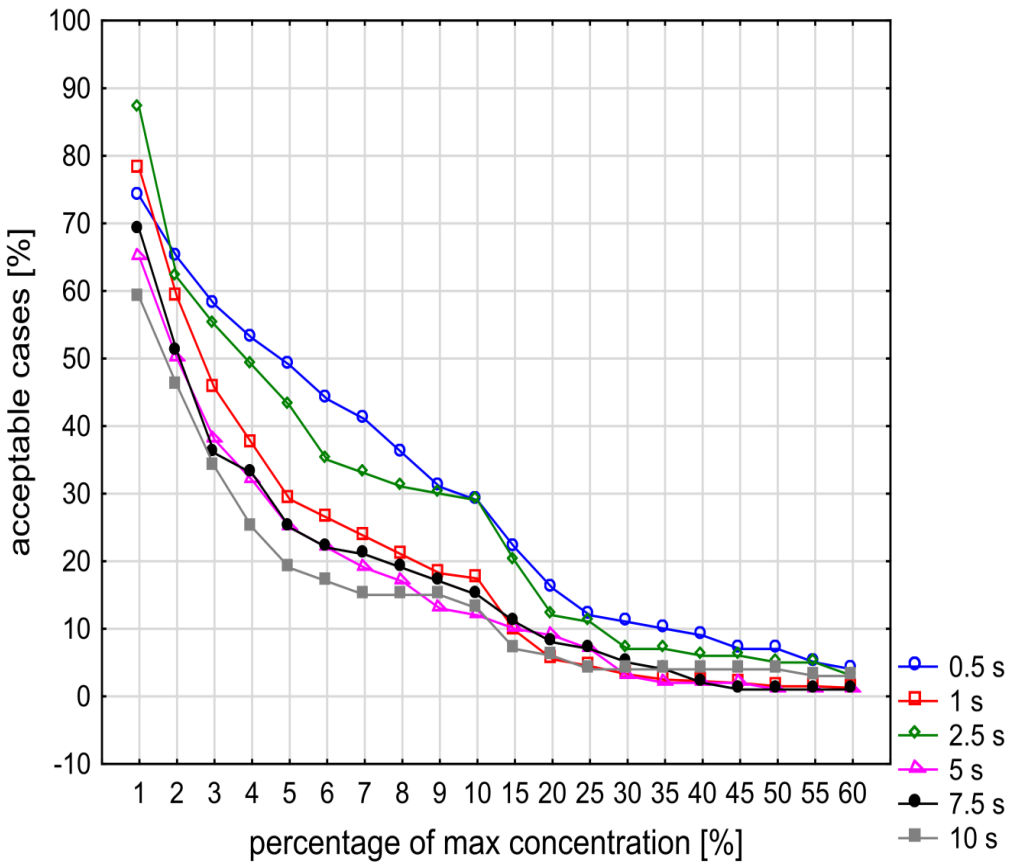

Figure 22. Comparing results of the threshold method with different percentages of maximum concentration with a visual approach for experiments with different release durations at position P2.

Fig. 22 displays the results comparing both methods for different durations of short-duration gas leakages. The character of curve behaviour for all puff durations is very similar. The curves reach their maximum immediately at the first tested percentage of maximum and then decrease as the percentage of maximum concentration utilized in the definition of arrival time increases. Fig. 22 reveals that the curves are organized neither increasingly nor decreasingly dependent on the leakage duration. Hence, the definition of arrival time based on a constant percentage of maximum concentration seems not to depend on the duration of leakage.

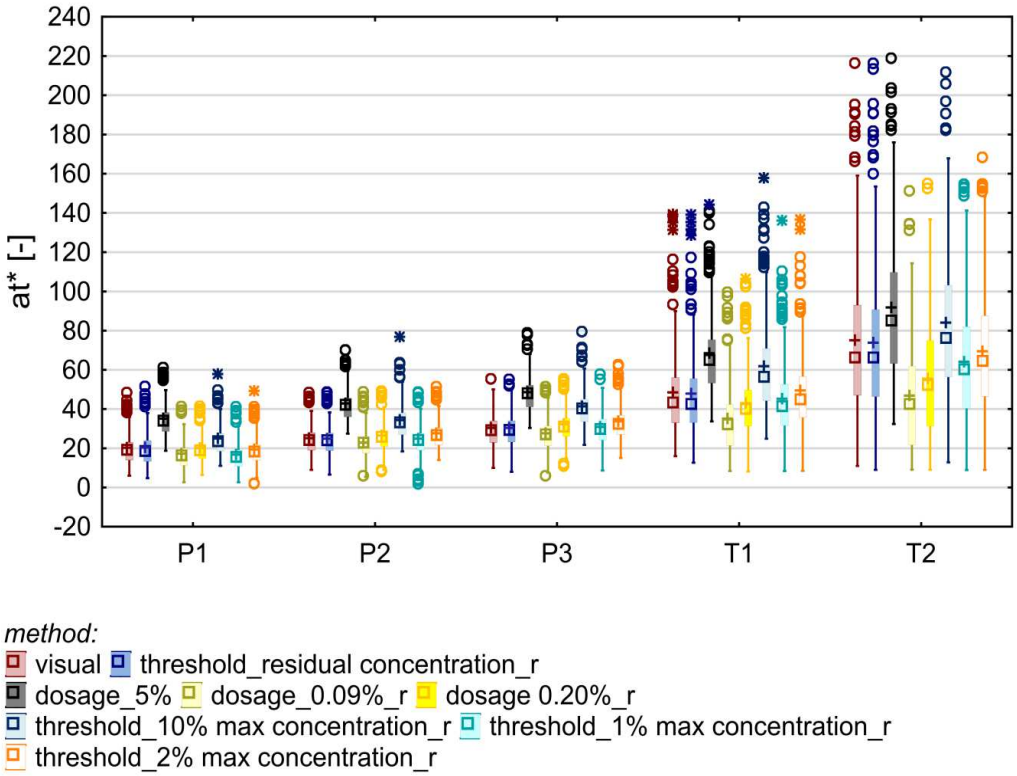

Figure 23. Overview of the results of different analysis methods for estimation of gas arrival time.

2.3.5. Overview of results

Fig. 23 shows all the results of the different methods of analysis with revisions (omitting the unreal results from further analysis - Table 3) in one figure. The threshold method utilizing the residual concentration has the mean, median, lower and upper quartile values at all sampling places similar to the visual method. These values overlap in the 95% confidence interval. The reason is the similar approach used in the analysis of both methods (knowledge of the time series behaviour at the sampling place without cloud presence). The advantage of this approach is that it is the only one, from the observed methods, which can be used

operatively. The other observed methods can be used only as a post-processing tool (a prerequisite of knowledge of total dosage/value of maximum concentration). The disadvantage of this method is the false, near-zero values of arrival time found in at least one realisation at each sampling location. The dosage method estimates of the observed statistics (mean, median, lower and upper quartile) at each sampling place, with 5% of the total dosage used in the algorithm, seem to be overestimated. The values do not overlap in the 95% confidence interval. The scatter plots of the locations within the parallel street reveal that the results are not only systematically overestimated but only a weak relationship between the visual approach and the dosage method with a 5% dosage in the algorithm can be seen instead. Comparing the individual result values with the visual approach, it was discovered that the percentage of the dosage utilized in the definition should be much smaller. Utilizing the optimal percentage of dosage (0.20%), we can see the similarity between all observed statistics at the sampling places within the parallel street. At the position in the transverse street closer to the parallel street, agreement is found only in particular cases. And at the position of detection furthest from the source, all the observed statistics are underestimated. The main cause is probably the longer mean time interval beginning with the cloud release and ending with the cloud arrival to the sampling place. For the explored locations, it holds that the longer the distance from the source, the longer the mean time interval is observed before the cloud arrives to the detector. Another reason might be the decrease in the measured concentration with the growing distance from the source. Therefore, the amount of the concentration counted before the cloud arrival represents a higher percentage of the total dosage which is the detector exposed to in the individual realisations. Utilizing leakages of different durations, a logical weakness of the dosage definition can be seen. The shorter the duration of the puff is, the higher the percentage of dosage is needed in the definition to reach the optimal results. This characteristic of the definition also causes the dependence of the results on the duration of the recorded time series of the realisation. On the other hand, an advantage of the definition is that the dosage gradually changes in time and does not jump as the individual measured concentration values do. The observed statistics in the threshold method, utilizing a 10% peak concentration in the algorithm, are overestimated in the major majority of cases. Seeking an optimal percentage of maximum concentration in the definition reveals that the needed percentage of the maximum concentration is smaller than 10%. Employing the optimal 2% of peak concentration, it is seen that the observed statistics match in the 95% confidence interval with the visual approach at the first two sampling positions closest to the source within the parallel street and in all positions within the transverse street.

At the remaining position, only partial agreement can be found. A disadvantage of this definition is that it is based on only one detected value. But the obtained results show that despite this sensitivity the procedure seems to get sensible results.

position	residual concentration	dosage 5%	dosage 0.09%	dosage 0.20%	peak 10%	peak 1%	peak 2%
P1	0.25%	0.00%	0.50%	0.00%	0.00%	3.24%	0.00%
P2	0.25%	0.00%	0.00%	0.00%	0.00%	1.50%	0.00%
P3	0.50%	0.00%	2.00%	0.25%	0.00%	0.50%	0.00%
T1	1.25%	0.00%	8.23%	2.00%	0.00%	10.22%	2.49%
T2	1.04%	0.00%	18.80%	6.01%	0.52%	21.93%	9.40%

Table 3. Percentage of revisions at sampling positions in various methods (i.e., fraction of cases in which the computed arrival time is lower than the smallest possible one).

2.4. Conclusion

This paper presents a new method of finding the arrival time of a cloud within a concentration time series. This method uses knowledge of a concentration time series prior to a gas cloud's discharge. The reason for such a choice is the analogy between this method and the visual approach (e.g. Yee et al., 1998), in which a human analyses the concentration time series. According to the authors, this manual approach seems to be the most trustworthy since a human can react to the various behaviours of a concentration time series in individual realisations at the sampling places more flexibly than an algorithm. But the visual method cannot be utilized for large datasets. In the visual approach, a human uses the knowledge of the behaviour of the time series before the cloud arrives to reach a decision concerning when the cloud first arrives at the detected location. Utilizing this new method, the 99th percentile of a short time series just before the gas discharge is counted and used as the threshold value. As this threshold is a characteristic of the time series itself, it is needed to require its exceeding in more than one value in the algorithm. Therefore, exceeding of the threshold within a short time interval is demanded. But because of the time series intermittency, it is required at least in 35% of cases. This definition also solves the problem of false cloud identification because of spikes since such episodes are rare and influence only a very small number of measured values.

Moreover, unlike previous studies of short-term gas leakages, this is the first study to utilize more definitions of cloud arrival time on the same datasets - four different techniques were employed (the visual method, the threshold method utilizing the residual concentration, the

dosage method, and the threshold method utilizing the values of the peak concentration in the algorithm). For each of the automatic procedures, an optimal magnitude of its parameter was sought (using the results of the visual method) and used along with the parameter value found in the literature. The results of each automatic method were compared with the visual method. The magnitudes of the parameters found in the literature (5% of the total dosage, 10% peak concentration) turned out to be too high, since the results were overestimated in most cases. Employing the optimal magnitudes of the parameters, the threshold method that uses the residual concentration (with intermittency factor 0.35) showed the highest agreement. The threshold method utilizing the value of maximum concentration (with 2% peak concentration) showed a slightly worse agreement. And the dosage method (with 0.20% of the total dosage) turned out to show the least agreement.

All in all, the paper reveals that the arrival times depend deeply on the method of analysis utilized as well as the parameter used in the method. The choice of these parameters depends on the experiments and should be optimised to the experiment conditions. For example, using the dosage method, the optimal percentage of dosage is dependent on the length of the recorded concentration time series as well as on the duration of the discharge. The inaccurate determination of the arrival time can also affect other puff characteristics such as puff duration, concentration percentiles, and dosage. An example is the 99th percentile of concentration counted from the time interval when the cloud is presented at the place of detection. In the case of an overestimation of the arrival time and in the case at which the concentrations on the leading edge of the cloud are smaller than those in the central part of the cloud, the counted 99th percentile will be higher than the true one. As a consequence, the cloud might be considered more dangerous than it truly is. And what is most important, inaccurate data of arrival time (especially overestimated values) utilized during the development of prediction tools for quick response of emergency services to a leakage of a toxic material can cause fatal damage.

References

Balczo, M., Di Sabatino, S., Franke, J., Grebec, M., Karpinnen, A., Meijer, E., Moussafir, J., Reif, B.P., Tinsrelli, G., Trijssenaar-Buhre, I., 2012. COST – Background and Justification Document, COST Action ES1006.

Baumann-Stanzer, K., Andronopoulos, S., Armand, P., Berbekar, E., Efthimiou, G., Fuka, V., Gariazzo, C., Gasparac, G., Harms, F., Hellsten, A., Jurcakova, K., Petrov, A., Rakai, A., Stenzel, S., Tavares ,R., Tinarelli, G., Trini Castelli, S., 2015. COST ES1006 – Model Evaluation Case Studies, COST Action ES1006.

Britter, R.E., Hanna, S.R.,2003. FLOW AND DISPERSION IN URBAN AREAS. Annual Review of Fluid Mechanics 35, 469-496.

Chaloupecká, H., Janour, Z., Nosek, Š., 2016. Short-term gas dispersion in idealised urban canopy in street parallel with flow direction. EPJ Web of Conferences 114.

Davison, A.C., Kinkley, D.V.,1999. Bootstrap Methods and their Application, Cambridge University Press, USA.

Doran, J.C., Allwine, K.J., Clawson, K.L., Carter, R.G., 2006. 6.2 RETENTION OF TRACER GAS FROM INSTANTANEOUS RELEASES OF SF6 IN AN URBAN ENVIRONMENT. 14th Joint Conference on the Applications of Air Pollution Meteorology with the Air and Waste Management Assoc.

Doran, J.C., Alwine, K.J., Flaherty, J.E., Clawson, K.L., Carter, R.G., 2007. Characteristics of puff dispersion in an urban environment. Atmospheric Environment 41, 3440-3452.

Good, P., 2005. Permutation, Parametric, and Bootstrap Tests of Hypotheses. Springer, USA.

Good, P.I., 2006. Resampling Methods, A Practical Guide to Data Analysis. Birkhäuser, USA.

Grimmond, C.S.B., Oke, T.R., 1999. Aerodynamic Properties of Urban Areas Derived from Analysis of Surface Form. Journal of Applied Meteorology 38, 1262-1292.

Harms, F., Leitl, B., Schatzmann, M., Patnaik, G., 2009. VALIDATING AN LES-BASED PUFF DISPERSION MODEL. International workshop on Physical Modelling of Flow and Dispersion Phenomena.

Harms, F., Leitl, B., Schatzmann, M., Patnaik, G., 2011. Validating LES-based flow and dispersion models. Journal of Wind Engineering and Industrial Aerodynamics 99, 289-295.

Harms, F., Hertwig, D., Leitl, B., Schatzman, M., Patnaik, G., 2013. CHARACTERIZATION OF TRANSIENT DISPERSION PROCESSES IN AN URBAN ENVIRONMENT. 14th Conference on Harmonisation within Atmospheric Dispersion Modelling for Regulatory Purposes.

Heathcote, E., 2014. The historic mixed-use courtyard buildings of central Europe. Global Property Insight, Financial Times.

Hesterberg, T., Monaghan, S., Moore, D.S., Clipson, A., Epsteinm, R., 2003. BOOTSTRAP METHODS AND PERMUTATION TESTS, In THE PRACTICE OF BUSINESS STATISTICS. W. H. Freeman and Company USA.

Homann, S.G., Aluzzi, F., 2014. HotSpot, Health Physics Codes, Version 3.0, User's Guide, National Atmospheric Release Advisory Center, Lawrence Livermore National Laboratory, Livermore.

HFR400 Atmospheric Fast FID, User Guide. Cambustion Ltd., Cambridge, version 1.0.

ISO, 1993. Guide to the Expression of Uncertainty in Measurement. Prepared by ISO Technical Advisory Group 4 (TAG 4), Working Group 3 (WG 3).

Jones, R., Lehr, W., Simecek-Beatty, D., Reynolds, R.M., 2013. ALOHA® (Areal Locations of Hazardous Atmospheres) 5.4.4: Technical Documentation, U. S. Dept. of Commerce, NOAA Technical Memorandum NOS OR&R 43. Seattle, WA: Emergency Response Division, NOAA..

Orica. https://en.wikipedia.org/wiki/Orica (accessed 28.6.2017).

Pontiggia, M., Landucci, G., Busini, V., Derudi, M., Alba, M., Scaioni, M., Bonvicini, S., Cozzani, V., Rota, R., 2011. CFD model simulation of LPG dispersion in urban areas. Atmospheric Environment 45, 3913-3923.

Roberts, J.W., Webster, D.R., 2002. Turbulent diffusion, in: Shen, H. H. (Ed.), Environmental Fluid Mechanics-Theories and Application, New York: Amer. Soc. Civil Eng., pp.7 - 47.

Varma, R., Varma, D.R., 2005. The Bhopal Disaster of 1984. Bulletin of Science, Technology and Society.

Van der Hoven, I., 1957. Power spectrum of horizontal wind speed in the frequency range from 0.0007 to 900 cycles per hour. Journal of Meteorology 14, 160-164.

VDI - Verein Deutcher Ingenier, 2000. Environmental meteorology Physical modelling of flow and dispersion processes in the atmospheric boundary layer, Application of wind tunnels, VDI-Standard: VDI 3783 Blatt 12, Dusserdorf.

Yee, E., Chan, R., Kosteniuk, P.R., Chandler, G.M., Biltoft, C.A., Bofers, J.F., 1994. Experimental Measurements of Concentration Fluctuations and Scales in a Dispersing Plume in the Atmospheric Surface Layer Obtained Using a Very Fast Response Concentration Detector. JOURNAL OF APPLIED METEOROLOGY 33, 996-1016.

Yee, E., Kosteniuk, P.R., Bowers, J.F., 1998. A STUDY OF CONCENTRATION FLUCTUATIONS IN INSTANTANEOUS CLOUDS DISPERSING IN THE ATMOSPHERIC SURFACE LAYER FOR RELATIVE TURBULENT DIFFUSION: BASIC DESCRIPTIVE STATISTICS. Boundary-Layer Meteorology 87, 409-457.

Zhiyin, Y., 2015. Large-eddy simulation: Past, present and the future. Chinese Journal of Aeronautics 28(1), 11-24.

Zhou, Y., Hanna, S.R., 2007. Along-wind dispersion of puffs released in a built-up urban area. Boundary-Layer Meteorology 125, 469-486.

Zimmerman, W.B., Chatwin, P.C., 1995. Fluctuations in dense gas concentrations measured in a wind tunnel. Boundary Layer Meteorology 75, 321-352.

Acknowledgement

This work was supported by the Czech Science Foundation GA CR - GA15-18964S and the Institute of Thermomechanics, AV CR - RVO: 613899

H. Chaloupecká et al. (2018), Journal of Loss Prevention in the Process Industries 56, 242-253.

3. Sensitivity of puff characteristics to maximum-concentration-based definition of departure time

Hana Chaloupecká[a,b*], Zbyněk Jaňour[a], Klára Jurčáková[a], Radka Kellnerová[a]

[a] Institute of Thermomechanics, Czech Academy of Sciences, Dolejškova 1402/5, Prague, Czech Republic

[b] Faculty of Mathematics and Physics, Charles University in Prague, Ke Karlovu 3, Prague, Czech Republic

Abstract

During a hazardous situation, its dangerousness has to be estimated. An important category of such situations is the one in which hazardous gas clouds are released into the atmosphere. The gas clouds are described by their characteristics at exposed locations. But their values are usually dependent on the parameters utilized in their definitions. Hence, the aim of this paper is to examine how the choice of parameter value in a definition of departure time can affect its value. Moreover, it evaluates how this change influences other characteristics which utilize the departure time in their definitions. To study these situations, wind-tunnel experiments of short-duration gas releases were conducted. The ground-level releases of ethane were performed on a model of an idealized urban canopy. The model was composed of houses with pitched roofs organized into closed courtyards. Concentrations were measured by a fast flame ionisation detector. The experiments were repeated about 400 times at each measurement position to get statistically representative datasets. In the analysis, two departure time definitions, based on a detected maximum concentration with various parameters, were utilized. Moreover, other derived puff characteristics were computed. The results showed that when a suitable range of parameters is used, the differences in mean departure times are significant. In contrast, some other characteristics which use puff departure times in their definitions (e.g. mean dosage) are usually not significantly different.

Keywords: wind tunnel; short-duration gas release; puff; departure time; peak concentrations; dosage.

3.1. Introduction

Environmental disasters are unfortunately inseparable from the history of humankind. In the past, such disasters were mostly caused by earthquakes, volcanic eruptions or tsunamis (e.g., Kozák and Čermák, 2010). One example is the destruction of Pompeii by the Vesuvius explosive eruption in 79 AD (e.g., Luongo et. al, 2003). Nowadays, environmental disasters are often connected with human activities (e.g., Chernobyl accident - Pollanen et. al, 1997; Kuwaiti oil fires - Husain, 1993). Moreover, the number of deaths and damage is increasing, as suggested by Alexander (1999). An important category of human-caused disasters is the one in which radioactive or toxic material is released into the atmosphere (e.g., accidents in the Fukushima Daiichi Nuclear Power Plant in Japan - Chino et al., 2011; Bhopal Union Carbide in India - Varma and Varma, 2005; Flix in Spain - Marco et al., 1998). After the detection of such a disaster, emergency services need to estimate its evolution over time and also its consequences for the environment and people's health. For such purposes, models are utilized (e.g., HotSpot - Homann et al., 2014). These models should give the most accurate results as possible. Hence, they have to be correctly developed. During the development, simulations of such incidents are utilized to validate the models. These simulations are usually performed using physical modelling (e.g., Santiago et al., 2007) or field experiments (e.g., Chan and Leach, 2007).

The results of experiments simulating short-term releases of toxic materials – both from field and laboratory campaigns – are usually concentration time series recorded at individual exposed locations (e.g., Chaloupecká et al., 2017). These data have to be analysed to assess the evaluation of the incident. The results of this analysis are characteristics describing release at the given location (e.g., arrival and departure time of toxic material, ascent time period of concentrations, descent time period of concentrations, dosage). An overview of frequently used characteristics is given e.g. by Zhou and Hanna (2007). Most of these variables are dependent on a determination of the times at which the material gets to and leaves the monitored location. Unfortunately, these times are very difficult to determine. This difficulty is mainly caused by the noise of the detector utilized for concentration measurements, the residue of tracer gas or dust particles sucked into the detector, as suggested by Chaloupecká et al. (2017). Hence, many definitions exist for how to determine them. Chaloupecká et al. (2017) utilized four different types of definitions of arrival time of material on one dataset and suggested the best option for the automatic usage. While the determination of the arrival time is definitely crucial for emergency services, the precise determination of departure time seems not to be as important at first glance. One reason is

that the determination of the ending of the evacuation and the return of people to the exposed regions can be inspected by the direct measurements utilizing detectors at the exposed locations (e.g., Mitchell et al., 2005). The predicted departure time is therefore only a helpful tool, which should estimate the time when firefighters and the army can perform direct measurements at the exposed locations. On the other hand, the value of the departure time enters into the definitions of other variables - e.g. dosage or high percentiles of concentrations. Such variables help to evaluate the hazardous effects of the emergency incident (e.g, Efthimiou et al., 2016; Yee and Chan, 1997).

The aim of this paper is to estimate how slight changes in a method of determination of departure time affects its values and the other derived puff characteristics. The main question we would like to answer is: Is a precise determination of puff departure time important for the evaluation of hazardous effects of an emergency situation, or not? To answer this question, we utilized a definition of departure time based on the last detection of a concrete percentage of maximum concentration in a concentration time series (e.g. Zhou and Hanna, 2007) with various values of percentages in the algorithm. During the analysis, it was seen that this method shows false long departure times in cases where a background signal is noisy (a higher concentration is observed one or more times). Hence, we modified the method to be resistant to this phenomenon. The modified method also utilizes the information of the recorded maximum concentration as the first one. But the difference is that it looks at a difference of local maxima of concentrations during a specific time interval instead of looking at only one value of concentration. This method trades on the fact that concentration levels after a gas cloud departure exhibit almost no change or the change is very slow over time. In contrast, concentration levels change over time much more during the presence of a gas cloud. Investigating the concentration level is aggravated by intermittency, when we detect in a short time interval transitions between high and almost zero concentration values. Therefore, local maxima are utilized in the method. Connecting these local maxima with lines, we create an envelope curve around the concentration time series. Using these envelope data, we can investigate from which time changes in the concentration level almost stop and we set this point in time as the departure time of a gas cloud.

3.2. Materials and Methods

3.2.1. Experimental set-up

The experiments were conducted in an open, low-speed wind tunnel specialised in boundary layer modelling. The boundary layer utilized in the experiments had a scale of 1:400 and a neutral stratification. The modelled boundary layer characteristics agree with the recommendations of VDI (2000) for flows found in cities (Grimmond and Oke, 1999; Britter and Hanna, 2003). More details about the wind tunnel and the boundary layer can be found in Chaloupecká et al. (2017). In the experiments, a model of an idealised city to the scale of 1:400 was used (Fig. 1). The model consisted of 63 mm high and 38 mm wide houses with pitched roofs. The height of the roofs constituted 13 mm of the height of houses. The houses were organised into 150 mm x 300 mm courtyards (outer dimensions) placed 50 mm from each other. A short-duration, ground-level point gas source with a circular orifice of 4 mm in radius was used in the experiments. Tracer gas discharges of 1 s set on a timer relay, which operated an electromagnetic valve, were utilized in the experiments. Pure ethane was used as the tracer gas. The placement of the source and measurement positions of concentrations within the model is displayed in Fig. 2. The measurement positions were set in the street parallel to the incoming flow (parallel street) and to three streets transverse to the incoming flow (transverse streets). The concentration time series were measured with a fast flame ionisation detector (FFID) at a human breathing zone. The detector response time was measured by a flick test (HFR400 User Guide). The flick test showed that the response time is better than 6 ms (see Chaloupecká et al., 2017 for more details). During the experiments, data were sampled at 1000 Hz rate and smoothed to 6 ms averages.

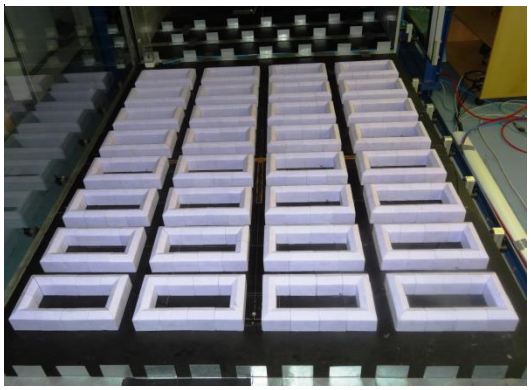

Figure 1. Model of an idealised urban canopy placed in the wind tunnel.

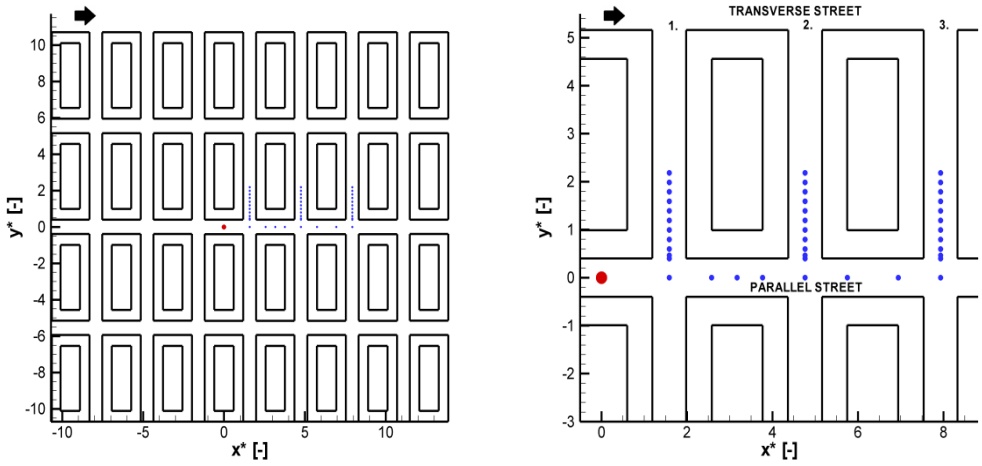

a. b.

Figure 2. Scheme of model, source dimensions in scale (red filled circle – source location, arrow – direction of incoming flow, blue squares – sampling positions): a. non-zoomed scheme of model, b. zoomed scheme of investigated area.

3.2.2. Data analysis

In the paper, the results are presented in dimensionless forms. The following relations as found in VDI (2000) were used to recalculate the variables into a dimensionless form:

- for coordinates

$$x^* = \frac{x}{H}, y^* = \frac{y}{H}. \quad (1)$$

In this relation, *H* stands for the characteristic height (the height of the modelled houses 63 mm), *x* and *y* are horizontal coordinates.

- for concentrations

$$C^* = \frac{CU_{ref}H^2}{Q}. \quad (2)$$

In this relation, U_{ref} stands for the reference speed (measured at the middle height of the wind tunnel), *H* is the characteristic height and *Q* is the source intensity. This relation is valid for a point source (VDI, 2000). Tests of independence of dimensionless concentration values on Reynolds number and on source intensity were conducted to set appropriate experimental conditions.

- for time

$$t^* = \frac{tU_{ref}}{H}. \quad (3)$$

In this relation, U_{ref} stands for the reference speed, and *H* is the characteristic height.

The uncertainty of the instruments used can be seen in Table 1. The experiments were repeated under the same experimental set-up around 400 times to get statistically representative ensembles. Each concentration time series was analysed to obtain puff characteristics (e.g. departure time, dosage). From these values, the ensemble statistics (e.g. mean values, interquartile ranges) were computed. The procedure is depicted in Fig. 3. The uncertainties of the ensemble statistics were computed with the help of an approach based on bootstrapping. We utilized Percentile Bootstrap Confidence Intervals based on 10,000 bootstrap samples (e.g., Davison and Kinkley, 1999; Good, 2005 and 2006; Hesterberg et al., 2003). The uncertainties are depicted by error bars in the Figures in the article. They represent 95% confidence intervals. Lincoln University (2014) defines a confidence interval as an interval within which it can be estimated, with a determined confidence, that the true parameter lies. For the 95% confidence interval of the population mean, this definition can be interpreted that we are 95% confident that the interval contains the population mean (Lincoln University, 2014).

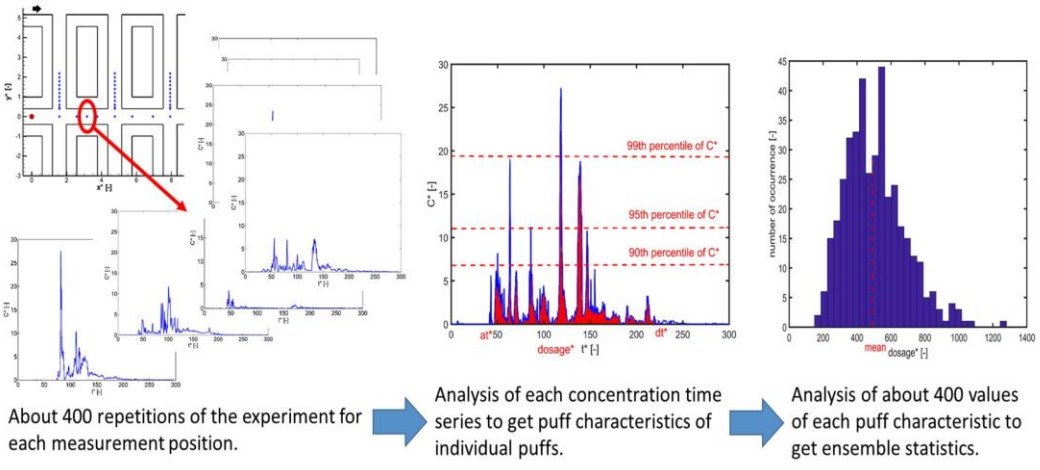

Figure 3. Procedure in measurements and analyses of concentration time series.

Instrument	Accuracy	
Model manufactured to 1:400 scale	1 mm	
Instruments placement to a sampling position	1 mm	
Approach flow direction	0.5°	
DANTEC LDA	0.05 m/s	
Cambustion HFR400 Atmosperic Fast FID	Noise	< 1%
	Peak-peak	< 1%
	Time response	< 6 ms
	Calibration	< 1%
Cole-Parmer Flowmeter	+-2% of full scale	
Prandtl tube with Baratron MKS, Typ 226A/228A (MKS Instruments)	+- 0.5% of full scale	

Table 1. Uncertainty of utilized instruments (adopted from Chaloupecká et al., 2017).

In the paper, we use the following puff characteristics:

3.2.2.1. Arrival time of a gas cloud (*at*)

For definition of arrival time, the method utilizing residual concentrations with intermittency factor 0.35 was used (e.g. Chaloupecká et al., 2017). It is a threshold method which uses the 99th percentile as counted from a concentration time series registered before the cloud release. This threshold has to be exceeded at arrival time value and also at least in 35% values of a short time interval to set the arrival time by the algorithm.

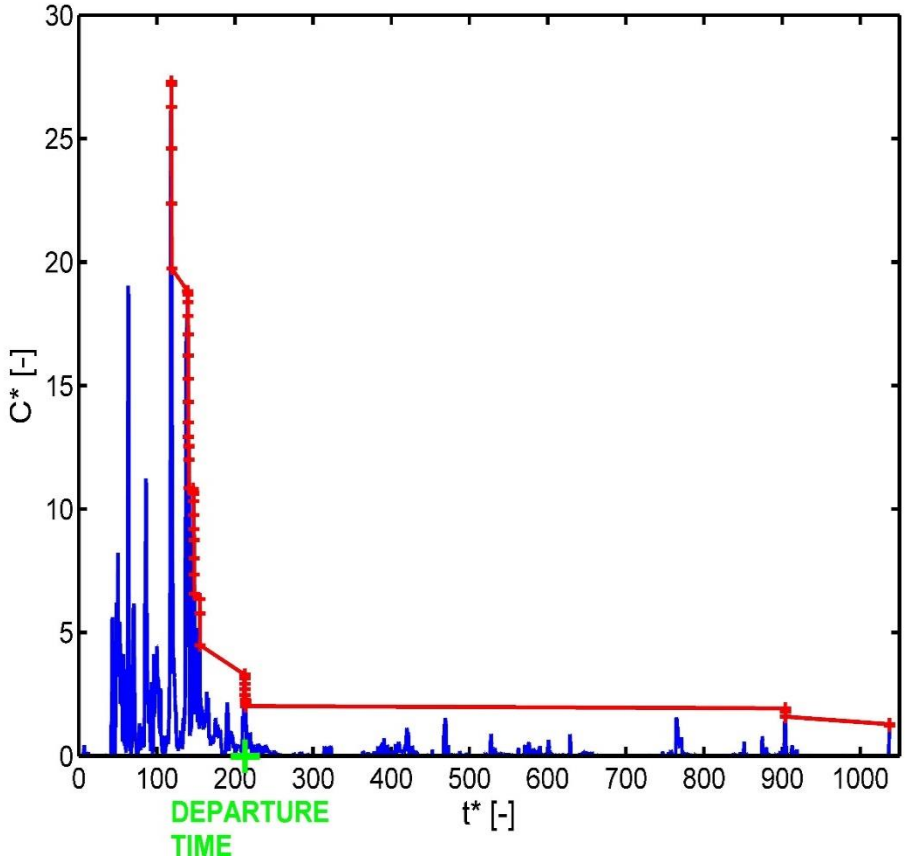

Figure 4. Example of concentration time series analysed by envelope method for puff departure time. The red crosses represent absolute maximum and following local maxima, they are connected by red lines. The green cross shows analysed departure time found with 3% absolute maximum value utilized in the algorithm.

3.2.2.2. Departure time of a gas cloud (*dt*)

a. Threshold method utilizing the value of detected maximum concentration

This method uses a certain percentage of maximum concentration (parameter) registered in the concentration time series as the departure time of a gas cloud (e.g. Zhou and Hanna, 2007).

b. Envelope method

In the envelope method, the absolute maximum concentration detection time and the local maxima as registered after the absolute maximum up to the end of the concentration time series are found (see Fig. 4). The values are checked due to possible false extremely high signal caused by dust particles. They must not be higher than ten times of the 95th percentile of concentrations counted from the time interval Δt^* = 200 with the investigated maximum

as its middle value. Otherwise, they are neglected. These local maxima are then analysed to find a departure time. The algorithm takes the individual local maxima one by one in time from the absolute maximum. For each investigated local maximum, the algorithm looks for the last local maximum registered in Δt^* = 200 distanced from it. If there is none, the algorithm sets the departure time as the time when the investigated local maximum was detected. If such a local maximum exists but the decrease in concentrations between these two values is less than a certain percentage of the absolute maximum concentration (parameter), the algorithm sets the time of detection of the investigated local maximum as the departure time. The time interval Δt^* = 200 was chosen to fulfil two conditions. On one hand, the interval should not be too long because of puff realisations in which a slow decrease of background concentrations can be seen. On the other hand, the value should not be too short because of the cases in which the puff is split into more parts.

3.2.2.3. Peak concentrations (*pc*)

Concentration time series starting with arrival time and ending with departure time were analysed to obtain high percentiles of concentrations. Dekking et al. (2004) defines the 100p-th percentile of a dataset as a value which divides the dataset in two parts in such a way that a proportion p is less than a certain number and proportion 1-p is greater than this number. We counted the 99th, 95th and 90th percentiles of concentrations from these time intervals.

3.2.2.4. Dosage

Dosage (e.g. Baumann-Stanzer et al., 2015) is the amount of concentrations detected during time interval starting with puff arrival time and ending with puff departure time.

In the article, we use a mean value of puff characteristics, which is counted by the following relation

$$mean\ A = \frac{\sum_{r=1}^{n} A_r}{n} \tag{4}$$

In this relation A_r is a value of puff characteristic for one realisation and n is the number of realisations.

To compare the results for a different parameter choice, we use the following variable

$$delta_{mean\ A} = \frac{abs(mean\ A^{3\%} - mean\ A^{6\%})}{mean\ A^{3\%}} * 100 \tag{5}$$

The superscript in percentage represents the value of parameter utilized in the departure time definition.

In the paper, we also depict the results by means of box plots (see Fig. 5 for their structure). The box plots depict the structure of the ensembles of the puff characteristics. The central boxes of the box plots contain 50% of the data. The structure of the rest of the data is displayed by non-outliers, outliers and extreme values.

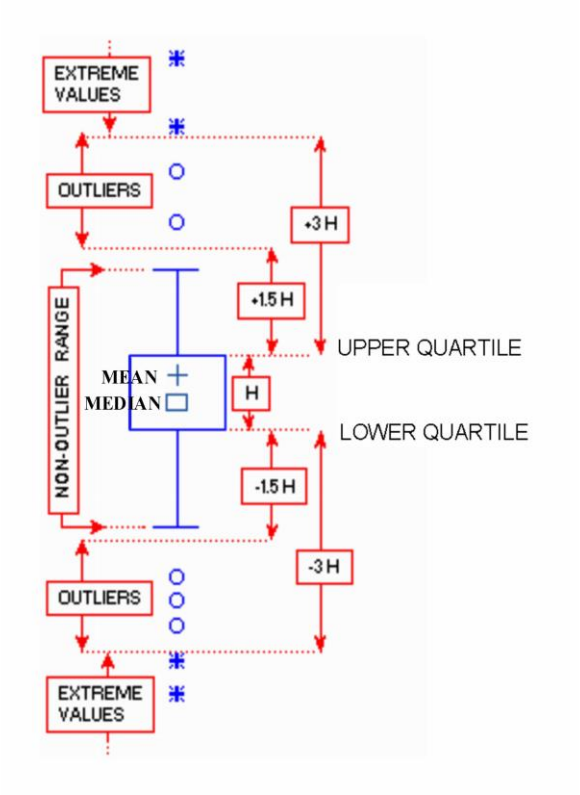

Figure 5. Scheme of box plot (adopted with modifications from STATISTICA software documentation at http://documentation.statsoft.com).

3.3. Results

3.3.1. Threshold method utilizing the value of maximum concentration

3.3.1.1. Departure time

Fig. 6a indicates how the value of departure time varies with changes of the percentage of the maximum concentration utilized in the departure time definition. With an increase in the percentages, the decrease of the value is rather steep at first but then the difference between the neighbouring values becomes smaller. The reason is that the results for low percentages of maximum concentration represent rather the behaviour of the background

concentrations than the gas cloud itself since the departure time is set to the time when we can see only background concentrations in the signal. These background concentrations are caused, for example, by a small amount of hydrocarbons present in the air and sucked into the tunnel from the laboratory surroundings or by tracer gas residue.

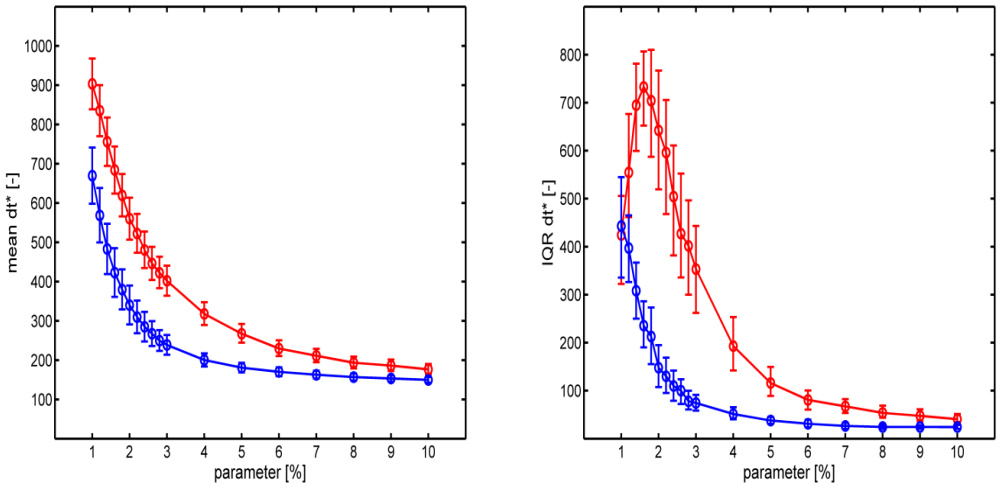

a. b.

Figure 6. Change of mean departure time (a) and the interquartile range of departure time (b) with change of utilized percentage of maximum concentration (parameter) in the departure time definition at two measurement positions.

The change in the behaviour for low and high percentages of maximum concentrations can be also seen at interquartile ranges for departure time, which cover the core 50% of departure times from ensembles (Fig. 6b). The interquartile range behaves dissimilarly in individual positions of measurements for definitions with low percentages of maximum concentrations. In some measurement positions, the value of interquartile range decreases with the increasing percentage of maximum concentrations. In other measurement positions this value at first increases, reaches its peak and then declines. The beginning of the decrease varies at individual measurement positions but it is approximately before 2.6%. Hence, we chose 3% of maximum concentrations - the nearest upper integer - as the lowest percentage of concentrations suitable for an analysis of puff departure time. As the highest suitable parameter, 6% of maximum concentrations were chosen. The reason is the behaviour of the mean differences of the results calculated for two integer parameters following each other. This mean difference is almost constant with further increase of the parameter.

We evaluated the difference between the results found by usage of the lowest and the highest percentage of concentrations regarded as suitable in the departure time definition (Fig. 7). Fig. 7a presents the situation for measurement positions set to a street transverse to the incoming flow (transverse street). The investigated difference varies roughly between 30% and 40% but no trend with respect to the measurement positions is noticeable in the investigated transverse streets. On the contrary, this variable seems to have a decreasing trend in the street parallel with the incoming flow - parallel street (see Fig. 7b). The difference changes from approximately 50% for the measurement position closest to the gas source to roughly only a half of this value at the end of the investigated area in the parallel street. One of the reasons contributing to the observed behaviour might be the vast changes in the value of measured maximum concentrations in the parallel street. The maximum decreases quickly with the increase of the distance of the measurement position from the gas source. Hence, the difference of the concentrations between 6% and 3% maximum is much bigger for the positions close to the source than for the positions relatively far from the source. The other reason might be the difference in behaviour of the concentration time series after the departure of the majority of contaminant with the change of the measurement position in the parallel street. In the positions close to the gas source, from time to time relatively high values of concentrations can be seen. These peaks of the concentrations are sharp and of not very different values, divided by relatively low concentrations. In contrast, we cannot usually spot so quick and frequent changes between small and high contaminant values far from the source. To evaluate this behaviour, we utilized the time interval between the last achievement of 3% and 6% maximum concentrations in the time series. We counted the mean number of percentages in which the value of concentrations exceeds a half from 3% maximum concentrations. This number increases in the parallel street from the position of the measurement closest to the source (14%) to the one furthest from the source (54%). In contrast, such a change in the percentages cannot be seen in the transverse streets. One similarity that is seen for all of the measurement positions is a statistically significant difference (significance level 0.05) in the values of mean departure times with the change in the percentage of maximum concentrations in the departure time definition. Hence, the results of departure time should be handled very carefully when used during an emergency situation or during an interpretation of puff behaviour.

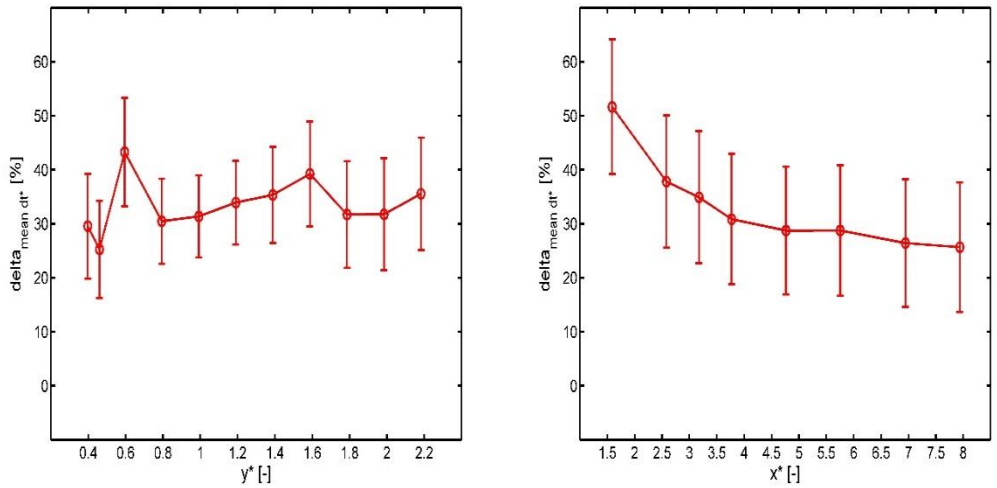

a. b.

Figure 7. Relative difference delta (equation (5)) of mean departure time for transverse street (a) and parallel street (b).

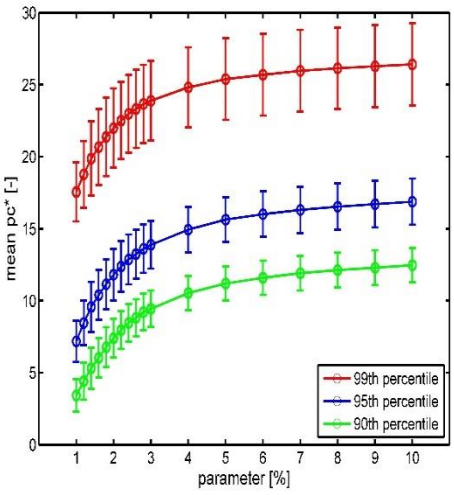

Figure 8. Change of the value of mean high percentiles of concentrations (99th, 95th, 90th percentile) with change of utilized percentage of maximum concentration (parameter) in departure time definition.

3.3.1.2. Peak concentrations

Fig. 8 shows the change of the mean 99th, 95th and 90th percentiles of concentrations with the change of the percentage of maximum concentrations utilized in the departure time definition. The mean high percentiles evince an opposite character of behaviour than the mean departure times. The value of mean high percentiles increases steeply with the increase of the parameter at first but then this increase becomes slower. The increase in the

values between the individual percentages is not relatively so different for the three investigated high percentiles. Hence, studying the percentage changes in the values, this increase is usually the largest for the 90th percentiles and the smallest for the 99th percentiles (see Fig. 9).

Fig. 9 shows how the difference between the high percentiles of concentrations for 3% and 6% of maximum concentrations utilized in the definition of departure time (delta) changes with a change of the measurement location. One can observe a decreasing trend of the variable delta for all three investigated percentiles in the parallel street similarly to the delta for the mean departure time (Fig. 7b). Moreover, an increasing trend is seen for all three investigated transverse streets for the delta of the mean 99th percentiles of concentrations from the position $y^*\approx 1$ and beyond. The position $y^*=1$ roughly corresponds to the mean location of the recirculating vortex edge (e.g., Hunter et al., 1992) located in the transverse street (see Fig. 9a). This statement is also true for the mean 95th and 90th percentiles for the second and third transverse street but not for the first transverse street. This exception might be connected with the uncertainties of the measurements. The delta for the mean 95th percentiles seems to be approximately two times higher than the delta for the mean 99th percentiles. In contrast, such a big difference is usually not seen between the mean 95th percentiles and the mean 90th percentiles. The difference in the values for the 3% and 6% parameter, as used in the departure time definition, is statistically insignificant in all measurement positions except for a few positions in the transverse street closest to the source. In contrast, the same difference calculated for the mean 95th percentile of concentrations is statistically insignificant only in a few measurement positions. The same can be stated about the mean 90th percentile of concentrations but the number of measurement positions in which the investigated difference is statistically significant is even higher. To sum up, the mean 99th percentile of concentrations seems to be a suitable variable to use in describing a hazardous situation thanks to its usually insignificant dependence on the percentage of maximum concentration utilized in the departure time definition in most measurement positions.

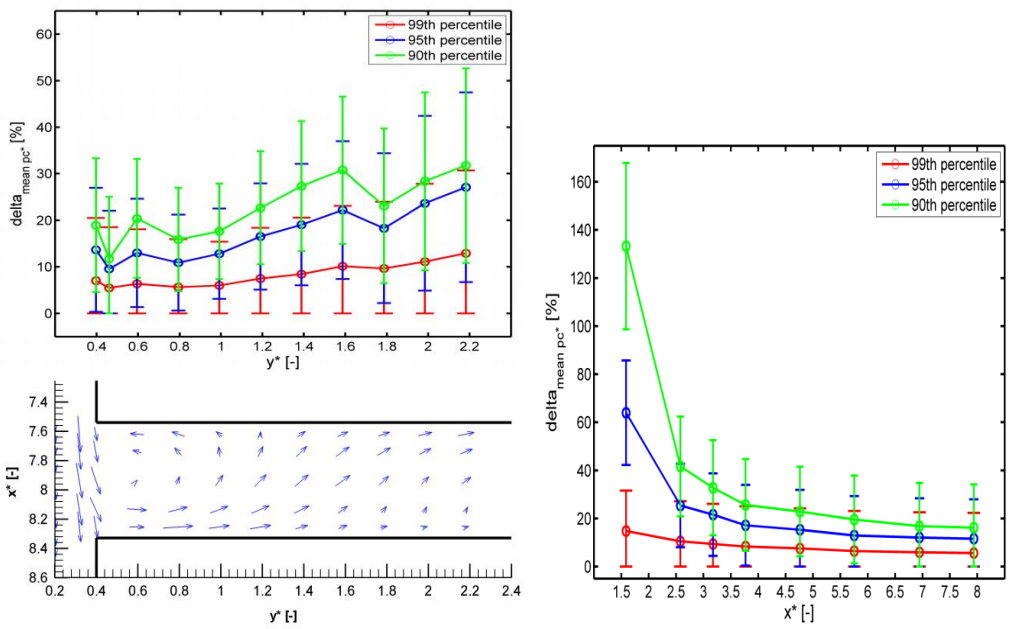

a. b.

Figure 9. Relative difference delta (equation (5)) of mean 99th, 95th and 90th percentiles of concentrations for measurement positions in middle of transverse street with horizontal mean flow (a) and middle of parallel street (b).

3.3.1.3. Dosage

Fig. 10 indicates how the mean dosage varies with different percentage values of maximum concentrations utilized in the departure time definition. Contrary to the mean peak concentrations and mean departure time, the change in the value of mean dosage is not so steep for small percentages of maximum concentrations. Though the percentage change of values decreases with an increase in the percentage of maximum concentrations utilized in the definition, this decrease is relatively not big. The reason is that dosage is an integral variable. The time interval used while calculating the change in dosage value with individual parameters in the departure time definition is bordered by times when individual percentages of concentrations (thresholds) were detected for the last time in the signal. This time interval is relatively long for small percentages of maximum concentrations (e.g. the time interval bordered by the threshold 1% and 2% maximum concentrations). But for bigger percentages (e.g. 7% and 8%), this time interval becomes shorter. In contrast, the detected concentrations are small for time intervals bordered by small threshold values (e.g. 1% and 2%) but they are bigger for the time intervals bordered by bigger thresholds (e.g. 7% and 8%). Hence, the area under the curve of signal bordered by times when the individual percentages of maximum concentrations were detected for the last time changes not so much for small

and bigger percentages of maximum concentrations. This behaviour indicates that no significant change in behaviour is noticeable when shifting from background concentrations to the time when a gas cloud can be seen in the signal in Fig. 10. The other thing that stands the mean dosage apart from the mean departure time and the mean peak concentrations is that the values of mean dosage sometimes overlap in the 95th confidence interval for all tested percentages of maximum concentrations utilized in the definition of departure time (see Fig. 10).

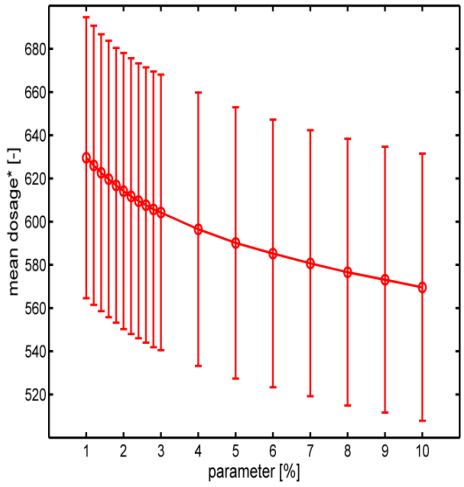

Figure 10. Change of the value of mean dosage with change of utilized percentage of maximum concentration (parameter) in departure time definition.

We evaluated the difference in mean dosage between the results found by the usage of 3% and 6% of maximum concentrations in the departure time definition (Fig. 11). This variable delta seems to have an increasing trend from the position $y^* \approx 1$ in all of the three investigated transverse streets. This situation is similar to the variable delta of the mean 99th percentiles of maximum concentrations (see Fig. 9a). Fig. 11a also shows a horizontal plot of mean velocity vectors in the street to point to the connection of the beginning of the curve increase with the edge of the recirculation vortex in the transverse street. The variable delta does not exhibit any noticeable trend in the parallel street. While the delta changes approximately from 4% to 6% in the transverse streets, its value in the parallel street is less than 4%. The difference between the results with a 3% and 6% parameter in the departure time definition is statistically insignificant in both the transverse streets and the parallel street. It becomes significant in most places only when a parameter value of around 15% and higher instead of 6% is utilized. Therefore, the mean dosage seems to be a suitable variable to use for the rating of hazardousness of a gas release.

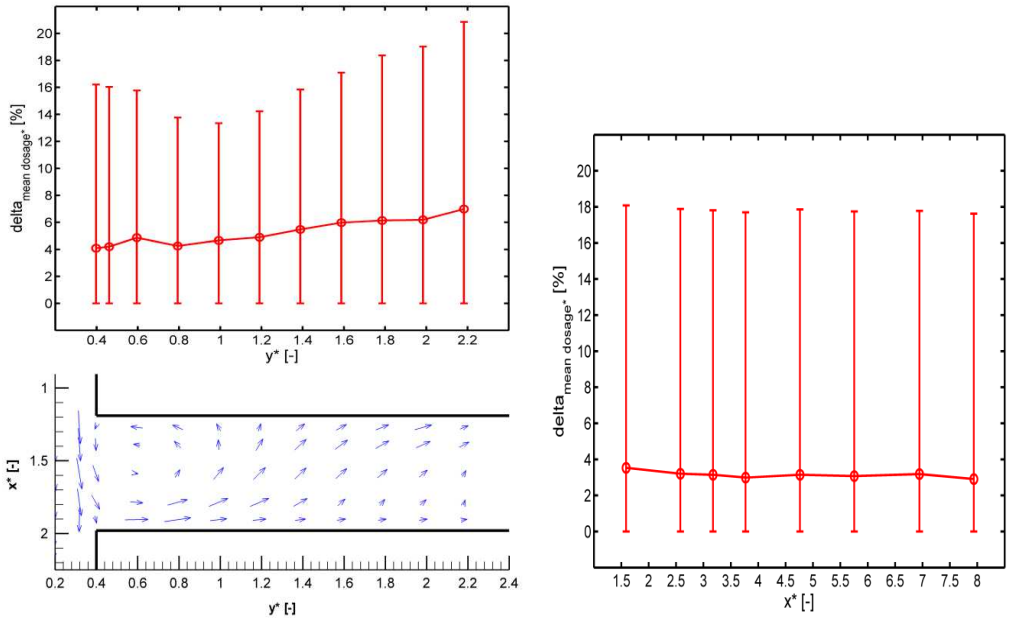

a. b.

Figure 11. Relative difference delta (equation (5)) of mean dosage for measurement positions in the middle of the transverse street with horizontal mean flow (a) and the middle of the parallel street (b).

3.3.2. Envelope method

3.3.2.1. Departure time

Fig. 12a shows a concentration time series of one realisation. The departure time found by the threshold method utilizing maximum concentration with the highest suitable parameter is marked by a violet cross. One can see that the departure time is set very late (dt^*=624) since only low concentrations can be seen from approximately t^*=200. The reason is that this departure time definition cannot cope with background concentrations very well. Therefore we modified this method to be able to get reasonable results in cases as in Fig. 12a. A green cross marks the position of departure time when a 3% maximum concentration is utilized in the modified definition (envelope method). One can see that the departure time is set to the time after which a red line is almost parallel with the horizontal axis until t^*=624 and one cannot therefore distinguish whether the concentrations registered after dt^* set by the envelope method are caused by a gas cloud or residual concentrations. Fig. 12b illustrates how the false values of departure time influence statistics of puff ensembles. The left box plot shows the results for the traditional method with the highest suitable parameter. The box plot on the right shows the results for the envelope method. The parameter value for the envelope method was set to provide departure times similarly to the traditional method

in most realisations. The biggest differences in both methods can be seen at higher values of departure time. While the box plot for the traditional method contains many outliers and extremes, the envelope method has far fewer of such values. These differences at the higher values are the reason that the mean values of both methods do not overlap in the 95th confidence intervals. The same can be stated about the upper quartiles. In contrast, the lower quartiles overlap in the 95th confidence intervals.

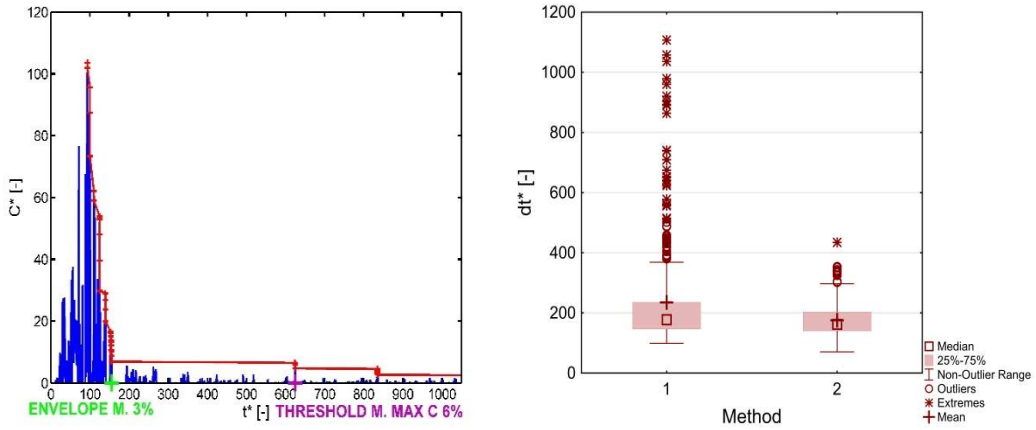

a. b.

Figure 12. Comparing the results of traditional and modified method of departure time definition: a. Example of concentration time series with marked results of analysis: violet cross - threshold method utilizing the value of detected maximum concentration with 6% max C., green cross - envelope method with 3% max C. Red crosses represent absolute maximum and following local maxima and they are connected by red lines. b. Box plots of departure times for traditional method (1) and envelope method (2).

Fig. 13 shows how the results of the mean departure time change with a change of the parameter utilized in the envelope method. In contrast with the previous method (Fig. 6), a transition of behaviour by small and high values of the parameter cannot be seen. Instead, the change in values with an increase of the parameter is rather more gradual, similarly to the mean dosage in Fig. 10. Compared to the first method, the mean values of the departure time are smaller for the same parameter values utilized in the definition. The reason is that the envelope method looks at the differences between concentration values instead of the values themselves.

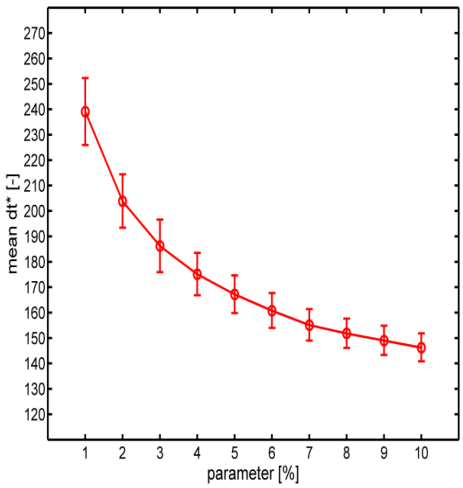

Figure 13. Change of value of mean departure time with change of utilized percentage of maximum concentration in departure time definition.

Taking the same values of parameters (3% and 6%) as in the previous method, the delta is also statistically significant in all measurement positions as in the traditional method but the values of delta are not so high (see Fig. 14). Their values vary from approximately 11% to 20% with respect to a sampling position. Similarly to the first method, no noticeable trend of the investigated difference can be seen in all three transverse streets but a decreasing trend can be spotted in the parallel street.

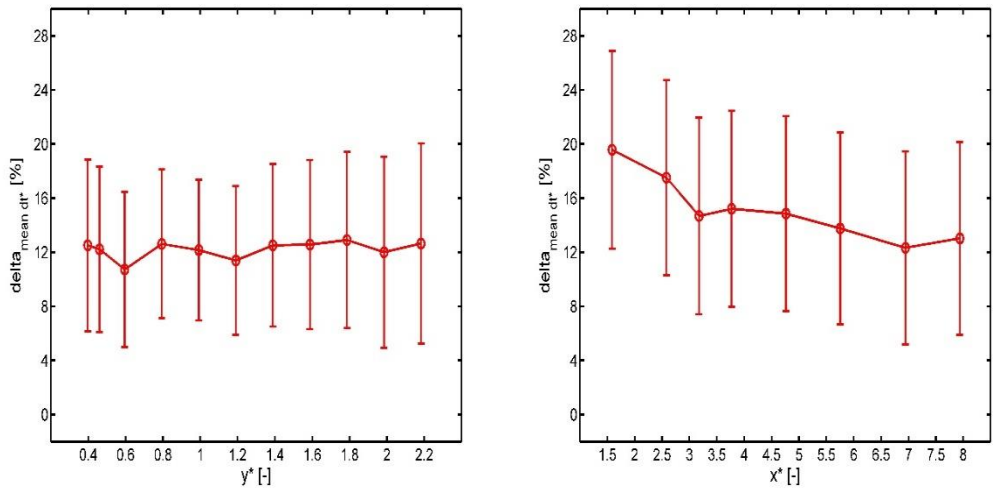

a. b.

Figure 14. Relative difference delta (equation (5)) of mean departure time for transverse street (a) and parallel street (b).

3.3.2.2. Peak concentrations

Fig. 15 depicts the change in values of peak concentrations with the change of percentages of maximum concentrations used in the envelope departure time definition. The character of behaviour of the three investigated high percentiles seems to be similar to the results found by the first method apart from the fact that no steep increase for small percentages can be seen. The reason is the behaviour of the departure time when using the envelope method in which such a steep change for small percentages is also not seen.

Fig. 16 shows the variable delta which describes what variations in values can be expected when 3% and 6% maximum concentrations are utilized in the definition of the departure time. As for the first method, the highest variations can be seen for the mean 90th percentiles and the smallest for the mean 99th percentile. Values of delta vary roughly from 2% to 8% for the mean 99th percentiles in the transverse streets and between 3% and 4% for the positions in the parallel street. They seem to be usually about two times lower than for the mean 95th percentile of concentrations. In contrast, such a big difference between the values is not seen for the delta of the mean 95th and the mean 90th percentile of concentrations. The trends, which were seen for the first method, are not statistically significant in all investigated streets. It is mostly due to variations in the two values furthest from the source for the transverse streets and the value closest to the source in the parallel street. Omitting these measurement positions, similar trends as in the first method can usually be seen. The change in the results, when 3% or 6% maximum concentrations are utilized, is statistically insignificant for the mean 99th percentiles of concentrations in all measurement positions. This difference becomes statistically significant in most values only when the parameter around 30% and higher is utilized instead of 6%. For the mean 95th percentile of concentrations, the difference between the values is statistically insignificant in all positions except for a few positions in the transverse street closest to the source. By the mean 90th percentile of concentrations, statistically significant differences can be found not only in the transverse street closest to the source but also in the parallel street. Therefore, the mean 99th percentile of maximum concentrations is the most suitable variable to describe the dangerousness of a gas cloud from the investigated high percentiles.

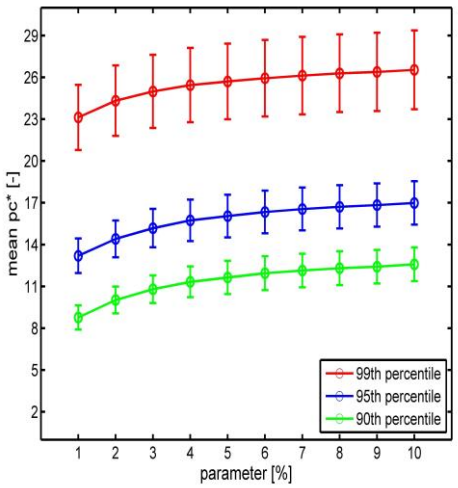

Figure 15. Change of value of mean high percentiles of concentrations (99th, 95th, 90th percentile) with change of utilized percentage of maximum concentration (parameter) in departure time definition.

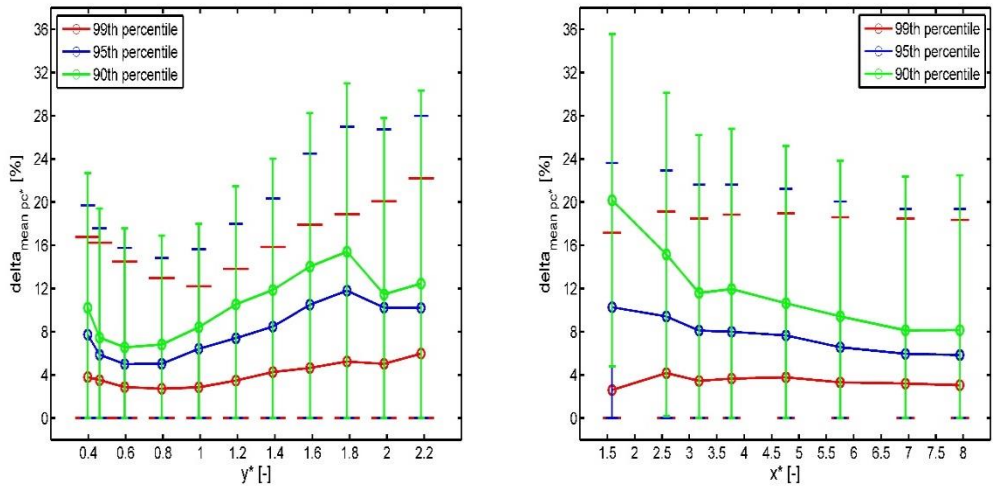

a. b.

Figure 16. Relative difference delta (equation (5)) of mean peak concentrations for transverse street (a) and parallel street (b).

3.3.2.3. Dosage

Fig. 17 indicates how the value of mean dosage varies with a change of the value of the parameter in the envelope departure time definition. One can see that the behaviour of the mean values is very similar to the one seen in the first method (Fig. 10). The values decrease gradually with the increase in the percentage of the maximum concentration and no difference in behaviour for the small and higher percentages can be seen.

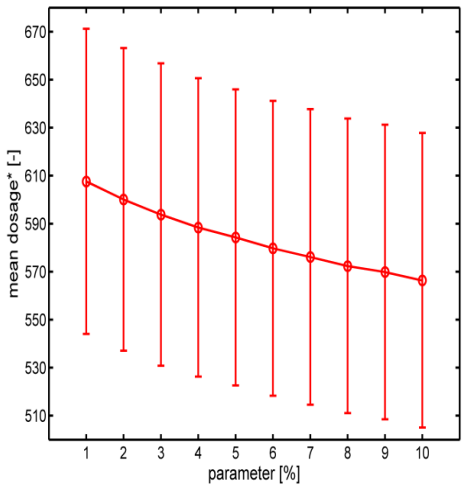

Figure 17. Change of the value of mean dosage with change of utilized percentage of maximum concentration in the envelope departure time definition.

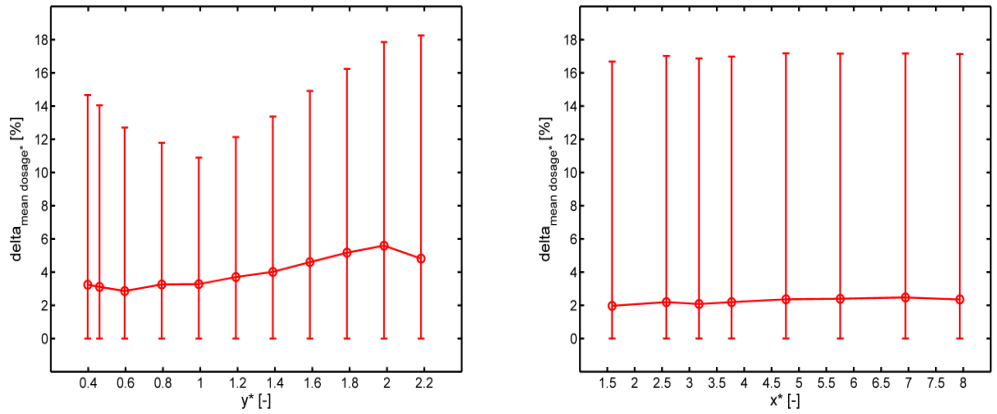

a. b.

Figure 18. Relative difference delta (equation (5)) of mean dosage for transverse street (a) and parallel street (b).

The character of behaviour of the variable delta (Fig. 18) is also very similar to the first method. The mean values vary between 3% and 5% for the sampling positions in the transverse streets. In the parallel street, the delta is roughly 2% for each measurement position. In all sampling positions, the difference between the results found with usage of 3% and 6% maximum concentrations in the definitions is statistically insignificant. It becomes significant in the majority of measurement positions when a parameter value around 10% instead of 6% is utilized. Hence, on one hand mean dosage is a suitable variable to describe the hazardousness of a gas cloud. On the other hand, this variable is not as resistant to a

parameter choice as the mean 99th percentile of maximum concentrations. The main reason is that the mean dosage changes more than the mean 99th percentiles of maximum concentrations when comparing the differences of values for two high parameters used in the departure time definition.

3.4. Conclusions

The paper showed how changes in the value of the parameter in departure time affect its values and the values of derived puff characteristics. We utilized the definition based on a selected percentage of a maximum concentration (parameter). A traditional approach searches for a last detection of the selected percentage of the maximum concentration in concentration time series. But the definition seems to have problems with residual concentrations, which affects not only the departure time of individual realisations but also the statistical values counted from ensembles (see Figure 12 for instance). Hence, we proposed a new method. The new method utilizes the fact that levels of concentrations vary considerably and often when a gas cloud is present at a sampling position. But they are almost constant when a gas cloud is absent. To overcome the effects of the intermittency in concentration signals, this new method uses local maxima, which if connected by lines represent an envelope over the concentration signals. Utilizing the local maxima, this envelope method searches for the time when a gradient in the concentration level becomes smaller than a certain percentage of the maximum concentration (parameter). Comparing the ensembles of departure times for both methods, one can see that the biggest difference is at higher values of departure time where the effect of residual concentrations is crucial (see Figure 12b).

The results of both methods - the traditional and the modified one - showed that the differences in values of departure time, when suitable values of parameters are utilized, are statistically significant. Hence, the results of departure time should be handled very carefully when used during an accident or an interpretation of puff behaviour. In contrast, the situation seems to be better with some other puff characteristics which utilize the value of departure time in their definitions. In high percentiles of concentrations, the situation is dependent on the choice of the concrete percentile. From the investigated percentiles of concentrations, relative differences delta are the highest for the mean 90th percentiles of concentrations. The mean 95th percentiles of concentrations usually have two times higher relative differences than the mean 99th percentiles of concentrations. The mean 99th percentiles of concentrations usually have only insignificant variations in values when the

different parameters are utilized. The same can be stated about the mean dosage. Therefore, these two variables seem to be the most suitable ones in the describing and rating of a hazardous situation. Using these variables, the dangerousness of an accident seems to be rated well even if the departure times are slightly inaccurate.

To conclude, the relatively strong dependence of the departure time on its precise definition means that during a hazardous situation emergency services should not rely so much on the model results of the departure time. But instead, direct measurement by detectors at the exposed locations are the best option according to the authors. In contrast, the variable dosage and the 99th percentile of concentrations seem to be trustworthy variables, since they do not rely as much on the precise definition of the departure time. They can be utilized while evaluating the hazardousness of an accident. These findings will be utilized while developing an emergency model for the Czech Ministry of Interior, which will be used by Czech emergency services (project TACR TJ01000383).

References

Alexander, D., 1999. Natural Disasters, Kluwer Academic Publishers, Netherlands.

Baumann-Stanzer, K., Andronopoulos, S., Armand, P., Berbekar, E., Efthimiou, G., Fuka, V., Gariazzo, C., Gasparac, G., Harms, F., Hellsten, A., Jurcakova, K., Petrov, A., Rakai, A., Stenzel, S., Tavares, R., Tinarelli, G., Trini Castelli, S., 2015. COST ES1006 Model evaluation case studies: Approach and results.

Britter, R.E., Hanna, S.R., 2003. FLOW AND DISPERSION IN URBAN AREAS. Annual Review of Fluid Mechanics 35, 469-496.

Chaloupecká, H., Jaňour, Z., Mikšovský, J., Jurčáková, K., Kellnerová, R., 2017. Evaluation of a new method for puff arrival time as assessed through wind tunnel modelling. Process Safety and Environmental Protection 111, 194-210.

Chan, S.T., Leach, M.J., 2007. A Validation of FEM3MP with Joint Urban 2003 Data. Journal of applied meteorology and climatology 46, 2127-2146.

Chino, M., Nakayama, H., Nagai, H., Terada, H., Katata, G., Yamazawa, H., 2011. Preliminary Estimation of Release Amounts of 131I and 137Cs Accidentally Discharged from the Fukushima Daiichi Nuclear Power Plant into the Atmosphere, Journal of Nuclear Science and Technology, 48 (7), 1129-1134.

Davison, A.C., Kinkley, D.V., 1999. Bootstrap Methods and their Application, Cambridge University Press, USA.

Dekking, F.M., Kraaikamp,C., Lopuhaa,H.P., Meester,L.E., 2005. A Modern Introduction to Probability and Statistics: Understanding Why and How, Springer, London.

Efthimiou, G.C., Andronopoulos, S., Tolias, I., Venetsanos, A., 2016. Prediction of the upper tail of concentration probability distributions of a continuous point source release in urban environments. Environmental Fluid Mechanic, 16 (5), 899–921.

Good, P., 2005. Permutation, Parametric, and Bootstrap Tests of Hypotheses, Springer, USA.

Good, P.I., 2006. Resampling Methods, A Practical Guide to Data Analysis, Birkhäuser, USA - Boston.

Grimmond, C.S.B, Oke, T.R., 1999. Aerodynamic Properties of Urban Areas Derived from Analysis of Surface Form. Journal of Applied Meteorology 38, 1262-1292.

Hesterberg, T., Monaghan, S., Moore, D.S., Clipson, A., Epstein, R., 2003. BOOTSTRAP METHODS AND PERMUTATION TESTS, In THE PRACTICE OF BUSINESS STATISTICS, W. H. Freeman and Company, USA - New York.

HFR400 Atmospheric Fast FID, User Guide. Cambustion Ltd., Cambridge, version 1.0.

Homann, S.G., Aluzzi, F., 2014. HotSpot, Health Physics Codes, Version 3.0, User's Guide. National Atmospheric Release Advisory Center, Lawrence Livermore National Laboratory, Livermore, CA 94550, LLNL-SM-636474.

Hunter, L.J., Johnson, G.T., Watson, I.D., 1992. An investigation of three dimensional characteristics of flow regimes within the urban canyon. Atmospheric environment 26B, 425-432.

Husain, T., 1994. Kuwaiti oil fires — Source estimates and plume characterization. Atmospheric environment 28 (13), 2149-2158.

Kozák, J., Čermák, V., 2010. The Illustrated History of Natural Disasters, Springer, Dordrecht.

Lincoln University, 2014. Library, Teaching and Learning: Confidence Intervals, QMET201. Lincoln University. https://library2.lincoln.ac.nz/documents/Confidence-Intervals.pdf

Luongo, G., Perrotta, A., Scarpati, C., 2003. Impact of the AD 79 explosive eruption on Pompeii, I. Relations amongst the depositional mechanisms of the pyroclastic products, the framework of the buildings and the associated destructive events. Journal of Volcanology and Geothermal Research 126, 201-223.

Marco, E., Pena, J.A., Santamarıa, J., 1998. The chlorine release at Flix (Spain) on January 21st 1996: a case study. Journal of Loss Prevention in the Process Industries 11, 153–160.

Mitchell, J.T., Edmonds, A.S., Cutter, S.L., Schmidtlein, M., McCarn, R., Hodgson, M.E., Duhé, S., 2005. Evacuation Behaviour in Response to the Graniteville, South Carolina, Chlorine Spill.. QUICK RESPONSE RESEARCH REPORT 178, University of South Carolina.

Pöllänen, R., Valkama, I., Toivonen, H., 1997. Transport of radioactive particles from the Chernobyl accident. Atmospheric Environment 31 (21), 3575-3590.

Santiago, J.L., Martilli, A., Martín, F., 2007. CFD simulation of airflow over a regular array of cubes. Part I: Three-dimensional simulation of the flow and validation with wind-tunnel measurements Boundary-Layer Meteorology 122, 609–634.

Varma, R., Varma, D.R., 2005. The Bhopal Disaster of 1984. Bulletin of Science, Technology and Society.

VDI - Verein Deutcher Ingenier, 2000. Environmental meteorology Physical modelling of flow and dispersion processes in the atmospheric boundary layer. Application of wind tunnels. VDI-Standard: VDI 3783 Blatt 12. Dusserdorf.

Yee, E., Chan, R.A., 1997. Simple model for the probability density function of concentration fluctuations in atmospheric plumes. Atmospheric Environment 31, 991–1002.

Zhou, Y., Hanna, S.R., 2007. Along-wind dispersion of puffs released in a built-up urban area. Boundary-Layer Meteorology 125, 469-486.

Acknowledgement

This work was supported by the Czech Science Foundation GA CR - GA15-18964S and the Institute of Thermomechanics, AS CR - RVO: 6138998.

Declarations of interest: none.

4. Model of arrival time for gas clouds in urban canopy

Hana Chaloupecká[1,2*], Zbyněk Jaňour[1], Klára Jurčáková[1] & Radka Kellnerová[1]

[1] Institute of Thermomechanics, Czech Academy of Sciences, Prague, Czech Republic

[2] Faculty of Mathematics and Physics, Charles University, Prague, Czech Republic

*hana.chaloupecka@it.cas.cz

Abstract

The aim of this paper is to present a new model of arrival time for gas clouds. To create such a model, simulations of short-term gas leakages were conducted in a wind tunnel with a neutrally stratified boundary layer. Into the tunnel, a model of an idealized urban canopy in scale 1:400 was placed. For simulations of the short-term gas discharges, ethane was utilized. Concentration time series were measured by a fast flame ionisation detector. The experiments were repeated about 400 times to get statistically representative datasets. The ensembles of concentration time series were measured at about 50 individual positions. From these data, puff arrival times were computed. The results showed that a suitable probability distribution to describe the variability in values at individual positions for arrival time is lognormal. Moreover, the parameters of this distribution do not change randomly with the change in the measurement position but their change can be described by functions. Utilizing them, probability density functions of arrival time can be constructed and whatever quantile of arrival time at a chosen position can be computed. Such a model could help emergency services to estimate how the situation could look like during the accident not only in the most frequently occurred but also in the extreme cases.

4.1. Introduction

Leakages of gases during an accident last very often less than one hour (e.g., Chaloupecká et al., 2017). The dispersion of these gas clouds depends on the actual turbulent flow present in the time and the place. Hence, wide range of dispersion scenarios can happen under the same mean ambient conditions. To be able to react effectively to an accident, emergency services need to know how the situation after the leakage can look like in mean as well as in extreme cases.

One of the crucial information for emergency services is the time when a gas cloud gets into individual places affected by the incident. Chaloupecká et al. (2017) compared arrival times

as found by different definitions and proposed a new method applicable also in the operative stage. Lübcke et al. (2013) found out that the mean value of arrival time increases with the increasing distance from the gas source but this increase seems to be higher close to the source. Chaloupecká et al. (2016) discussed the mean arrival time in an urban canopy in which flow was parallel with a street. Within this parallel street, the mean value of arrival time increases linearly with the increasing distance from the source. But a range of values of an arrival time ensemble at each measurement position is very wide and therefore a change of values of different quantiles at individual sampling positions is also an important aspect. Hence, we propose a new model describing an evolution of probability density functions of arrival time in an idealized urban canopy.

4.2. Methods and experimental set-up

The experiments were conducted in a wind tunnel with a neutrally stratified boundary layer. Its characteristics agreed with the recommendations of VDI (2000) for flows found in towns (see Chaloupecká et al., 2017 for more details). Into the tunnel, a model of an idealized urban canopy with pitched roofs in scale 1:400 was placed (Figure 1). This type of urban canopy is typical for European cities (e.g., Heathcote, 2014). For simulations of the short-term gas discharges, ethane was utilized. The discharges of 1 s set on a programmer logic controller were created by an electromagnetic valve. Concentration time series were measured by a fast flame ionization detector. The experiments were repeated about 400 times to get statistically representative datasets. The ensembles of concentration time series were measured at about 50 individual positions within human breathing zone at the model (see Figure 1b). From these data, puff arrival times (at*) were computed. We utilized a threshold method utilizing residual concentrations for finding arrival time, which is described in Chaloupecká et al. (2017).

In the paper, we use dimensionless quantities (e.g., VDI, 2000)

$$x^* = \frac{x}{H}, y^* = \frac{y}{H}, t^* = \frac{tU_{ref}}{H} \quad (1)$$

In these relations, *x, y* stand for horizontal coordinates, *H* the characteristic height (the height of modelled buildings), t time, U_{ref} reference speed (measured in the middle of the wind tunnel). The probability density function (pdf) of lognormal distribution (e.g., Wilks, 2006) with parameters μ, σ is defined as

$$f(x|\mu,\sigma) = \frac{1}{x\sigma\sqrt{2\pi}} exp\left\{\frac{-(lnx-\mu)^2}{2\sigma^2}\right\}; x > 0 \quad (2)$$

A quantile function is defined as

$$Q(p) = inf\{x \epsilon R; p \leq F(x)\} \quad (3)$$

for a probability $0 < p < 1$ and a cumulative distribution function *F* of a random variable *X*. The sample quantile *Q(p)* is approximately the value expected to exceed a randomly chosen member of the dataset with probability *p*, as suggested Wilks (2006).

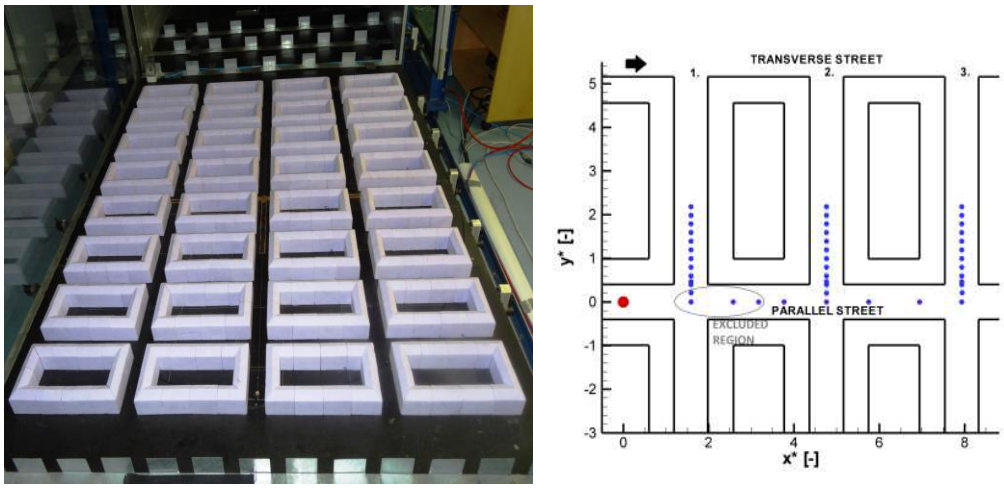

a. b.

Figure 1. Model of idealized urban canopy: placement in wind tunnel (a), scheme of investigated area (b) - big circle - position of ground-level point source, small circles - sampling positions, arrow - flow direction

4.3. Results

The results showed that the ensembles of arrival time usually follow a lognormal distribution according to Chi-square-goodness-of-fit-test (e.g., Hoel, 1966) with significance level 0.05. Along the parallel street, all datasets can be fitted by a lognormal distribution. But within the transverse streets, some measurement positions in which the data do not seem to follow the lognormal distribution exist. These positions are highlighted by star markers in Figures 2 and 3.

The parameters of the fitted distributions do not change randomly with the increasing distance from the gas source, but seem to chance according to some rules and therefore could be fitted by functions. For the analysis, we used least square method (e.g., Hoel, 1966).

The value of the parameter μ increases with the increasing distance from the source in the parallel street. This increase is approximately linear. An approximately linear increase of the parameter μ can also be seen with the increasing distance from the middle of the parallel street into the transverse street in all three investigated transverse streets. But one can spot

a variation of this behaviour just behind the intersection. In this region, a "hump" (a bigger increase and after a few sampling positions a decrease of the parameter value) can be seen. This behaviour is apparently connected with the presence of a recirculation vortex (e.g., Soulhac et al., 2009) in this region. Comparing the transverse streets, the slope of the fitted linear function decreases from the first to the third transverse street. But this change is not statistically significant; the values of the slope overlap in the 95% confidence intervals (CIs). Hence, we did not distinguish the slopes during creation of the model. Utilizing the linear approximation, the overall model describing an evolution of μ in the investigated area is

$$\mu = 0.083x^* + 0.30y^* + 2.93 \quad (4)$$

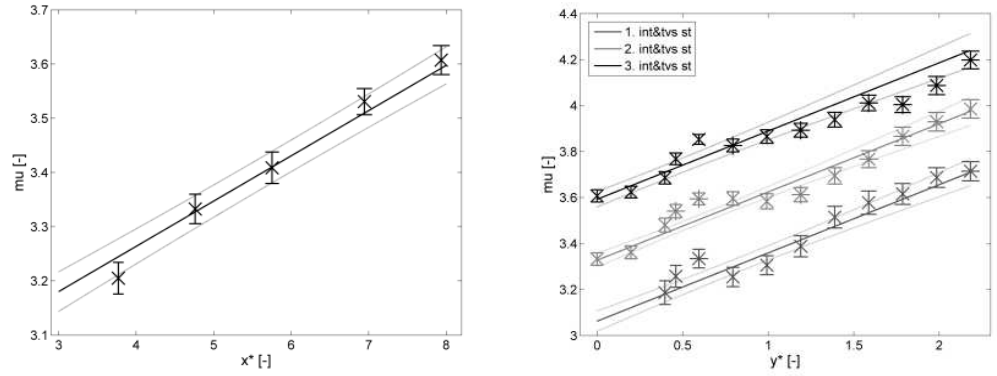

a. b.

Figure 2. Parameter μ of arrival time with 95% CI in the parallel street (a) and in the intersections (int) and transverse streets (tvs st) (b) with fitted model (thick line) and its 95% CI (thin line).

The model (Figure 2) is valid for all the sampling positions except for an excluded region (see Figure 1b). The coefficient of determination R^2 for the model is 0.97.

The second parameter of the lognormal distribution σ decreases with the increasing distance from the source in the parallel street. In contrast, the value of the parameter σ has an increasing tendency looking from the middle of the parallel street into the second or the third transverse street. In the first transverse street, such tendency is not noticeable. The appropriate model describing an evolution of σ in the investigated area is

$$\sigma = \frac{0.39}{x^*} + 0.01y^{*2} + 0.21 \quad (5)$$

The model (Figure 3) is valid for the same sampling positions as the parameter μ above. The coefficient of determination R^2 for the model is 0.89.

We utilized the proposed model to calculate the 0.05, 0.25, 0.5, 0.75 and 0.95 quantiles of at^* and compared them with the same quantiles derived from the data from the experiments. The values matched in the 95% CIs except for a few quantiles for positions close to the source (not showed).

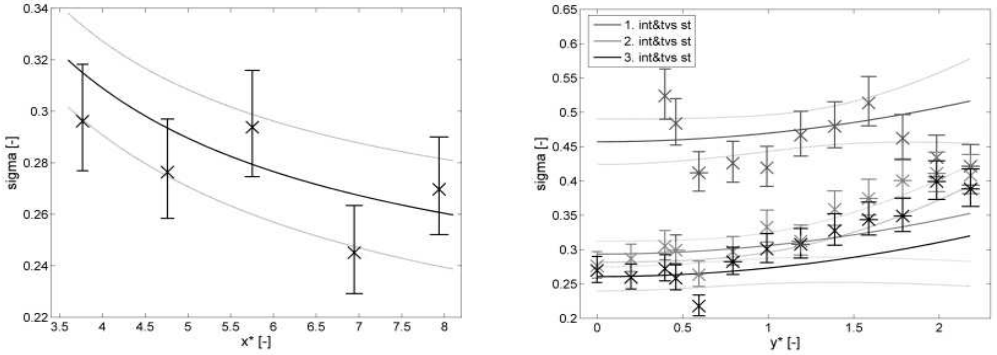

a. b.

Figure 3. Parameter σ of arrival time with 95%CI in the parallel street (a) and in the intersections (int) and transverse streets (tvs st) (b) with fitted model (thick line) and its 95% CI (thin line).

4.4. Conclusion

The paper dealt with arrival time of gas clouds. It proposed the new model for construction of the probability density function of arrival time within the idealized urban canopy. Arrival time ensembles in our experiments usually follow a lognormal distribution. The evolution of its parameters within our model can be described by the equations $\mu = 0.083\mathrm{x}^* + 0.30\mathrm{y}^* + 2.93$, $\sigma = 0.39/x^* + 0.01y^{*2} + 0.21$. Such models could be utilized to predict the situation after the short-term gas leakage not only in the most frequently occurred (mode of pdf) but also in extreme cases (e.g., 0.95 quantile of pdf).

Acknowledgments

The authors would like to thank the Technical Agency of the Czech Republic - TA CR (TJ01000383) and the Institute of Thermomechanics (RVO 61388998) for their financial support.

References

Chaloupecká, H., Jaňour, Z., Mikšovský, J., Jurčáková, K., Kellnerová, K. (2017), *Evaluation of a new method for puff arrival time as assessed through wind tunnel modelling*, PSEP, Vol. 111, pp. 194-210.

Chaloupecká, H., Jaňour, Z., Nosek, Š. (2016), *Short-term gas dispersion in idealised urban canopy in street parallel with flow direction*, EPJ Web of Conference.

Heathcote, E. (2014), The historic mixed-use courtyard buildings of central Europe, Global Property Insight, Financial Times.

Hoel, P.G. (1966), *Introduction to Mathematical Statistics*, Wiley, USA, 427 p.

VDI (2000), Environmental meteorology, Physical modelling of flow and dispersion processes in the atmospheric boundary layer, Application of wind tunnels, VDI-Standard: VDI 3783 Blatt 12.

Lubcke, L., Harms, H., Berbekar, E., Leitl, B. (2013), *Puff dispersion in a simplified central-European city,* International Workshop on Physical Modelling and Dispersion Phenomena.

Soulhac, L., Garbero, V., Salizzoni, P., Mejean, P. and Perkins, R.J. (2009), *Flow and dispersion in street intersections*, Atmospheric Environment, Vol. 43, pp. 2981–2996.

Wilks, D.S. (2006), *Statistical methods in the Atmospheric Sciences*, Academic Press, USA, 626 p.

5. Equations of a new puff model for idealized urban canopy

Hana Chaloupecká[a,b*], Michala Jakubcová[a], Zbyněk Jaňour[a], Klára Jurčáková[a], Radka Kellnerová[a]

[a] Institute of Thermomechanics, Czech Academy of Sciences, Dolejškova 1402/5, Prague, Czech Republic

[b] Faculty of Mathematics and Physics, Charles University in Prague, Ke Karlovu 3, Prague, Czech Republic

*corresponding author, email: hana.chaloupecka@it.cas.cz, telephone: +420 266 053 203

Abstract

During a leakage of hazardous materials, emergency services need to predict the evolution of the accident. In such situations, fast models are used. Such models can produce reasonable results for long-term leakages but the results for short-term leakages can be underestimated even by one order of magnitude as was shown in the project COST ES1006. Hence, the main aim of this paper is to present equations for recalculating the results valid for the continuous source to the ones valid for the short-term source. The model would consist of a model utilized for the continuous source and the equations introduced in the paper. The outputs obtained are the probability density functions of the puff characteristics: dosage, maximum concentration, and 99th and 95th percentiles of concentrations. These functions can help to estimate the situation not only for the mean case but also for the extreme cases.

Keywords: short-term gas leakage; long-term gas leakage; continuous release; operational model.

5.1. Introduction

Chemical industry products simplify people's lives each and every day. But the chemical industry also possesses a darker, less visible side. One of the negative aspects is chemical plant accidents. Inhabitants living close to chemical plants are particularly threatened by spills and accidents, often accompanied by large fires [1,2] or by toxic gas leakages into the air [3,4]. Such leakages often last less than one hour and the dispersion of the toxic material is strongly influenced by turbulence [5,6].

In case of a hazardous situation, emergency services need to have a prediction of its evolution to prevent loss of lives and environmental disasters. This prediction can be performed using mathematical models. The Direct Numerical Simulation (DNS) solves the Navier-Stokes equations without any turbulence model. It provides accurate results [7,8], but its demands on calculations are for high Reynolds numbers out of range even for available supercomputers [9]. The Large Eddy Simulation (LES, [10,11]) computes only large scales, which are affected much more by boundary conditions than the small ones, and utilizes a subgrid-scale model for the small scales. Though the LES in comparison with the DNS decreases the demand on computers, the demand is still very high [12]. Further decrease of the time demands on the calculations can be achieved by Reynolds' averaging [13]. It utilizes averaging over a time interval much longer than all the time scales of the turbulent flow [14]. Applying this averaging to the Navier Stokes equations, one obtains the Reynolds Averaged Navier Stokes equations (RANS,[15,16]). These equations can be utilized in combination with the LES, which is performed in the Detached Eddy Simulation (DES,[17,18]). Nevertheless, RANS are usually used in engineering practice on their own [12].

In an operational practice, usage of even a much simpler approach, which provides results in almost no time, is more common [14,19]. This approach is called the Gaussian dispersion modelling. Apart from the time issue, one of the reasons for their usage is their recommendation in regulatory guidelines[20,21]. The Gaussian models can be divided into two main types, the plume and the puff. The basic of the plume type [14] is a constant mean transport wind in the horizontal plane and the Gaussian concentration distributions in directions perpendicular to the wind direction. It is applicable for accidents in which the gas is leaking for a relatively long time (e.g. hours to days). The puff type [14] has a Gaussian concentration distribution in all three directions and it is useful for those cases in which the duration of the leakage is within the time scales in which the turbulent motions in flow are crucial.

Results of the project COST ES1006 revealed that fast models utilized for the actual emergency phase for long-term gas leakages can get reasonable results but the results for short-term ones can be underestimated even by one order of magnitude [21]. The solution to this problem might be to find relations for the recalculations of the results from the long-term to the short-term sources. In this paper, we present such relations for a built-up environment consisting of closed courtyards with pitched roofs. To find the relations, wind tunnel experiments were utilized. For short-term gas leakages, many possible dispersion scenarios for an exposed position and the same mean conditions exist [5,22]. Hence, the

result of our recalculation is not one value of a quantity describing the short-term leakage at the exposed location but a probability density function of the quantity, instead. The probability density function enables one to count the most probable value as well as the extreme cases which can occur. This stands our model apart from the models usually utilized during accidents in which only the ensemble-averaged puff outline and concentration field can be predicted [14]. The main aim of this paper is to present the relations for recalculations of the result from the long-term to the short-term sources for the variables: dosage, maximum concentrations, 99th percentiles of concentrations and 95th percentiles of concentrations. Such variables are important in emergency situations while assessing of the hazardousness of the incident [23].

The rest of the paper is organized as follows. Section 2 explains the methodology. Its subsections describe the wind-tunnel experiments, data processing, utilized puff characteristics, uncertainties, and the special functions utilized. Then, the method of validation is introduced. At the end, the entire approach utilized is summarized in a short paragraph and visualized by a scheme. Section 3 summarizes the results which are being discussed. This section is divided into two subsections. In the first one, the results for the variable dosage are presented. The second subsection describes the results for maximum and high percentiles of concentrations. The main findings are concluded in Section 4.

5.2. Methods

5.2.1. Wind-tunnel experiments

The datasets utilized for the development of the mathematical model were obtained by measurements in a wind-tunnel, which is specialized in boundary layer modelling. We used the boundary layer in scale 1:400 and verified its characteristics with the recommendations in [24] - see [6] for more details. Into the wind-tunnel, the model of an idealized urban canopy in scale 1:400 was placed (Fig. 1). The model was composed of buildings with pitched roofs to the height of 50 mm in basements and 13 mm roofs (total height H = 63 mm) [25]. The source was ground-level, circular with a 4 mm radius. The short-term releases of 1 s set on the time relay at the model were performed by an electromagnetic valve. The concentrations were measured by a fast flame ionisation detector (fast FID) with a resolution of 6 ms (estimated by a flick test [6]) at the height of human breathing zone. For the short-term releases, the experiments were repeated about 400 times for each measurement position to get statistically representative datasets. For the continuous releases, 180 s long concentration time series were recorded to get representative mean values of

concentrations. The sampling positions were chosen to cover the parallel street (pl st), three intersections (int) and three transverse streets (tvs st). The source was set as the origin of the coordinate system. The x* axis was set in the flow direction and the y* axis in the lateral direction, as depicted in Fig.1. Flow measurements were conducted by a Laser Doppler Anemometry (LDA).

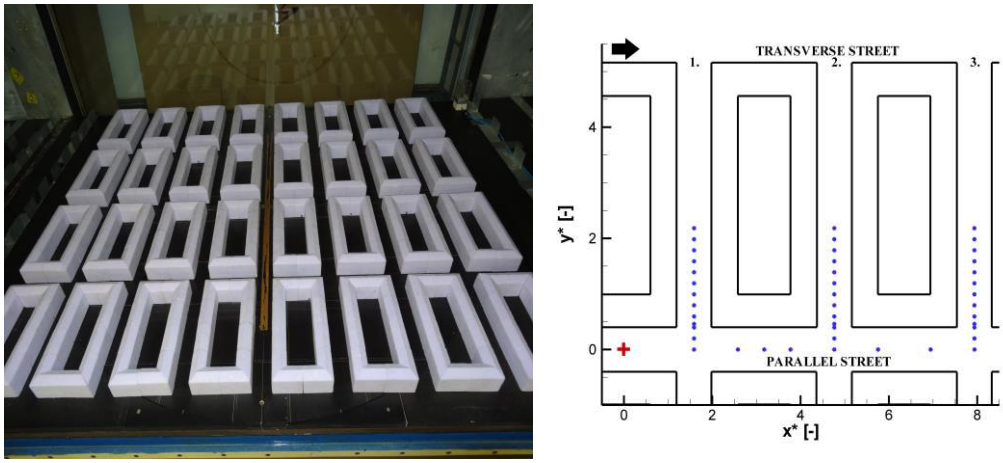

a. b.

Figure 1. Experimental set-up: a. placement of the model in the wind-tunnel, b. zoomed investigated section: red cross - position of source, blue circles - sampling positions, arrow - flow direction.

5.2.2. Data processing

The measured data were transformed into a dimensionless form [24]. To transform the coordinates in the horizontal plane x, y into the dimensionless form x*, y*, the following equations were applied

$$x^* = \frac{x}{H}, y^* = \frac{y}{H} \quad (1)$$

In the equation, H is the characteristic length (i.e. height of the modelled buildings).

The concentrations C were transformed into the dimensionless form C* using the relation

$$C^* = \frac{CU_{ref}H^2}{Q}, \quad (2)$$

where U_{ref} is the reference speed (measured at the middle height of the wind tunnel), Q is the source intensity. This relation is valid for a point source [24]. The tests of independence

of dimensionless concentration values on Reynolds number and on source intensity were conducted to set appropriate experimental conditions.

To transform time t into a dimensionless form t^*, we used the relation

$$t^* = \frac{tU_{ref}}{H}. \quad (3)$$

5.2.3. Puff characteristics

In the paper, we used four puff characteristics for analyses. These characteristics are: dosage, maximum concentration, 99th and 95th percentiles of concentrations. All of these characteristics depend on the determination of the times when the gas cloud arrived at the sampling position and when it left this position. Hence, these two characteristics (arrival time, departure time) are also explained in this section.

5.2.3.1. Arrival time (at*)

The arrival time definition introduced in [6] was utilized. It is a threshold method that utilizes the residual concentration. The method computes the 99th percentile of residual concentrations [26]. The arrival time is set if this value is exceeded in the first value as well as in at least 35% of the values of a short time interval beginning with this value.

5.2.3.2. Departure time (dt*)

For the departure time definition, we utilized the envelope method [23]. In the method, an envelope utilizing the absolute maximum and the following local maxima over the data is created. The departure time is set if the decrease between two following local maxima is less than 4% of the absolute maximum or if these two local maxima are distanced more than Δt^* = 200.

5.2.3.3. Dosage

The variable dosage [22] represents a sum of concentrations, which is exposed to the place of detection during the presence of the cloud.

5.2.3.4. Maximum concentration (Cmax*)

The maximum concentration is the highest value of concentration registered during the presence of the cloud at the observed detection position.

5.2.3.5. Peak concentrations (C99*, C95*)

Peak concentrations are high percentiles of concentrations [26] counted from the time interval when the gas cloud was observed at the detection position. In the paper, we use the 99th and 95th percentiles of concentrations (C99*, C95*).

5.2.4. Uncertainties

In the paper, uncertainties are represented by 95% confidence intervals [27] of the values (CIs). For the continuous releases, the type A uncertainty [28] was estimated utilizing a block circular bootstrap [29,30] since the concentration time series are not independent. The block length was chosen according to [31,32]. For the short-term releases, we utilized the ordinary bootstrap [33] since the puff characteristics are independent. The type B uncertainty [28] appearing in the measurements due to the environment and the instruments [23] was estimated following the Bezpalcová [34] and Taylor and Kuyatt [35] instructions.

5.2.5. Utilized special functions

In the paper, we utilized two special functions within the modelling part:

5.2.5.1. Probability density function (pdf) of generalized extreme value (GEV) distribution

The probability density function of the generalized extreme value distribution for the variable var [27,36,37] can be written as

$$f(var|k,\mu,\sigma) = \left(\frac{1}{\sigma}\right)\exp(-(1+k\frac{(var-\mu)}{\sigma})^{-\frac{1}{k}})(1+k\frac{(var-\mu)}{\sigma})^{-1-\frac{1}{k}}$$

$$\text{for } 1+k\frac{(var-\mu)}{\sigma} > 0, \qquad (4)$$

where μ, σ and k are parameters of the distribution. The parameter μ is the location or shift parameter since it shifts the pdf on the horizontal axis. The parameter σ, which has to be greater or equal to zero, is the scale parameter. It stretches (if σ>1) or compresses (if σ<1) the pdf in the direction of the horizontal axis. The last parameter k is the shape parameter. This parameter determines the decrease of the distribution tail. If $k = 0$, the distribution is referred to as the type I extreme value distribution (Gumbel) and its tail decreases exponentially. The type II (Fréchet) corresponds to $k > 0$ and its tail is 'heavy', it decreases as a polynomial. For $k < 0$, the type III extreme distribution (Weibull), the upper tail is finite.

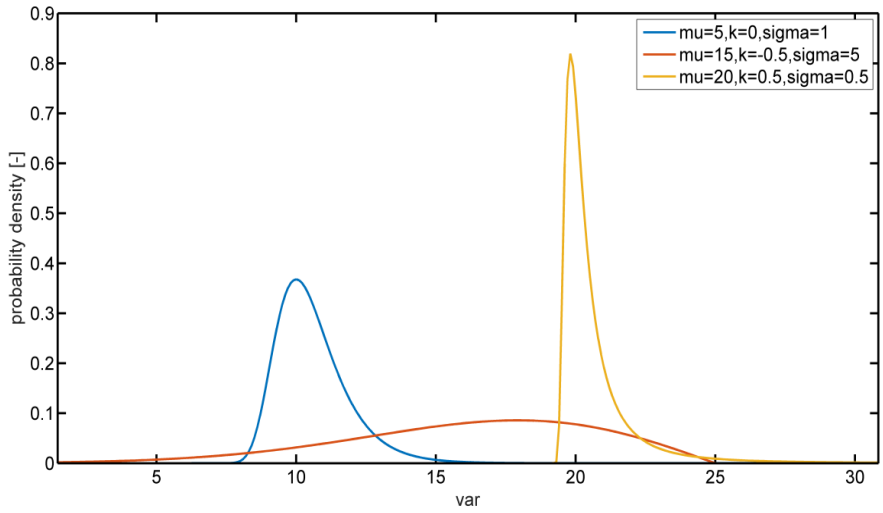

Figure 2. Example of probability density functions of GEV distribution with various parameters.

5.2.5.2. Logistic function

The logistic function [38] is an S-shaped (sigmoid) function in the form

$$f(x) = \frac{A}{1+e^{-b(x-r)}}. \quad (5)$$

In this relation, A denotes the curve's maximum value, b determines the steepness of the curve and r horizontally translates the function and hence it determines the location of the sigmoid midpoint.

5.2.6. Validation

To verify the found equations, we utilized the cross-validation [27]. In the cross-validation, the data are separated into subsets. On one (training) subset, the equation is fitted. Then one searches how well this equation fits for the other (validation) subset. A special type of cross-validation is called leave-one-out cross-validation, which we utilized in the paper. The reason was to be able to cover the behaviour of the variables in each region of the investigated section during the cross-validation from the dataset. In this special case, one value of the data is omitted from the dataset of n values in each step and the fitting procedure is repeated n times. In each step, the squared difference between the omitted value and the value predicted by the fitted model on n-1 remaining data is computed. In the end, these differences are averaged. By this procedure, the leave-one-out mean square error (LOO MSE) is obtained.

5.2.7. Overview of the utilized approach

We repeated short-term gas releases for each measurement position about 400 times. The recorded concentration time series were analysed. As a result, about 400 values of individual characteristics (e.g. dosage) for each measurement position were obtained. These ensembles were, for each measurement position, fitted with a suitable distribution by obtaining its parameters. For the same measurement positions, the experiments of continuous releases were conducted, and the concentration time series were recorded. From the recorded concentration time series, mean values of concentrations were calculated. In the end, relations between the puff parameters and mean values of concentrations for continuous source or the lateral and longitudinal distance from the source placed in [0,0] were searched. The entire process is schematically plotted in Fig. 3.

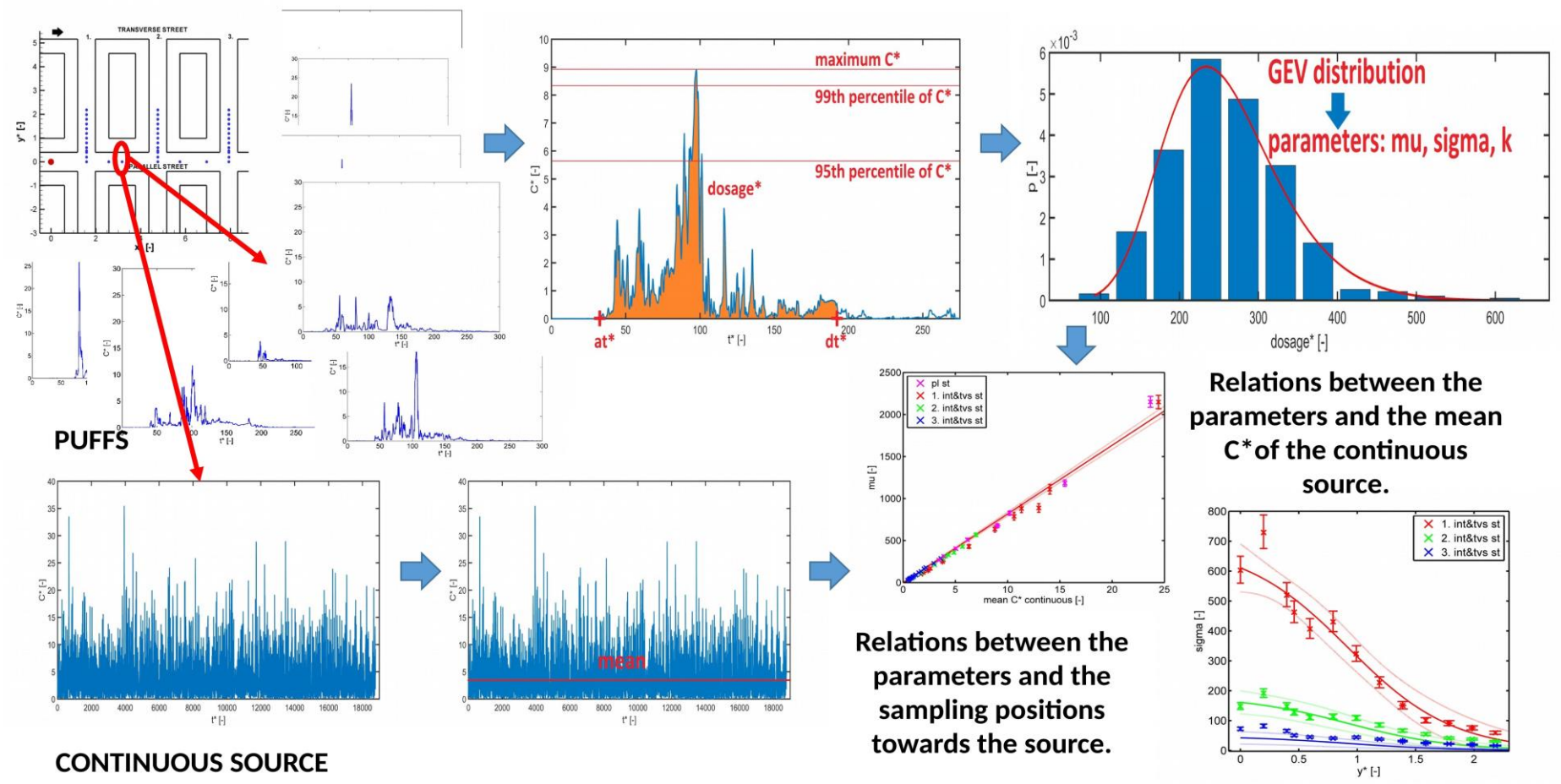

Figure 3. Overview of the utilized approach.

5.3. Results

In the results section, we propose the equations of a new model (Table 1). These equations, from many tested ones, fitted the data best according to the cross-validation. The results showed that LOO MSE changed around 20% compared to the mean square error (MSE) [27] of the fitted curves.

5.3.1. Dosage

The dosage ensembles at most sampling positions can be fitted by the GEV distribution according to the chi square goodness of fit test [39] with a significance level of 0.05. To distinguish whether the dataset at the sampling position was suitable for the fitting by the GEV distribution, two different symbols were utilized in the figures. Crosses are used for the datasets suitable for the GEV fitting, asterisks for the unsuitable ones. Though the data were not suitable for the GEV distribution according to the test, the found parameters of the GEV distribution usually agreed well with the trend shown by the neighbouring values suitable for the fitting. Hence, we did not eliminate these values from the analysis.

While the value of the location parameter of the GEV distribution can be easily predicted from the mean concentrations of the continuous source, the other two parameters of the GEV distribution are influenced rather by their location towards the source of contaminant and can be estimated by its usage.

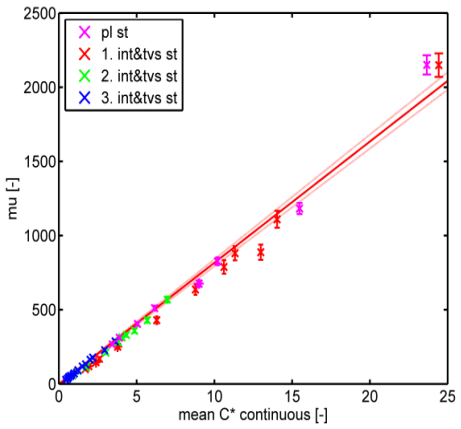

Figure 4. The relation between the location parameter μ and the mean concentrations for the continuous source for dosage (solid line denotes the fitted model, dashed lines denote 95% CIs).

Table 1. Equations for recalculation of the results from the long-term to the short-term source.

Parameter of GEV distribution	Equation	Equation parameters	Puff characteristic	Value
μ	**$\mu = a_\mu C^* - b_\mu$**	a_μ	dosage* Cmax* C99* C95*	82±2 5.2±0.3 4.2±0.2 2.6±0.1
		b_μ	dosage* Cmax* C99* C95*	insignificant 2.5±2.3 3±2 2.5±0.9
k	**$k = a_k x^* - b_k + (c_k - d_k x^*)y^*$**	a_k	dosage* Cmax* C99* C95*	0.017±0.007 0.07±0.02 0.06±0.02 0.03±0.01
		b_k	dosage* Cmax* C99* C95*	0.18±0.04 0.5±0.1 0.41±0.09 0.27±0.07
		c_k	dosage* Cmax* C99* C95*	0.18±0.03 0.37±0.09 0.37±0.08 0.34±0.06
		d_k	dosage* Cmax* C99* C95*	0.033±0.006 0.05±0.02 0.05±0.01 0.04±0.01
σ	**$\sigma = \exp(a_\sigma - b_\sigma x^*)/(1 + \exp(c_\sigma y^* - d_\sigma))$**	a_σ	dosage* Cmax* C99* C95*	7.2±0.2 3.6±0.2 3.6±0.2 3.7±0.2
		b_σ	dosage* Cmax* C99* C95*	0.42±0.05 0.32±0.08 0.37±0.06 0.44±0.04
		c_σ	dosage* Cmax* C99* C95*	2.2±0.7 4±3 3.6±0.2 2.2±0.5

		d_σ	dosage* Cmax* C99* C95*	2±1 6±5 5±2 2.3±0.9

The value of the location parameter μ increases with the increase of the mean concentrations of the continuous source (Fig. 4). This increase is approximately linear (Table 1). The coefficient of determination [40] for the linear relationship is 0.985. The location parameter shifts the whole distribution on the horizontal axis. Hence, the greater this parameter is, the greater e.g. the expectation of mean dosage. So, the increasing trend agrees with the following logical expectation. If huge mean concentrations are observed for a place by a continuous source, the huge mean dosage can also be seen by a short-term source. And on the contrary, if small mean concentrations are observed for a place by a continuous source, the small mean dosage can also be seen by a short-term source.

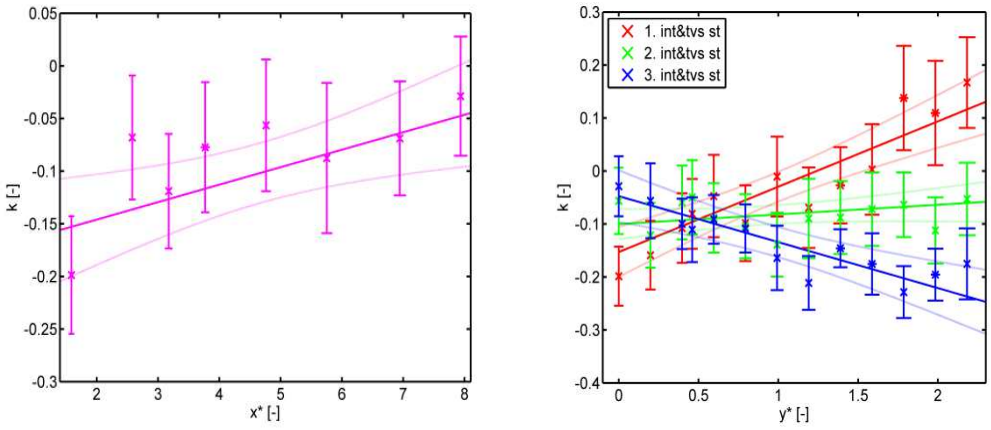

a. b.

Figure 5. The relation between the shape parameter k and the sampling positions towards the source for dosage (solid lines denote the fitted model, dashed lines denote 95% CIs).

The shape parameter k (Fig. 5) can be predicted from knowledge of the sampling position towards the source of contaminant (Table 1). In the parallel street, the parameter can be fitted by an increasing linear function. In the transverse street, the slope of the line declines when looking from the first to the third street. While the slope of the line increases with an increase in the distance from the intersection in the first transverse street, this slope declines in the third transverse street.

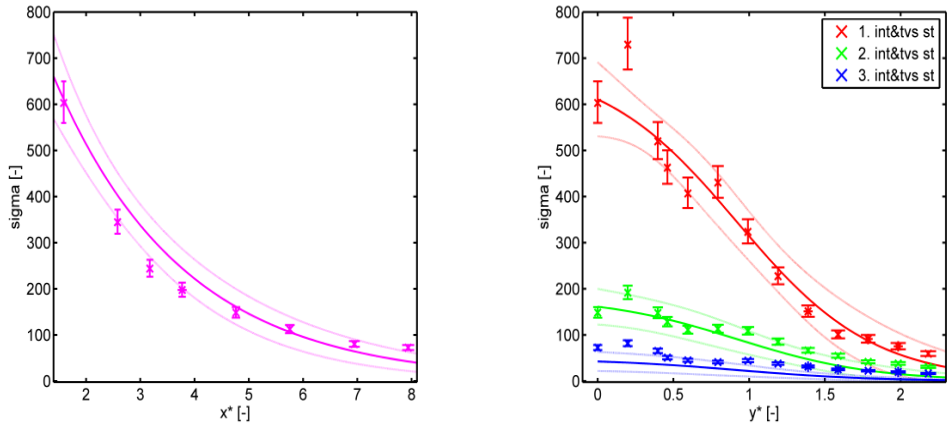

a. b.

Figure 6. The relation between the scale parameter σ and the sampling positions towards the source for the dosage (solid lines denote the fitted model, dashed lines denote 95% CIs).

The value of the scale parameter σ (Fig. 6) can be estimated from knowledge of the sampling position towards the source of contaminant like for the shape parameter. But the relation is different (Table 1). The trend is said to be broadly decreasing in the entire section of measurement with the increase of the distance from the source (with slight modifications in the region of the intersection and the mean position of the corner vortex [41,42]- Fig. 7). Since the shape parameter for σ>1 stretches the pdf, the range of values which can be seen in individual puff realisations tends to decrease. This behaviour could point out the tendency of more variable puff behaviour close to the source and this tendency seems to decrease as we move further form the source. Further from the source, the puff is wider, more mixed and with a smaller maximum concentration. In the parallel street, an exponential decrease with the increasing distance from the position of the source can be observed. In the intersections and transverse streets, this decrease is sigmoidal. A typical S-shaped curvature of the logistic function can be spotted. Over this curvature another flat inversed S-shaped function can be seen in the region of the intersection and the mean position of the corner vortex. But this function is not modelled by the model equation since it is indistinct. This inverse S-shaped function modifies a tendency of the parameter to decrease. In this region, the scale parameter first increases and hence the range of values is becoming larger, and then decreases by having the midpoint of the S shape approximately at the corner of the intersection. The lower arc of the S shape causes the parameter to increase again and finally it has an approximately exponential decrease to the end of the measurement section. The reason for the slight decrease of the parameter in the region of the corner vortex might be the increased isolation, and the protection of these positions inside the corner vortex.

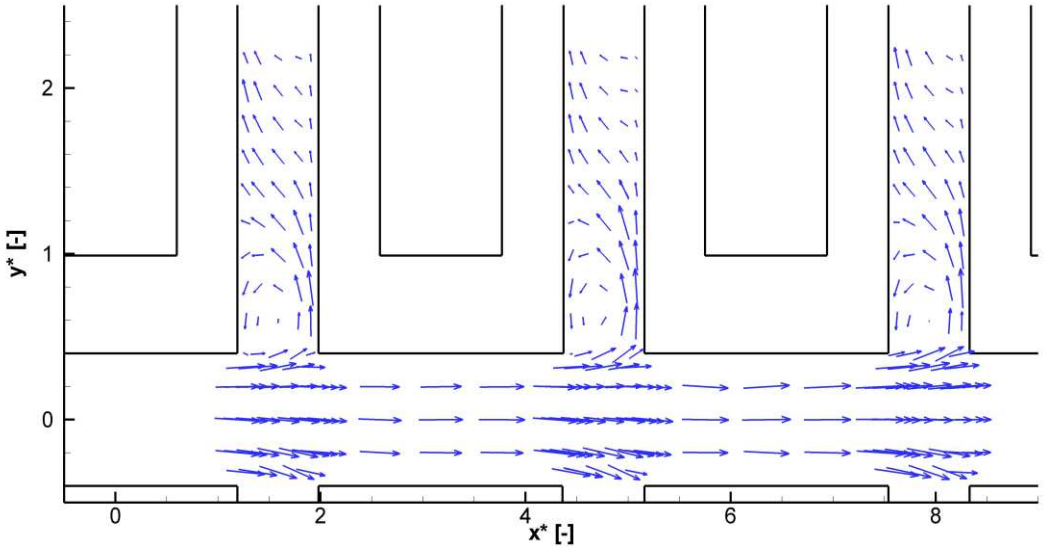

Figure 7. Vectors of mean flow in the investigated section.

5.3.2. Maximum and high percentiles of concentrations

To evaluate the hazardousness of the gas leakage, maximum concentrations and high percentiles of concentrations can be utilized. Knowledge of both types of variables is important because they both have different disadvantages. The problem of the maximum concentration is that it is only one value from a long time series. Hence, even one false value, caused e.g. by sucking a dust particle into the fast FID, can lead to an incorrect maximum concentration. In contrast, high percentiles are dependent on more values. But their disadvantage is their dependence on determination of puff arrival and departure time.

Like for the variable dosage, the GEV distribution turned out to be the best distribution to fit the datasets for the high percentiles of concentrations (95th and 99th percentiles) and maximum concentrations according to the chi square goodness of fit test (significance level 0.05). The value of the location parameter can be predicted utilizing the knowledge of mean concentrations for the continuous source. And for the other two parameters of the GEV distribution, utilizing the location of the sampling position towards the source is the best option. This is also the same as for the variable dosage.

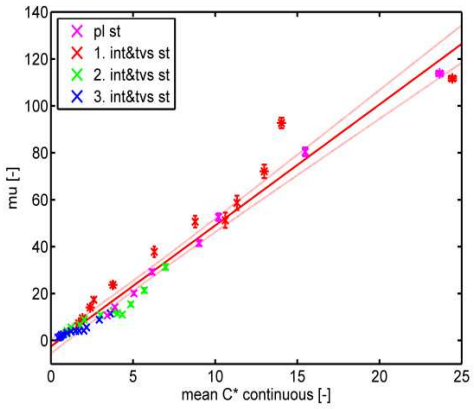

a.

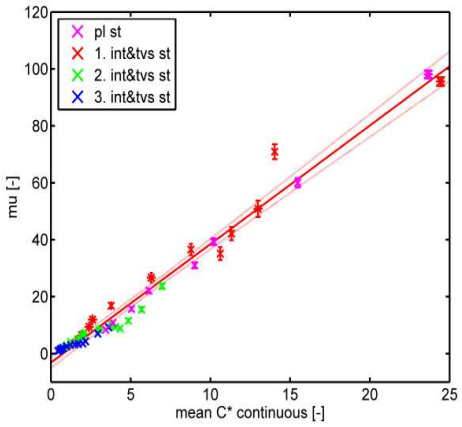

b.

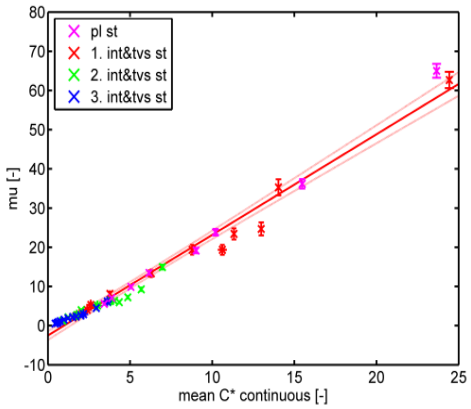

c.

Figure 8. The relation between the location parameter μ and the mean concentrations for the continuous source for maximum (a), 99th percentile (b) and 95th percentile of concentrations (solid lines denote the fitted model, dashed lines denote 95% CIs).

The relation between the location parameter of the maximum/high percentiles of concentrations μ and the mean concentrations for the continuous source (Fig. 8) is approximately linear (Table 1). The higher the mean concentrations for the continuous source are, the higher expected the value of the location parameter. The adjusted coefficient of determination [40] is 0.963 for the maximum concentrations, 0.976 for the 99th percentiles of concentrations and 0.979 for the 95th percentiles of the concentrations. The linear relationship of the explored variable with the mean concentrations was also observed by the variable dosage. But in contrast, the absolute value by the linear relation is not statistically insignificant (significance level 0.05) by the studied variables. It is a negative value, which overlap in the 95% confidence intervals for all of the three explored variables. The slope of the line increases with the movement to the variables towards the right edge of

the pdf. For instance, this slope is approximately two times higher for the maximum concentrations than for the 95th percentiles of concentrations.

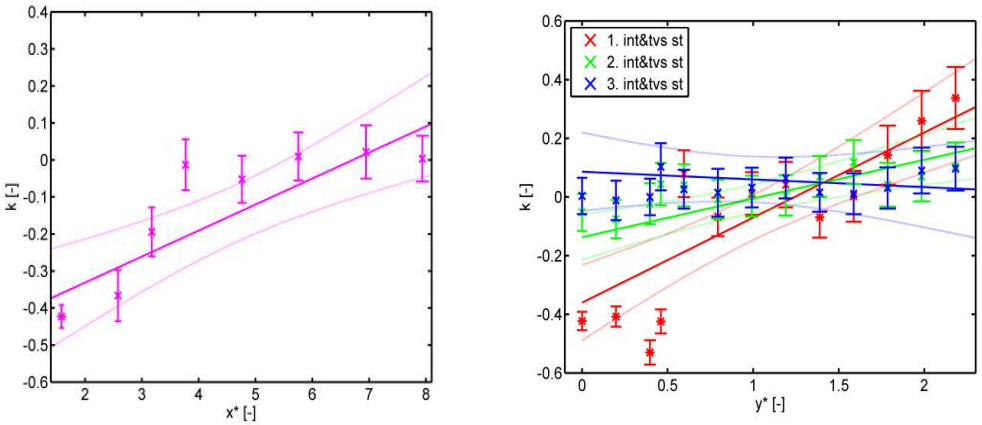

a. b.

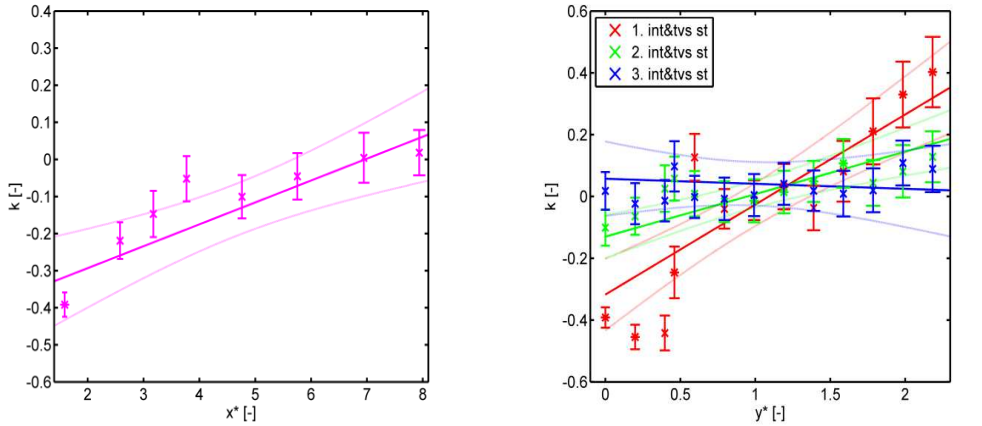

c. d.

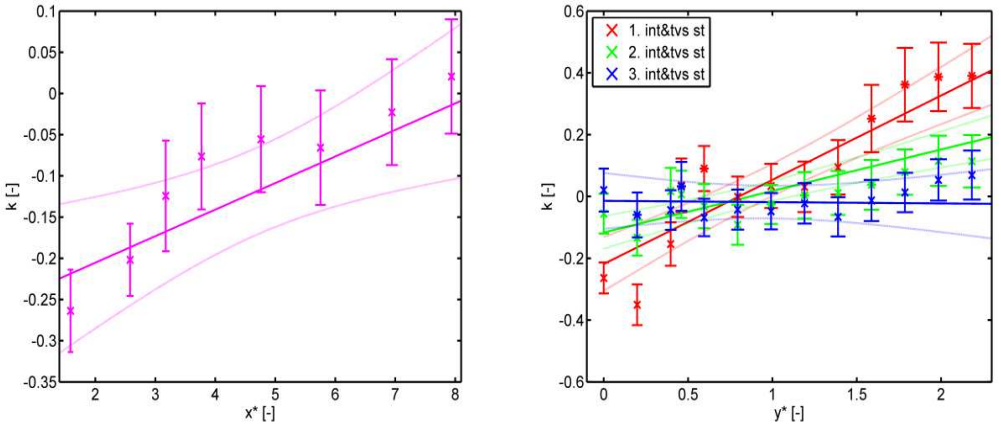

e. f.

Figure 9. The relation between the shape parameter k and the sampling positions towards the source for maximum concentration (a, b) / 99th percentile (c, d) / 95th percentile of concentrations (e, f) (solid lines denote the fitted model, dashed lines denote 95% CIs).

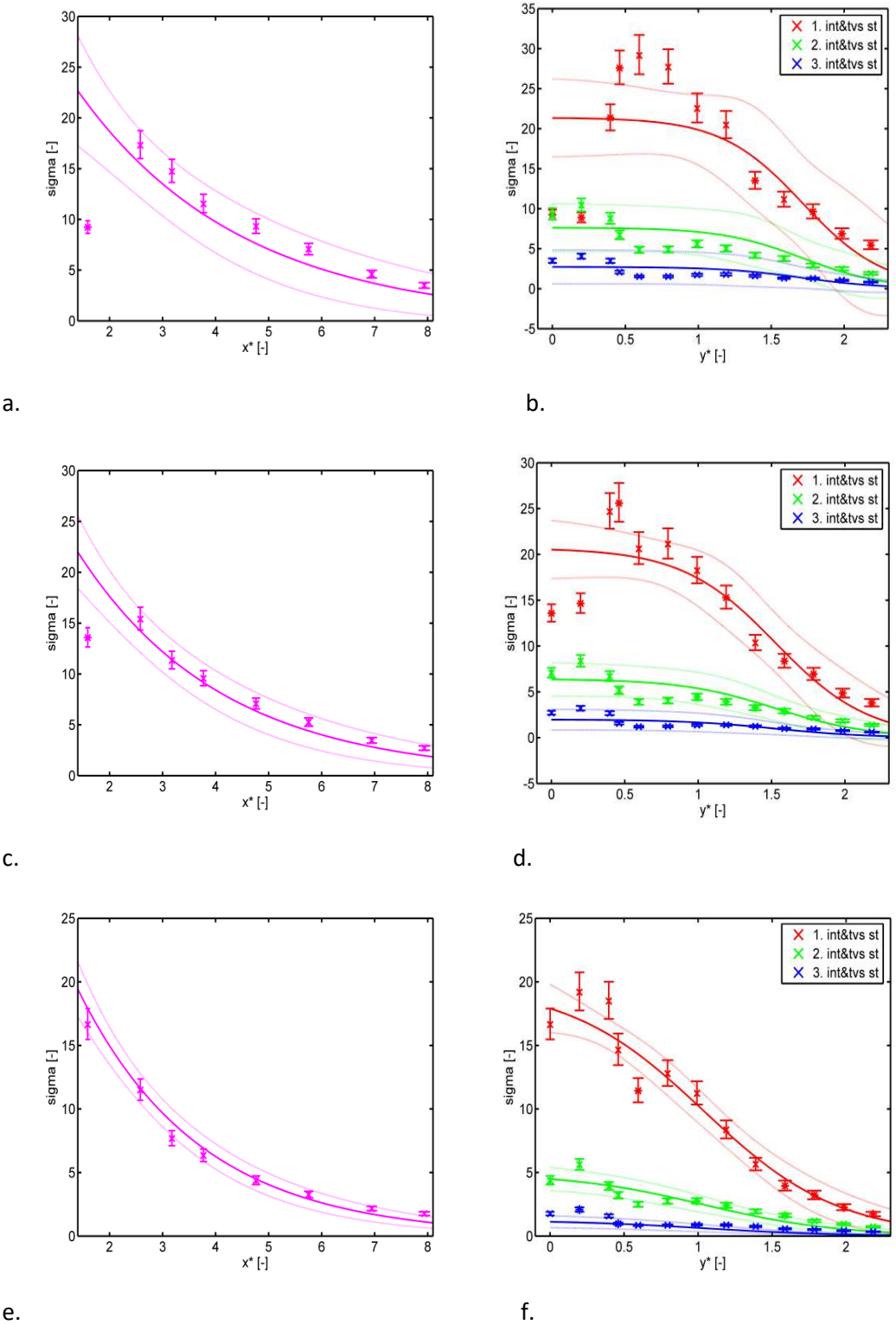

Figure 10. The relation between the scale parameter σ and the sampling positions towards the source for maximum concentration (a, b) / 99th percentile (c, d) / 95th percentile of concentrations (e, f) (solid lines denote the fitted model, dashed lines denote 95% CIs).

The shape parameter k (Fig. 9) changes approximately linearly with the change in the sampling position in the explored area (Table 1). The adjusted coefficient of determination is

0.786 for the 95th percentile of concentrations, 0.698 for the 99th percentile of concentrations and 0.698 for the maximum concentrations. The decrease of the coefficient with the movement to the variables towards the right edge of the pdf is probably caused by the increase of the extremity in variables, where e.g. the maximum concentration represents only one value from a long time series. The increase in values, with the increase of the distance from the source, is faster in all of the studied variables than for dosage in the parallel street. This increase is faster the more we move to the right edge of the pdfs. One can notice lower values for the sampling positions close to the source comparing e.g. the results for the 95th percentiles of concentrations and the maximum concentrations. For the maximum concentration, relatively low values of the parameter within the intersection can be also spotted. This phenomenon is expressed less by the 99th percentile of concentrations and least by the 95th percentile of concentrations. This feature is displayed in pdfs so that the pdfs decline faster to zero values at their right edges. By such pdfs, it is less probable to come across more outlier high values than for pdfs with more gradual decrease of the pdf tails.

For the scale parameter σ (Fig. 10), the adjusted coefficient of determination and MSE also decreases as one moves closer and closer to the edge of the pdfs as in the other two parameters. The scale parameter of the explored variables behaves similarly, as in the variable dosage. One can see an exponential decrease of the parameter with an increase in distance from the source in the parallel street. In the intersections and transverse streets, a sigmoidal decrease with slight modifications within the region of the intersections and the positions of the corner vortex can be observed (Table 1). We can spot a dissimilar behaviour of the flat S-shaped function at the position of the intersection and the corner vortex for the first transverse street by the variables. While by the 95th percentile of concentrations, the values of the parameter first increase and then decrease while approaching the midpoint of the S shape near the street corner and then after some distance, again decreases because of the lower arc of the S shape, the situation is different by the other two variables. The flat S is almost inversed. At first, one can spot relatively low values of the parameter near the middle of the intersection. These values then increase, reaching their maxima close to the corner of the intersection and then they start to decline. In the parallel street, this dissimilarity in the first transverse street by maximum concentration and 99th percentile of concentrations is visible from the first value, which deviates from the rest of the points by an unusually low value. Omitting the two sampling positions closest to the source, the adjusted coefficient of determination increases (from 0.779 to 0.958 for the maximum concentration, and from 0.908 to 0.979 for the 99th percentile of concentration). But the parameters of the equation

overlap in 95% CIs with only one exception of b_σ. This parameter is slightly higher when omitting the two positions for both of the studied variables. Because of only slight modifications in the equations with the omitted positions, and to keep the same number of sampling positions for all of the studied variables, we decided not to omit these two positions from the analysis.

5.4. Conclusions

The paper introduced new equations of a puff model for the idealized urban canopy (Table 1). The equations are utilized in the model for a recalculation of the results found for the continuous source by a model to the ones valid for the short-term source. As the outputs of the proposed model, probability density functions of the puff characteristics (dosage*, Cmax*, C99*, C95*) are constructed. This output in the form of pdfs is the main feature that stands our model apart from the models usually utilized during an accident, in which only the ensemble-averaged puff outline and concentration field can be predicted [14].

The results showed that the GEV distribution is the best one to fit the ensembles for all of the studied puff characteristics and showed as well the similarity in the behaviour of its parameters, too. The value of the location parameter of the GEV distribution was best predicted utilizing the mean concentrations of the continuous source. The relation between them was approximately linear in the explored section. The other two GEV parameters were best estimated using their location towards the source. The shape parameter had approximately a linear relationship with the location towards the source. The scale parameter changed exponentially in the parallel street and as a sigmoid function in the intersections and the transverse streets.

The proposed model must be further developed. The characteristics, such as dosage, depend on the duration of the gas release. Hence, the next step for our research is to find a relation that aims to recalculate the results for short-term releases of different durations. Then, the model must be validated on a different urban canopy and with different approach flow angles. The model must also be validated against other types of landscape (e.g. countryside, industry zone) and the equations adjusted for these different conditions.

Acknowledgement

This work was supported by the Technology Agency of the Czech Republic, TACR (TJ01000383) and the Institute of Thermomechanics, AS CR - RVO: 6138998.

References

[1] A. Scott, Fatal explosion hits BASF's Ludwigshafen site, Chem. Eng. News. 94 (2016) 13.

[2] A.H. Tullo, C&EN's Global Top 50 chemical companies: Chemical profits continue to rise as the global economy booms, C&EN Chem. Eng. News. 96 (2018).

[3] D.R. Varma, R. Varma, The Bhopal Disaster of 1984, Bull. Sci. Technol. Soc. (2005).

[4] F.P. Lees, Loss Prevention in the Process Industries – Hazard Identification, Assessment and Control, Volume 3, Butterworth Heinemann (1996).

[5] P.C. Zimmerman, W.B. Chatwin, Fluctuations in dense gas concentrations measured in a wind tunnel, Bound. Layer Meteorol. 75 (1995) 321–352.

[6] H. Chaloupecká, Z. Jaňour, J. Mikšovský, K. Jurčáková, R. Kellnerová, Evaluation of a new method for puff arrival time as assessed through wind tunnel modelling, Process Saf. Environ. Prot. 111 (2017) 194–210. doi:10.1016/j.psep.2017.07.006.

[7] N.N. Moser,R.D. Kim, J. Mansour, Direct numerical simulation of turbulent channel flow up to Reτ=590, Phys. Fluids. 11 (1999) 943–945.

[8] R. SCHLATTER, P. ÖRLÜ, Assessment of direct numerical simulation data of turbulent boundary layers, J. Fluid Mech. 659 (2010) 116–126.

[9] VKI, LES and related techniques.Theory and applications., von Karman institute for Fluid dynamics, 2016.

[10] U. Piomelli, Large-eddy simulation : achievements and challenges, 35 (1999) 335–362.

[11] T. Kobayashi, Large Eddy simulation for engineering applications, Fluid Dyn. Res. 38 (2006) 84–107. doi:10.1016/j.fluiddyn.2005.06.004.

[12] Y. Zhiyin, Large-eddy simulation: Past, present and the future, Chinese J. Aeronaut. 28 (2015) 11–24. doi:10.1016/j.cja.2014.12.007.

[13] B.R. Stull, An Introduction to Boundary layer Meteorology, Kluwer academic publishers, 2012.

[14] S. Pal Arya, Air Pollution Meteorology and Dispersion, Oxford University Press, 1999.

[15] P. Neofytou, A.G. Venetsanos, D. Vlachogiannis, J.G. Bartzis, A. Scaperdas, CFD simulations of the wind environment around an airport terminal building, Environmental

Modelling & Software 21 (2006) 520-524.

[16] T. Kajishima, K. Taira, Reynolds-Averaged Navier-Stokes equations, Springer, 2017.

[17] P.R. Spalart, Detached Eddy Simulation, Annu. Rev. Fluid Mech. 41 (2009) 181–202.

[18] Y.Ö. Özgür Yalçın, K. Cengiz, High-order detached eddy simulation of unsteady flow around NREL S826 airfoil, J. Wind Eng. Ind. Aerodyn. 179 (2018) 125–134.

[19] S. Şahin, M. Ali, Emergency planning zones estimation for Karachi-2 and Karachi-3 nuclear power plants using Gaussian puff model, Sci. Technol. Nucl. Install. 2016 (2016). doi:10.1155/2016/8549498.

[20] S.R. Hanna, G.A. Briggs, R.P.J. Hosker, Handbook on atmospheric diffusion, 1982. doi:10.2172/5591108.

[21] N.G. Jeff Bluett, Good Practice Guide for Atmospheric Dispersion Modelling, 2004.

[22] K. Baumann-Stanzer, S. Andronopoulos,P. Armand, E. Berbekar, G. Efthimiou, V. Fuka, C. Gariazzo, G. Gasparac, F. Harms, A. Hellsten, K. Jurcakova, A. Petrov, A. Rakai, S. Stenzel, R. Tavares,G. Tinarelli, S. Trini Castelli, COST ES1006 Model evaluation case studies: Approach and results, Cost Office, 2015.

[23] H. Chaloupecká, Z. Jaňour, K. Jurčáková, R. Kellnerová, Sensitivity of puff characteristics to maximum-concentration-based definition of departure time, J. Loss Prev. Process Ind. 56 (2018) 242–253. doi:10.1016/J.JLP.2018.09.007.

[24] VDI - Verein Deutcher Ingenier, Environmental meteorology Physical modelling of flow and dispersion processes in the atmospheric boundary layer, Application of wind tunnels, VDI-Standard: VDI 3783 Blatt 12, Dusserdorf., 2000.

[25] L. Kukačka, Urban Ventilation Dependence on Geometric Configuration, Doctoral Thesis, Charles University, Prague, 2018.

[26] F.M. Dekking, C. Kraaikamp, H.P. Lopuhaa, L.E. Meester, A Modern Introduction to Probability and Statistics, (2005) 485.

[27] D.S. Wilks, Statistical methods in the Atmospheric Sciences, Academic Press, USA, 2006.

[28] S. Bell, A Beginners Guide to Unceratinty of measurement, Natyonal Physical Laboratory, 2001.

[29] J.P. Politis, D.N. Romano, A circular block-resampling procedure for stationary data,

Tech. Rep. No. 370. (1991).

[30] A.C. Davison, D. V. Hinkley, Bootstrap Methods and their Application, Technometrics. 42 (1997) 216. doi:10.2307/1271471.

[31] H. Politis, D.N. White, Automatic Block-Length Selection for the Dependent Bootstrap, Econom. Rev. 23 (2004) 53–70.

[32] H. Patton, A. Politis, D.N. White, `CORRECTION TO "Automatic Block-Length Selection for the Dependent Bootstrap" by D. Politis and H. White', Econom. Rev. 28 (2009) 372–375.

[33] W. Piegorsch, Encyclopedia of Environmetrics, Wiley, 2012.

[34] K. Bezpalcova, Physical Modelling of Flow and Diffusion in Urban Canopy, Doctoral Thesis, Charles university, Prague, 2006.

[35] B.N. Taylor, C.E. Kuyatt, NIST Technical Note 1297 1994 Edition, Guidelines for Evaluating and Expressing the Uncertainty of NIST Measurement Results, Natl. Inst. Stand. Technol. (1994) 1–20.

[36] J. Beirlant, J. Goegebeur, Y. Segerrs, J. Teugels, Statistics of Extremes. Theory and Applications, John Wiley and Sons Ltd., 2005.

[37] E. Castillo, Extreme Value Theory in Engineering., Academic Press, 2012.

[38] N. Kyurkchiev, S. Markov, SIGMOID FUNCTIONS : SOME APPROXIMATION , 2015.

[39] J.P.M. de Sá, Applied statistics using SPSS, Statistica, Matlab and R, Springer, 2014.

[40] A. Anderson, Business Statistics for Dummies, A Wiley Br, 2013.

[41] L. Soulhac, V. Garbero, P. Salizzoni, P. Mejean, R.J. Perkins, Flow and dispersion in street intersections, Atmos. Environ. 43 (2009) 2981–2996. doi:10.1016/j.atmosenv.2009.02.061.

[42] H. Chaloupecká, Z. Jaňour, R. Kellnerová, K. Jurčáková, Influence of flow on puff characteristics, in: WIT Trans. Eng. Sci., 2017: pp. 37–48. doi:10.2495/CMEM170051.

6. Conclusion

The dissertation dealt with short-term gas releases studied utilizing wind tunnel modelling. The dispersion from short-term gas releases differs from long-term gas releases as their leakage duration falls into the turbulent part of the atmospheric spectrum (e.g., Van der Hoven, 1957). Many different accident scenarios can occur under the same mean ambient and leakage conditions (e.g., Zimmerman and Chatwin, 1995). This fact is one of the reasons why the research into short-term gas releases is so difficult and only a small number of studies focused on them exist. Because of the variability in results, many release realisations (a few hundred) under the same mean conditions are needed for risk assessment (e.g., Zimmerman and Chatwin, 1995; Chaloupecká et al., 2016). Such a research can be performed by wind tunnel modelling as it enables one to control ambient conditions very well.

I conducted such a research utilizing the wind tunnel modelling. I utilized an idealized urban canopy. The urban canopy was composed of buildings with pitched roofs organised into closed courtyards. Into it, a ground-level point gas source was placed. I conducted experiments of short-term as well as long-term gas releases. More than 30,000 repetitions of the short-term gas release experiment under the same mean ambient and release conditions were performed in my measurements, which lasted a few years, to get statistically representative datasets.

The first part of the dissertation is focused on specific definitions of puff characteristics. We presented new methods for determination of arrival time and departure time of a gas cloud at exposed places. Moreover, several definitions of cloud arrival time were applied on the same datasets and the results were compared. It was also revealed how slight changes in determination of departure time affect its values as well as values of other derived puff characteristics.

The new method of arrival time utilizes knowledge of a concentration time series prior to a gas cloud's discharge. The reason for such a choice is the analogy with the visual approach (e.g. Yee et al., 1998), in which a human analyses the concentration time series by hand. According to the authors, this manual approach seems to be the most trustworthy since a human can react to the various behaviours of a concentration time series in individual realisations at the sampling places more flexible than any algorithm. But the visual method cannot be utilized for large datasets. In the new method, we count the 99th percentile of a short time series just before the gas discharge and use this value as the threshold. The

threshold value is demanded to be exceeded in some percentage of cases of a short time interval because this threshold is a characteristic of the time series itself.

Moreover, unlike previous studies of short-term gas leakages, this is the first study to utilize more definitions of cloud arrival time on the same datasets. This procedure is highly important in order to be able to compare the results of different studies. We employed four different types of definitions (the visual method, the threshold method utilizing the residual concentration, the dosage method, and the threshold method utilizing the values of the peak concentration in the algorithm). Compared to the other methods, the advantage of the new presented method is that it is the only one which can be used operatively and not only as a post-processing tool. For each of the automatic procedures, we sought an optimal magnitude of its parameter as well as used the parameter value found in the literature. We compared the results of each automatic method with the visual method because this method (according to the authors) seems to be the most trustworthy one. The magnitudes of the parameters found in the literature were too high, since the results were overestimated in most cases. Employing the optimal magnitudes of the parameters, the threshold method that uses the residual concentration agreed the best. The threshold method utilizing the value of maximum concentration was a little worse. And the worst turned out to be the dosage method.

In the chapter focusing on departure time, we utilized the definition based on a selected percentage of a maximum concentration. But it had problems with residual concentrations, which affects not only the departure time of individual realisations but also the statistical values counted from ensembles. Hence, we proposed a new method. The method is based on the fact that concentrations levels change much more when a gas cloud is present at a sampling position than when a gas cloud is absent. Utilizing the method, an envelope (with help of local maxima) is created over the data. The envelope method searches for the time when a gradient in the concentration level becomes small.

Moreover, we studied the sensitivity of puff characteristics to slight changes in cloud departure time definition. The results revealed relatively strong dependence of the puff departure time on its precise definition. Hence, during a hazardous situation emergency services should not rely on the model results of the departure time as much. In contrast, the variables dosage and the 99th percentile of concentrations do not rely as much on the precise definition of the departure time and they can be therefore utilized while evaluating of the hazardousness of an accident.

The second part of the dissertation is focused on the reconstruction of probability density functions of puff characteristics in the exposed places. It used the knowledge of the sampling positions towards the source and the mean values of concentrations valid for the long-term gas source. The main aim is the usage of the found equations predicting probability density functions of puff characteristics in a new operational model. The reason why the model output is not only one value but a probability density function for each puff characteristic and the exposed place is the variability in the results of puff realisations. Many possible dispersion scenarios for an exposed position and the same mean conditions exist (Zimmerman and Chatwin, 1995). The probability density function enables one to count the most probable value as well as the extreme cases which can occur. This stands our model apart from the operational models usually utilized during accidents in which only the ensemble-averaged puff outline and concentration field can be predicted (Pal Arya, 1999).

The results revealed that the lognormal distribution is the best distribution to fit the arrival time ensembles. The GEV distribution turned out to be the best distribution to fit the ensembles of the puff characteristics: dosage, maximum concentration, and 99th and 95th percentiles of concentrations.

For arrival time, the parameters of the lognormal distribution were best estimated using the location of the sampling positions towards the source. The evolution of the parameter μ of the lognormal distribution within the explored section was linear. For the other parameter, the equation was a little more difficult: $\sigma = \frac{0.39}{x^*} + 0.01y^{*2} + 0.21$.

For the rest of the studied puff characteristics, the results showed the similarity in the behaviour of GEV distribution parameters. The value of the location parameter of the GEV distribution was best predicted utilizing the mean concentrations of the continuous source by a linear relation. The other two GEV parameters were best estimated using the location of the sampling positions towards the source. The shape parameter had approximately a linear relationship with the location of the sampling position towards the source. The scale parameter changed exponentially in the parallel street and as a sigmoid function in the intersections and the transverse streets.

The reconstruction of the probability density functions of puff characteristics is a part of work which is being done in the project TACR in collaboration with the Czech Ministry of Interior. The main aim of the project is developing of a software for emergency services. This software should contain an operational model to be used in case of long-term gas as well as short-

term gas leakages. The main demand for the model is its speed which should be very high. Moreover, the model should be able to be used on notebooks which are nowadays affordable for emergency services of the Czech Republic. The software will consist of a simple model utilized for the continuous source (Gaussian model) and the equations enabling to recalculate the results valid for the continuous source to the ones valid for the short-term source. The outputs for short-term gas releases will be probability density functions of puff characteristics.

Figure 1. Simulation of a rural area in the wind tunnel.

The characteristics, such as dosage, depend on the duration of the gas release. Hence, the next step for our research is to find a relation that aims to recalculate the results for short-term releases of different durations. Then, the model must be validated on a different urban canopy and with different approach flow angles. The model must be also validated against other types of landscape. In the project, we will utilize a rural area (Figure 1). The other landscape that will be used for validation is an industry zone (Figure 2).

Figure 2. An industry zone.

References

Chaloupecká, H., Jaňour, Z., Nosek, Š., 2016. Short-term gas dispersion in idealised urban canopy in street parallel with flow direction. EPJ Web of Conferences 114.

Pal Arya, S., 1999. Air Pollution Meteorology and Dispersion, Oxford University Press.

Van der Hoven, I., 1957. Power spectrum of horizontal wind speed in the frequency range from 0.0007 to 900 cycles per hour. Journal of Meteorology 14, 160-164.

Zimmerman, W.B., Chatwin, P.C., 1995. Fluctuations in dense gas concentrations measured in a wind tunnel. Boundary Layer Meteorology 75, 321-352.

Yee, E., Kosteniuk, P.R., Bowers, J.F., 1998. A STUDY OF CONCENTRATION FLUCTUATIONS IN INSTANTANEOUS CLOUDS DISPERSING IN THE ATMOSPHERIC SURFACE LAYER FOR RELATIVE TURBULENT DIFFUSION: BASIC DESCRIPTIVE STATISTICS. Boundary Layer Meteorology 87, 409-457.